Report No. NA-69-27
(DS-69-16)

AD712308

Interagency Agreement No. FA66NF-AP-15

Project No. 520-002-03X

A COMPARISON OF NATURAL LIGHTNING AND THE LONG LABORATORY SPARK WITH APPLICATION TO LIGHTNING TESTING

Reproduced by the
CLEARINGHOUSE
for Federal Scientific & Technical
Information Springfield Va. 22151

(ACCESSION NUMBER) (THRU)
(PAGES) (CODE)
(NASA CR OR TMX OR AD NUMBER) (CATEGORY)
FACILITY FORM 602

AUGUST 1970

SEP 1970
RECEIVED
NASA STI FACILITY
INPUT BRANCH

FINAL REPORT

Prepared for

DEPARTMENT OF TRANSPORTATION
FEDERAL AVIATION ADMINISTRATION
National Aviation Facilities Experimental Center
Atlantic City, New Jersey 08405

D D C
OCT 13 1970
RECEIVED

by

WESTINGHOUSE RESEARCH LABORATORIES
Pittsburgh, Pennsylvania 15235

93

DISCLAIMER NOTICE

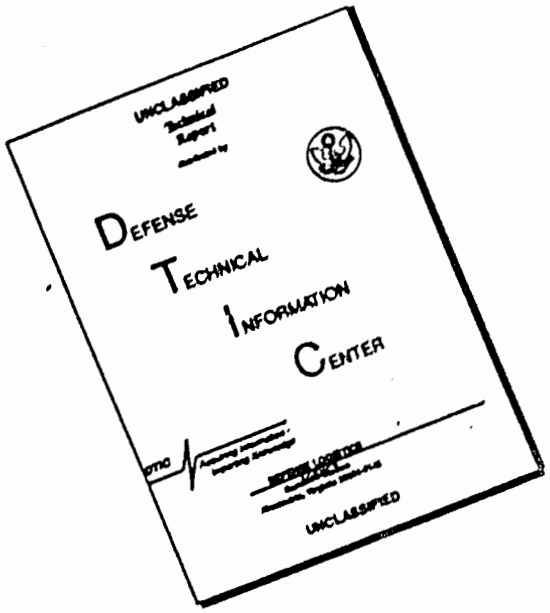

THIS DOCUMENT IS BEST QUALITY AVAILABLE. THE COPY FURNISHED TO DTIC CONTAINED A SIGNIFICANT NUMBER OF PAGES WHICH DO NOT REPRODUCE LEGIBLY.

FINAL REPORT

Interagency Agreement Number: FA66NF-AP-15 and NONR 4838(00)

Project Number: 520-002-03X

Report Number: NA-69-27
(DS-69-16)

A COMPARISON OF NATURAL LIGHTNING AND THE LONG LABORATORY SPARK WITH APPLICATION TO LIGHTNING TESTING

August 1970

Prepared by

Martin A. Uman

Distribution of this document is unlimited. This report has been prepared by the Westinghouse Research Laboratories for the Department of Transportation, Federal Aviation Administration, National Aviation Facilities Experimental Center, Atlantic City, New Jersey, under Contract No. FA66NP-AP-15 through the Office of Naval Research. The contents of this report reflect the views of the contractor, who is responsible for the facts and the accuracy of the data presented herein, and do not necessarily reflect the official views or policy of the FAA. This report does not constitute a standard, specification or regulation.

WESTINGHOUSE RESEARCH LABORATORIES
PITTSBURGH, PENNSYLVANIA 15235

FOREWORD

This report was prepared by the Westinghouse Research Laboratories for the Federal Aviation Administration. The work was part of a program of the Engineering and Safety Division, Aircraft Development Service, Washington, D. C. The contract which was cosponsored by the Office of Naval Research and the FAA was monitored by the Instruments and Flight Test Section, Aircraft Branch, Test and Evaluation Division, National Aviation Facilities Experimental Center, Atlantic City, New Jersey.

ABSTRACT

Laboratory sparks a few meters in length can be used to simulate lightning current rates-of-rise and peak values and to simulate some of the temporal characteristics of the lightning channel temperature. Long spark generators are inadequate for producing a simulation of the continuing current phase of lightning. Long sparks cannot be used to produce a simulation of the shock wave due to lightning except in that the spark data can be scaled by theory to predict the characteristics of the lightning shock wave. A short discussion is given of the several types of lightning which might be encountered by an aircraft. The validity of long-spark testing in determining the likely points of strike of a lightning discharge to an aircraft or other structure is briefly considered.

TABLE OF CONTENTS

	Page
FOREWARD	iii
ABSTRACT	v
TABLE OF CONTENTS	vii
LIST OF ILLUSTRATIONS	ix
INTRODUCTION	1
DISCUSSION	3
Electrical Properties	3
Thermal Properties	4
Acoustic Properties	5
Lightning Strikes to Aircraft	9
CONCLUSIONS	11
REFERENCES	12

APPENDIX I
"Temperature and Electron Density in Long Air Sparks" by Orville, Uman, and Sletten.

APPENDIX II
"Acoustic Output of a Long Spark" by Dawson, Richards, Krider, and Uman.

APPENDIX III
"Peak Power and Energy Dissipation in a Single-stroke Lightning Flash" by Krider, Dawson, and Uman.

APPENDIX IV
"Four-meter Sparks in Air" by Uman, Orville, Sletten, and Krider.

APPENDIX V
"A High-speed Time-resolved Spectroscopic Study of the Lightning Return Stroke, parts I, II, III" by Orville.

APPENDIX VI
"Determination of Lightning Temperature" by Uman.

APPENDIX VII
"Time Interval between Lightning Strokes and the Initiation of Dart Leaders" by Uman and Voshall.

LIST OF ILLUSTRATIONS

Figure		Page
1	Shock Wave Overpressure vs. Distance from an Infinite Cylindrical Source. (Adapted from Jones et al.[16].)	6
2	Shock Wave Overpressure vs. Distance at Mid-gap for a 4-m Spark of Energy Input per Unit Length 5×10^3 J/m. (The solid circles represent data taken with a piezoelectric microphone; the crosses, data taken with a condenser microphone.)	8

INTRODUCTION

It is thought that a lightning strike to an aircraft can result in the detonation of that aircraft's fuel, and it is known that lightning can cause the destruction or malfunction of unprotected electrical equipment. Long laboratory sparks are often used to test the vulnerability of aircraft and of electrical equipment to natural lightning.

In the present report, we consider the validity of the use of laboratory sparks in testing for lightning hazards. An up-to-date review of all known physical characteristics of natural lightning has been published by Uman.[1a] The physical characteristics of 4- to 5-meter laboratory sparks created by the Westinghouse 6.4-million-volt impulse generator located at Trafford, Pennsylvania have been studied by Orville et al.[2] (Appendix I*), Dawson et al.[3] (Appendix II), Krider et al.[4] (Appendix III), and Uman et al.[5] (Appendix IV). The papers by Dawson et al.[3] and Krider et al.[4] contain comparisons between some properties of lightning and of the long spark. Since the properties of long laboratory sparks are dependent upon the generator and associated electrical circuits which produce the sparks, we will, in this report, confine our discussion to those laboratory sparks created by the Westinghouse Trafford Generator. A detailed description of the generator and associated circuits is given by Uman et al.[5]

The following parameters of lightning and of the laboratory spark are considered of primary importance as regards the lightning hazard:

1. The maximum rate-of-change of electrical current, the maximum electrical current, and the duration of current flow in the object struck by lightning. These properties of the current are important in that they in part determine the power generated in the path of current-flow and the voltages induced in the vicinity of the discharge. Further a lightning current of considerable duration generates appreciable heat. The heat so produced could weaken mechanical structures and ignite flammable vapors.

2. The temporal characteristics of the temperature of the discharge channel. To weaken mechanical structures or to ignite flammable vapors it is necessary to apply a given temperature for a certain amount of time. In general, the higher the temperature, the shorter the necessary time of application.

3. The shock wave (close thunder) generated by the expanding discharge channel in its initial phase. There is evidence (Few et al.[6], Dawson et al.[3], Uman et al.[5]) that a significant fraction of the input energy to an electrical

---

*The research described in the published papers reprinted in Appendices I through VII as well as that contained in the body of this report was supported in part by the Federal Aviation Administration. The papers are reprinted with permission of their authors and publishers.

discharge is transmitted to the shock wave. The shock wave is thus capable of damaging mechanical structures and may be able to ignite flammable vapors.

It is shown in this report that the laboratory spark and natural lightning can be considered similar in some, but not all, of the above stated parameters; and thus that, with caution, the laboratory spark can be used for lightning testing. In the following section we will consider the electrical, thermal, and acoustical properties of the usual cloud-to-ground lightning and of the laboratory spark.

DISCUSSION

Electrical Properties

When the lightning stepped-leader approaches to some tens of meters above the earth, an upward-propagating discharge is launched from earth to the leader tip. The initial current measured at ground due to lightning is that of the upward-propagating discharge. When the lightning leader and upward-propagating discharge completely bridge the gap between cloud and ground, a highly luminous return stroke is propagated from earth to cloud. The rapid current rise to peak measured at ground is associated with the return stroke. The return stroke discharges to earth the charge, of the order of 5 coulombs for first strokes and 1 coulomb for subsequent strokes, stored on the leader. The time from detection of measurable current to peak current is generally a few microseconds for first stroke and can be less than 0.1 μsec for subsequent strokes (Berger and Vogelsanger,[7] Uman[1b]). Current rates-of-rise in excess of 80 kA/μsec have been measured (Berger and Vogelsanger[7]). Peak currents are generally 10 to 20 kA, but a few reliable values in excess of 100 kA have been obtained (Uman[1b]). Brook et al.[8], Kitagawa et al.[9], and Williams and Brook[10] report that continuing currents of the order of a hundred amperes may flow in the lightning channel for tens or even hundreds of milliseconds. The input energy to a typical lightning stroke channel is thought to be of the order of 10^5 J/m and the peak power input is thought to be in excess of 10^9 watts/m (Dawson et al.[3], Krider et al.[4]).

The laboratory spark can be used to simulate the lightning rate-or-rise of current, peak current, and possibly peak power input. However, the spark generator goes not supply a lightning-like input energy nor the type of continuing current characteristic of natural lightning. The Westinghouse 4- to 5-meter spark has a maximum current rate-of-rise of the order of 80 kA/μsec, a peak current of about 8 kA, a peak power input of about 10^9 watts/m, and an energy input of 5×10^3 J/m (Uman et al.[5]). The current waveform is lightning-like in shape, rising from zero current to peak current in a few microseconds and then decaying relatively slowly to zero again (Uman et al.[5]). Current flow is interrupted at about 70 μsec from spark initiation (Uman et al.[5]).

It is to be emphasized that changes in the generator and associated circuit parameters will yield changes in the observed spark parameters and that the spark referred to in this report is that described by Uman et al.[5]

Thermal Properties

Time-resolved lightning temperatures and electron densities have been measured by Orville[11] (Appendix V). Similar data on the laboratory spark have been published by Orville et al.[2] A discussion of the validity of the temperature measurements has been given by Uman[12] (Appendix VI). Both lightning and spark temperatures measured with microsecond time-resolution have peak values near 30,000°K. The lightning temperature decays to the 10,000°K to 15,000°K range in several tens of microseconds. The temperature decay of the spark is qualitatively similar to that of lightning but takes place on a time scale about a factor of 3 faster. The lightning continuing current is essentially a 100 amp air arc and thus should have a temperature of the order of 10,000°K (e.g., Maecker[13]). The continuing current may last tens or even hundreds of milliseconds. The laboratory spark has no continuing current, although in principle a low voltage arc source could be paralleled with the spark generator and switched into the channel at the appropriate time to simulate the continuing current. After the current in the lightning or spark channel is interrupted, the channel temperature may still remain relatively hot for an appreciable length of time. According to the theory of Uman and Voshall[14] (Appendix VII), the channel cooling time is proportional to the square of the channel radius. A lightning channel with a radius of about 1 cm can be expected to take tens of milliseconds to cool from 10,000°K to 2,000°K. The fully developed spark channel radius has been measured by Uman et al.[5] to be between 0.5 and 1.0 cm. Lightning channel radii after the initial breakdown phase are usually considered to be about 1.0 cm or slightly larger (Uman[1c]).

The electron density in both the spark and in lightning has a value averaged over the first few microseconds of the discharge of about 10^{18} cm^{-3}. The lightning channel reaches pressure equilibrium with the ambient atmosphere in a time of the order of 20 μsec; the spark channel in a time of the order of 5 μsec. After pressure equilibrium is reached, the electron density in both the spark and lightning will be of the order of 10^{17} cm^{-3} until the temperature of the discharge decreases to below about 15,000°K. Values for electron density as a function of time after current interruption are given by Uman and Voshall.[14]

Acoustic Properties

The acoustic output of lightning has been studied by Few et al.[6], Few[15], Dawson et al.[3], and Jones et al.[16] The acoustic output of the long spark has been studied by Dawson et al.[3] The theory of Few et al.[6] which relates the dominant acoustic frequencies present far from the discharge to the input energy to the discharge yields reasonable results for both lightning and sparks.

The theoretical overpressure generated as a function of distance for various energy inputs to an infinite cylindrical channel is given in Figure 1, which is adapted from a similar figure given by Jones et al.[16] According to all modern theories of cylindrical shock wave propagation, the shock front pressure for a cylindrical shock wave can be expressed to a good approximation as

$$P = 0.2 \times 10^{-5} \frac{W}{r^2} \text{ atmospheres} \qquad (1)$$

where the validity of (1) is restricted to $P > 10$ atm, the strong-shock regime, and distances from the channel of more than several initial channel diameters; "W" is the energy input to the channel in joules/m assuming that the bulk of the energy input takes place in less than a few microseconds (which has been measured by Uman et al.[5] to be the case for long sparks); and "r" is the radial distance from the center of the channel in meters.

As previously noted, the energy input to a typical lightning channel is thought to be of the order of 10^5 J/m. For this energy input the theoretical shock front pressure for a cylindrical shock wave at a radius of 0.02 m is about 500 atm, at $r = 0.05$ m is about 80 atm, and at $r \approx 0.14$ m is about 10 atm. According to the theory of Jones et al.[16] and of Few et al.[6], for an energy input of 10^5 J/m, the shock wave pressure will decay to near atmospheric in a radial distance of a few meters. Severe lightning discharges might be expected to have energy inputs an order of magnitude greater than typical discharges.

For the laboratory spark with an energy input of 5×10^3 J/m the theoretical shock front pressure for a cylindrical shock wave at a radius of 0.02 m is about 25 atm, decaying to near atmospheric in a few tens of centimeters. The availability of theory describing the cylindrical shock wave makes it possible to scale up the laboratory results for a given energy input to the case of natural lightning with a larger energy input. Direct lightning shock-wave simulation cannot, however, be done with the laboratory spark.

The cylindrical shock wave theory is only valid if the channel producing the shock wave is straight and is considerably longer than the distance at which the shock is observed. Since both lightning and long sparks are tortuous, Few[15] has suggested that various sections ("tortuosity lengths") of a channel

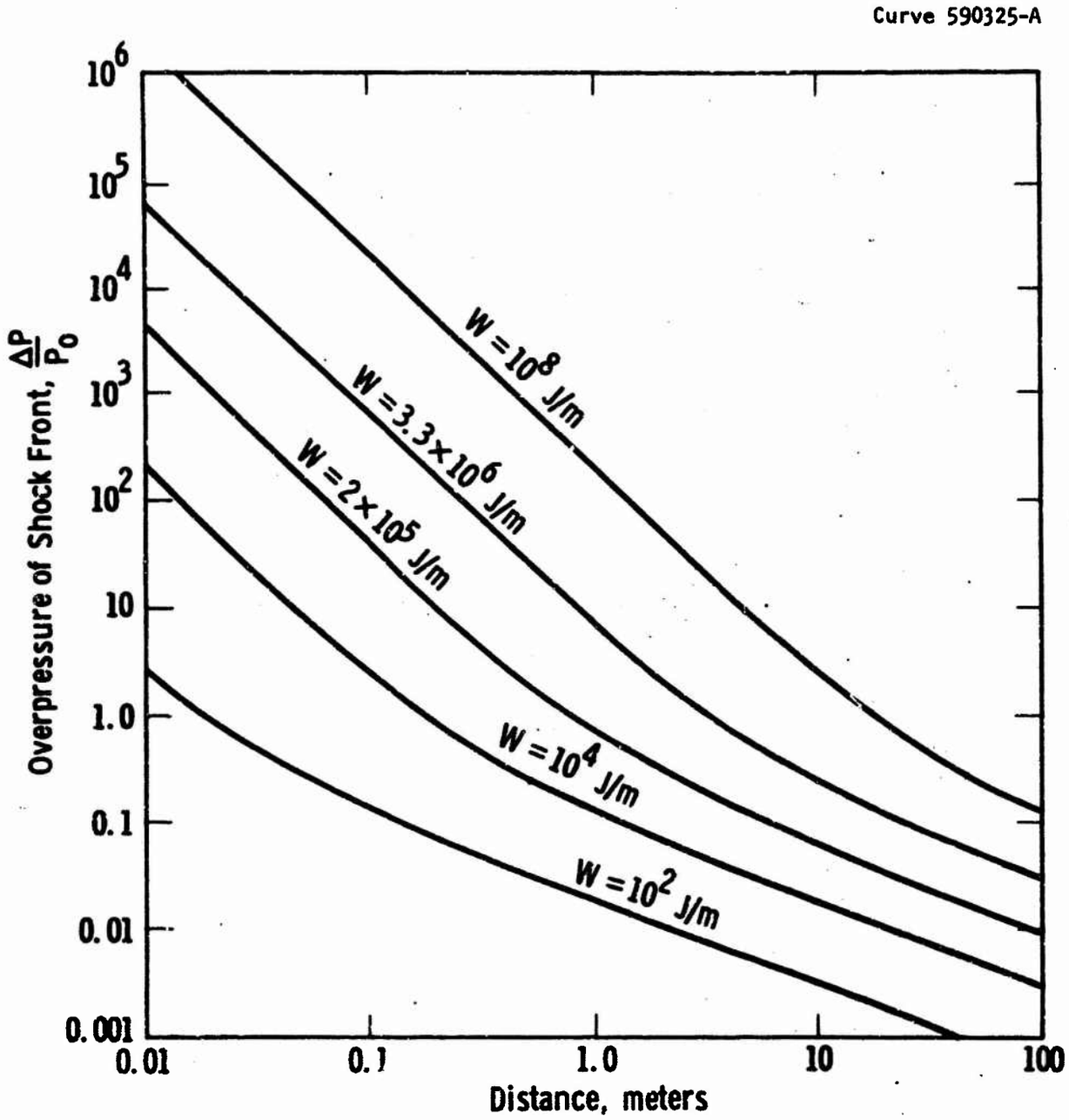

Fig. 1 - Shock Wave Overpressure vs. Distance from an Infinite Cylindrical Source. (Adapted from Jones et al.[16])

will produce individual shock waves. When the observer is closer to a radiating channel section than the length of the section, the shock wave will be cylindrical. When the observer is much further from the radiating channel section than the length of the section, the observed shock wave will be a spherical shock wave. In fact, far from the channel many spherical shock waves should be observed, one from each radiating section of the channel.

To investigate the validity of the ideas presented above, measurements were made at the Westinghouse Research Laboratories of the overpressure vs distance and the shock wave-shape vs distance for the 4-m laboratory spark. Measurements have been made at distances of 34 cm to 16 m from the channel. Additional measurements are planned. We show in Fig. 2 the overpressure data along with the best available theory. The dashed curve is Plooster's[17] cylindrical shock wave theory which is essentially the same as the theory shown in Fig. 1. The solid lines represent the spherical shock wave theory of Brode[18] for various assumed tortuosity lengths L for the spark channel; that is, the energy input for the spherical shock wave is WL where $W = 5 \times 10^3$ J/m. The experimental shock overpressures fall significantly below the cylindrical curve. They fit best a spherical curve due to a tortuosity length between 6 and 50 cm. Measurements much closer to the spark are needed to determine if the overpressure approaches the cylindrical curve at distances less than the tortuosity length. At distances of several meters from the channel, multiple shock waves are observed in accord with the idea of sound radiating from separate tortuosity lengths. Nevertheless, the analysis of the data using the tortuosity-length concept of Few[15] is not a unique analysis. Other analyses are possible. For example, one could argue that only a small fraction of the energy input is transmitted to the shock wave. (To make a cylindrical shock wave curve go through the experimental points, the energy transmitted to the shock wave would have to be about 0.2 of the total energy input.)

One very important point is evident from the spark shock wave measurements. It is that the measured shock overpressure is always less than that predicted by cylindrical shock wave theory. It follows that conservative specifications for equipment or structures designed to withstand the lightning shock wave can be obtained using the cylindrical shock wave theory.

Curve 590326-A

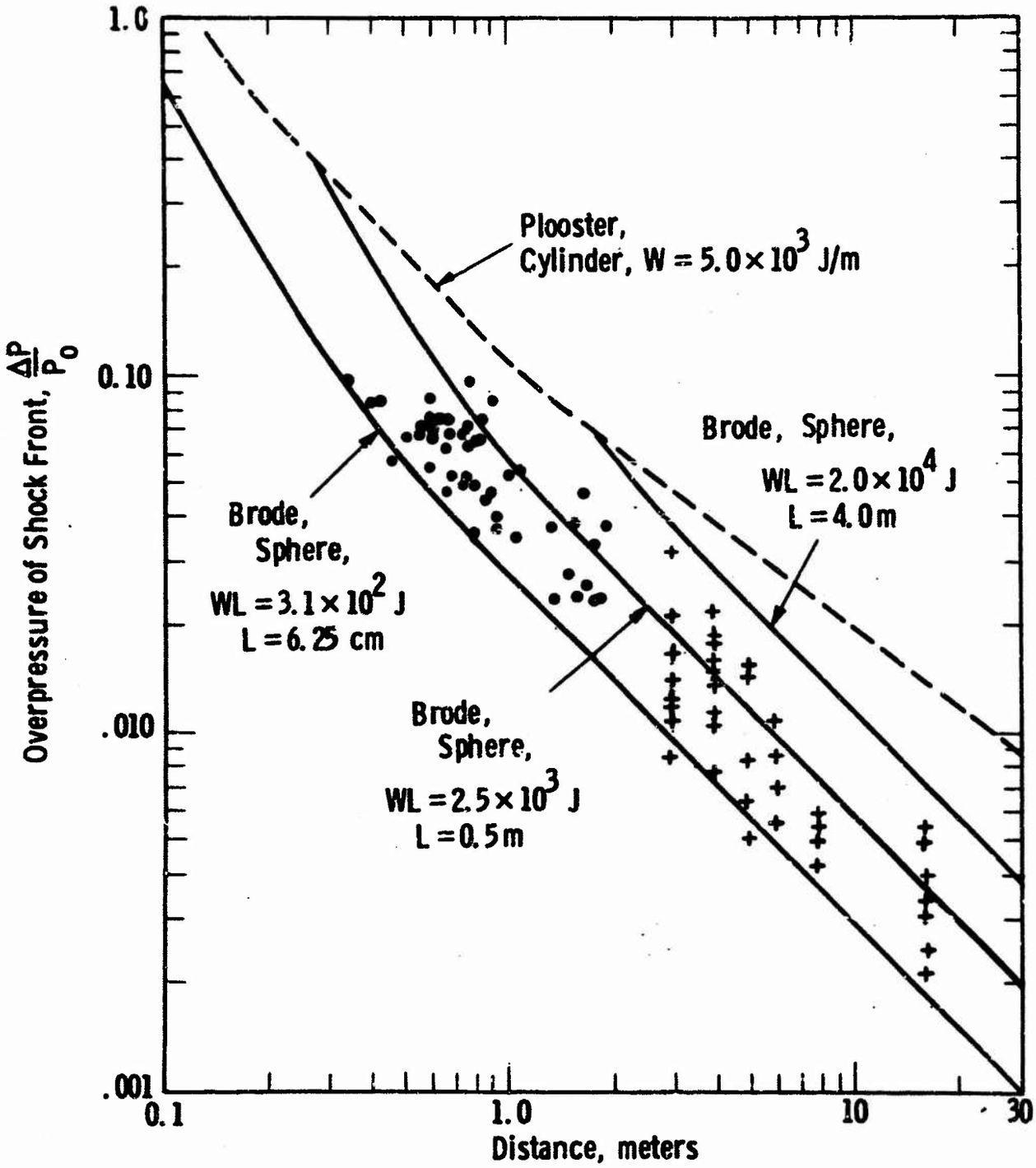

Fig. 2 - Shock Wave Overpressure vs. Distance at Mid-gap for a 4-m Spark of Energy Input per Unit Length 5 x 10^3 J/m. (The solid circles represent data taken with a piezoelectric microphone; the crosses, data taken with a condenser microphone.)

Lightning Strikes to Aircraft

The preceding sections of this report have been concerned with the usual cloud-to-ground lightning. An aircraft, however, is most often struck by a lightning discharge which ends in the air, by an intracloud discharge, or by an intercloud discharge. There is some evidence that all three of these lightning forms are similar (Brook[19]). The intracloud discharge has been the most studied of the three types of discharges but still there is little definite information concerning it (Uman[1d]). It is thought that intracloud discharges generally take place between an upper positive cloud charge center and a lower negative charge center; that a leader of moderate luminosity bridges this gap in tenths of a second; and that a number of relatively weak return strokes (K-changes) with peak currents of the order of 1 kA occur when the propagating leader contacts pockets of charge of opposite polarity to that of the leader. The total charge neutralized in an intracloud discharge is thought to be of the same order of magnitude as the charge transferred in a cloud-to-ground discharge. It would thus appear that protection of aircraft from the deleterious effects of cloud-to-ground lightning would suffice to protect the aircraft from the effects of intracloud discharges.

The usual cloud-to-ground lightning discharges lowers negative charge to ground. Occasionally a discharge occurs which lowers positive charge (Uman[1e]). The positive strokes have relatively slow rates-of-rise of current compared to negative strokes, have peak currents of about the same order of magnitude as negative strokes, but transfer relatively large amounts of charge. Berger and Vogelsanger[7] found that positive strokes transferred on the average about 3 times the charge of negative strokes. They found a maximum value of 300 C for a positive discharge. Thus positive strokes may present a considerable hazard insofar as their high currents flow for a relatively long time.

Aircraft flying in strong electric fields may initiate lightning discharges. It might be expected that leaders would propagate in two directions from the aircraft toward charge concentrations in the cloud. This type of discharge would probably be similar to discharges initiated by upward-propagating leaders from towers or high structures (Uman[1f]). In discharges initiated by upward-propagating leaders, typically the leader current measured at the ground merges smoothly into a more or less continuous current of a few hundred amperes. The current rise time to peak is of the order of milliseconds. Occasionally return strokes, with their associated rapid increase of current, may traverse the leader channel. The aircraft-initiated discharge should present no additional lightning hazards from those of the usual cloud-to-ground discharge.

In a study of lightning strikes to an instrumented aircraft, Petterson and Wood[20] found that peak currents in the struck aircraft were generally a few thousand amperes and rise times to peak were of the order of milliseconds.

It is tempting to associate the relatively long rise times to current peak with discharges initiated by the aircraft since, as noted in the previous paragraph, similar rise times are found in discharges initiated from grounded towers. On the other hand, since the properties of intracloud discharges are not well documented, the discharges to the aircraft could well have been normal intracloud discharges. In fact, the peak currents measured by Petterson and Wood[20] are of the order of magnitude thought to be characteristic of intracloud K-changes. The question of whether an aircraft actually triggers lightning or merely gets in the way of it has been discussed in more detail by Vonnegut[21] and by Petterson and Wood.[20]

We consider now briefly the validity of long spark testing in determining the likely points of strike of a lightning discharge to a flying aircraft or to a grounded structure. Since the characteristic step-length of the lightning-initiating stepped leader is some tens of meters and since the length of laboratory sparks is always less than that step length, it would appear that lightning and long-spark breakdown might well differ in significant aspects. On the other hand, spark testing can be justified from an intuitive point of view by the argument that the strike point of lightning is determined by the electrostatic field distribution on the structure and that this is relatively independent of the source of the field. This argument ignores, among other effects, the effect of space-charge field distortion which may be dependent on the temporal characteristics of the applied field. Thus, from the results of laboratory model tests using long sparks, one would expect natural lightning always to strike the tops of tall buildings. This is not always the case as evidenced by numerous examples of seemingly "impossible" lightning strikes (e.g., to the sides of the Empire State Building, to the base of the 42-story Cathedral of Learning Building in Pittsburgh). Just how valid the laboratory tests are is not known. They are certainly better than no tests at all and may, indeed, be reasonably valid.

CONCLUSIONS

On the basis of the preceding discussion and the research performed for the FAA, the following conclusions are drawn:

1. The long laboratory spark can be used to simulate many properties of the usual cloud-to-ground lightning. In particular, the spark can be used to simulate lightning current rates-of-rise and peak values and to simulate the temporal characteristics of the lightning temperature for the initial few tens of microseconds of the discharge and possibly during the time after current interruption. The long spark, by itself, cannot be used to simulate the continuing current phase of lightning. The spark cannot be used to simulate the shock wave due to lightning except that the spark results can be scaled by theory to predict the characteristics of the lightning shock wave.

2. An upper limit to the shock wave overpressure expected near a lightning channel can be obtained by use of cylindrical shock wave theory. Overpressure values can be read from Fig. 1 once the energy input W is chosen. A reasonable upper limit to W might be 10^6 J/m.

3. If aircraft are not vulnerable to the deleterious effects of the usual cloud-to-ground lightning, they are probably protected from the effects of intracloud, intercloud, and air discharges. On the other hand, very little is known about intracloud, intercloud, and air discharges, so that a reliable listing of their characteristics must await further research.

4. There are several obvious areas of lightning study relative to aircraft safety which need more research. (a) More information in needed on the properties of intracloud, intercloud, and air discharges, on the processes which initiate these discharges and the processes which initiate ground discharges, and on the effects of aircraft on the initiation processes. (b) Additional research is needed on the shock wave generated by an electrical discharge, so that a reliable estimate of the lightning shock wave properties can be made over a distance ranging from the strong shock regime very close to the channel to the acoustic regime many meters away from the channel. (c) While most research into the effects of lightning has been primarily concerned with direct strikes to aircraft, more attention should be paid to the effects of close lightning strikes. For example, a lightning discharge occurring several hundred meters from an aircraft generates relatively large electric and magnetic fields at the aircraft. These fields can do considerable damage to sensitive electronic systems. Very little is known about these close fields, although, in principle, a calculation of their characteristics is straightforward once a specification of the channel currents is made.

REFERENCES

1. Uman, M. A., Lightning, McGraw-Hill Book Co., New York, 1969; (a) Chapter 1; (b) Section 4.3; (c) see "radius of return stroke" in subject index; (d) Section 3.8; (e) Sections 3.7.6 and 4.3; (f) Sections 2.5.4 and 4.4.

2. Orville, R. E., Uman, M. A., and Sletten, A. M., "Temperature and Electron Density in Long Air Sparks, J. Appl. Phys., 38, 895, 1967. [See Appendix I].

3. Dawson, G. A., Richards, C. N., Krider, E. P., and Uman, M. A., Acoustic Output of a Long Spark, J. Geophys. Res., 73, 815, 1968. [See Appendix II].

4. Krider, E. P., Dawson, G. A., and Uman, M. A., Peak Power and Energy Dissipation in a Single-stroke Lightning Flash, J. Geophys. Res., 73, 3335, 1968. [See Appendix III].

5. Uman, M. A., Orville, R. E., Sletten, A. M., and Krider, E. P., Four-meter Sparks in Air, J. Appl. Phys., 39, 5162, 1968. [See Appendix IV].

6. Few, A. A., Dessler, A. J., Latham, D. J., and Brook, M., A Dominant 200 hz Peak in the Acoustic Spectrum of Thunder, J. Geophys. Res., 72, 6149, 1967.

7. Berger, K. and Vogelsanger, E., Messungen und Resultate der Blitzforschung der Jahre 1955-1963 auf dem Monte San Salvatore, Bull. Schweiz. Electrotech. Vereins, 56, 2, 1965.

8. Brook, M., Kitagawa, N., and Workman, E. J., Quantitative Study of Strokes and Continuing Currents in Lightning Discharges to Ground, J. Geophys. Res., 67, 649, 1962.

9. Kitagawa, N., Brook, M., and Workman, E. J., Continuing Currents in Cloud-to-ground Lightning Discharges, J. Geophys. Res., 67, 637, 1962.

10. Williams, D. P. and Brook, M., Magnetic Measurement of Thunderstorm Currents, Pt. 1, Continuing Current in Lightning, J. Geophys. Res., 68, 3243, 1963.

11. Orville, R. E., A High-speed Time-resolved Spectroscopic Study of the Lightning Return Stroke, parts I, II, III, J. Atmosph. Sci., 25, 827, 1968. [See Appendix V].

12. Uman, M. A., On the Determination of Lightning Temperature, J. Geophys. Res., 74, 949, 1969. [See Appendix VI].

13. Maecker, H., Elektronendichte und Temperatur in der Säule des Hockstromkohlebogens, Z. Phys., 136, 119, 1953.

14. Uman, M. A., and Voshall, R. E., Time Interval between Lightning Strokes and the Initiation of Dart Leaders, J. Geophys. Res., 73, 497, 1968. [See Appendix VII].

15. Few, A. A., Thunder, Ph.D. Thesis, Rice University, Houston, Texas, 1968.

16. Jones, D. L., Goyer, G. G., and Plooster, M. N., Shock Wave from a Lightning Discharge, J. Geophys. Res., 73, 3121, 1968.

17. Plooster, M. N., Shock Waves from Line Sources, NCAR-TN-37, National Center for Atmospheric Research, Boulder, Colorado, 1968.

18. Brode, H. L., The Blast Wave in Air Resulting from a High Temperature, High Pressure Sphere of Air, Research Memo RM-1825-AEC, The Rand Corporation, Santa Monica, California, 1956.

19. Brook, M., private communication, 1968.

20. Petterson, B. J. and Wood, W. R., Measurements of Lightning Strikes to Aircraft, Final Report, FAA Project No. 520-002-03X, Sandia Laboratory Report Number SC-M-67-549, Albuquerque, New Mexico, January 1968.

21. Vonnegut, B., Electrical Behavior of an Airplane in a Thunderstorm, Technical Report, FAA Contract FA64WA-5151, Arthur D. Little, Inc., Cambridge, Massachusetts, February 1965 (available from DDC as AD614914).

APPENDIX I

"Temperature and Electron Density in Long Air Sparks"

by Orville, Uman, and Sletten

Reprinted from JOURNAL OF APPLIED PHYSICS, Vol. 38, No. 2, 895-896, February 1967
Copyright 1967 by the American Institute of Physics
Printed in U. S. A.

Temperature and Electron Density in Long Air Sparks

R. E. ORVILLE*
Institute of Atmospheric Physics, University of Arizona, Tucson, Arizona
AND
M. A. UMAN AND A. M. SLETTEN
Westinghouse Research Laboratories, Pittsburgh, Pennsylvania
(Received 26 September 1966; in final form 26 October 1966)

ALTHOUGH the long laboratory spark in air has been studied extensively using electrical and photographic techniques, we have found nothing in the literature to indicate that quantitative spectroscopy has been used in such studies. In this communication, we present the results of a spectroscopic study of long laboratory sparks in air.

Five-meter-long air discharges were created between a negative rod and a grounded plane with a 6.4 MV impulse generator. The voltage applied to the spark gap reached its maximum value in 1.5 μsec. In addition to electrical measurements, spectra (3900 to 8900 Å) were recorded on film with 2-μsec time resolution. The near ir spectrum and current to ground for the long spark are shown in Fig. 1. The zero-time values for the spectrum and for the current may differ by 2 or 3 μsec.

The spectrometer used was composed of a transmission grating and associated optics coupled to a high-speed Beckman and Whitley drum camera. A 6-cm length of the spark channel was isolated for observation. Intensity calibration of the film was effected by passing the spark spectrum through a series of neutral density filters; wavelength calibration was done by photographing a standard source. Reciprocity failure should not occur for the short exposure times involved.[1]

It was not practical to attempt to measure radiative emission as a function of spark radius. Thus the spectra obtained represent the total emission from a short length of channel as a function of wavelength and time. In the analysis, we necessarily assumed physical conditions to be constant across the spark channel diameter.

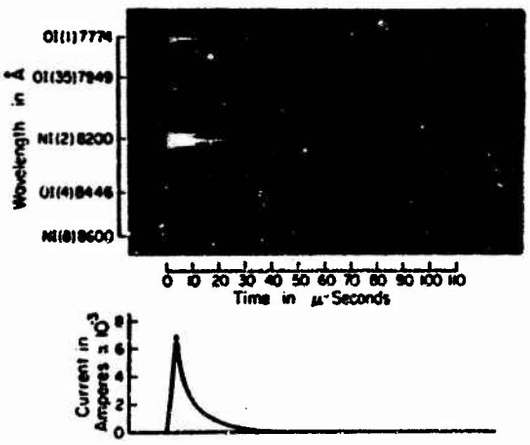

FIG. 1. The near ir spectrum and current of a 5-m spark in air.

Spark temperature may be calculated from the measurement of relative spectral line intensities and electron density from the Stark broadening of certain spectral lines. In order for these calculations to be meaningful, the channel must be optically thin to the wavelengths of interest. In addition, for there to exist a "temperature," local thermodynamic equilibrium (LTE) must be present to some approximation. That the channel is optically thin can be determined by comparing with measurements the predicted intensity ratios of lines due to transitions from approximately the same upper energy level. These intensity ratios are independent of temperature.

The opacity check was made in the visible within the *N*II(3) 5680-Å multiplet and in the near ir by comparing the intensity of the *O*I(1) 7774-Å multiplet to *O*I(4) 8446-Å multiplet. For LTE to exist in the temperature range of interest, an electron density in excess of 10^{16} cm^{-3} is required.[2] Although these high densities are attained in the early stages of the spark, the measurable electron density in the latter stages is near 10^{13} cm^{-3}. At these electron densities, "complete" LTE does not exist. However, all energy levels above the ground states of the ions and atoms of importance are populated in accordance with Boltzmann statistics (according to the criterion given by Griem[2a]). Thus, at worst, the temperature determined from relative line intensity measurements (from a given atom or ion) is the electron temperature. The electron-ion kinetic-energy equilibration time is of the order of 0.1 μsec.

Temperature determinations were made by measuring the following three line-intensity ratios: *O*I(1) 7774 Å/*O*I(35) 7947 Å, *O*I(4) 8446 Å/*O*I(35) 7949 Å, *N*II(39) 4041 Å/*N*II(12) 3995 Å; and by using the measured ratios in conjunction with the expression

$$T = (E' - E)/k \ln(I\lambda^3 g' f'/I'\lambda'^3 g f), \qquad (1)$$

where I, λ, g, and f are intensity, wavelength, statistical weight (of the upper state of the line), and emission oscillator strength, respectively, of one line with excitation potential E. The corresponding quantities for the other line are primed. Upper energy level differences $(E' - E)$ for the line pairs used were 3.35 eV, 3.10 eV, and 4.57 eV. Typical temperature-vs time values are given in Table 1. Temperature errors of about 15%, are present due to errors in intensity measurements and uncertainty in

TABLE I. Some properties of a 5-m spark in air.

Time (μsec)	Temperature (°K)	Electron density (cm^{-3})	Electrons per air atom	Pressure (atm)
0–2	3.4×10^{4}	11×10^{17}	1.4	13
2–4	2.8×10^{4}	3×10^{17}	1.1	2.4
4–6	2.6×10^{4}	2×10^{17}	1.1	1.3
6–8	2.4×10^{4}	2×10^{17}	1.0	1.1
8–10	2.2×10^{4}	2×10^{17}	1.0	1.0
10–12	2.0×10^{4}	2×10^{17}	0.97	0.93
12–14	1.9×10^{4}	2×10^{17}	0.95	0.87

transition probabilities. Agreement between temperatures determined by different line pairs is good. Temperatures determined from ion lines tend to be slightly higher than those determined from neutral lines, indicating that the ion radiation is emitted from the hotter center of the channel while the neutral radiction is emitted from the cooler outer regions. Note that the time resolution is 2 μsec so that if the temperature varies rapidly (as it does during the initial 4 μsec), some average temperature is determined.

Electron densities were estimated by comparing the Stark widths of $H\alpha$ at 6563 Å and of $OI(4)$ 8446 Å with theory.[3b] The instrument function as determined from the widths of intrinsically narrow lines was about 10 Å. Measured linewidths before correction for the instrument function varied between 17 and 33 Å. Thus, errors as large as a factor of two may be present in the electron density determination given in Table I.

From a knowledge of temperature and electron density and with the assumption of LTE, the remaining physical properties of the spark channel may be calculated.[4,5] Some of these data are given in the last two columns of Table I. The picture obtained is that of an expanding spark channel whose temperature and pressure decrease monotonically with time. Due to the errors present the pressure values may be in error by a factor as large as two. The temperature and electron density increase at spark initiation is not resolved with 2-μsec time resolution.

Experiments were also performed on a spark of 2.5-m length. The temperature and electron density for the 2.5-m spark were, within the experimental error, identical to those values given in Table I for the 5-m spark.

The research reported in this paper was supported in part by the Geophysics Branch of the Office of Naval Research.

* Now at the Westinghouse Research Laboratories, Pittsburgh, Pa.

[1] H. Souvenier, in *Proceedings of the 6th International Congress on High-Speed Photography* (Tjeenk Willink and Zoon, Haarlem, 1963), pp. 388–392.

[2] D. H. Sampson, Astrophys. J. 144, 96 (1966).

[3] H. R. Griem, *Plasma Spectroscopy* (McGraw-Hill Book Co., New York, 1964), (a) pp. 130, 145–149; (b) pp. 447, 448.

[4] F. R. Gilmore (private communication).

[5] B. H. Armstrong and M. Scheibe, Lockheed Missiles and Space Co., June 1964, available as AD-602866 from OTS, Dept. of Commerce, Washington 25, D.C.

APPENDIX II

"Acoustic Output of a Long Spark"

by Dawson, Richards, Krider, and Uman

JOURNAL OF GEOPHYSICAL RESEARCH VOL. 73, NO. 2 JANUARY 15, 1968

Acoustic Output of a Long Spark

G. A. DAWSON, C. N. RICHARDS, AND E. P. KRIDER

Institute of Atmospheric Physics, The University of Arizona
Tucson, Arizona 85721

M. A. UMAN

Westinghouse Research Laboratories, Pittsburgh, Pennsylvania 15230

In a recent paper [*Few et al.*, 1967] measurements of the average power spectrum of thunder were reported. The results indicated a very broad maximum at about 200 Hz. A short theoretical analysis was also given that set a lower limit on the expected dominant frequency of about 57 Hz. In the analysis, the dominant frequency was shown to be inversely proportional to the square root of the energy per unit length dissipated in the discharge channel.

Measurements have now been made on the acoustic output of the spark from the Westinghouse 6.4 Mv impulse generator at Trafford. For these experiments, the applied generator potential was 4.8 Mv, with a 1.5 μsec rise time, and the rod-plane gap length was set at 4 meters. The acoustic detector was a miniature piezo-electric pressure transducer fitted into a small megaphone to improve coupling.

At a distance of 17 meters from the spark, the dominant frequency (as determined by the separation between pressure extrema) lay in the range 1350 to 1650 Hz, with a most frequent occurrence of approximately 1550 Hz. The signals were characterized by an initial large amplitude wave, the first excursion of which corresponded to a compression, followed by a long-duration, small amplitude component of similar frequency, as shown in Figure 1. In this oscillogram, the vertical and horizontal scales are 200 mv and 1 msec per major division respectively; more details of the long duration signal were obtained with increased gain. The beginning of the signal has been lost by the choice of triggering level which gave stability in the R F fields of the spark. All signals were very similar to that of Figure 1, with the exception of one signal that showed two quite separate large amplitude waves. It is assumed that this signal was produced by a channel with a pronounced fork.

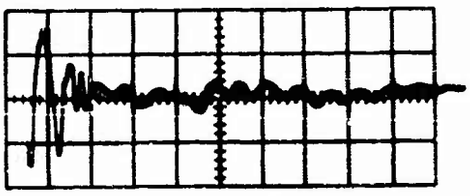

Fig. 1. Amplified output from pressure transducer. Sweep speed 1 msec per major division.

The energy per unit length dissipated in the channel has been determined by two independent calculations from data supplied by A. M. Sletten of Westinghouse. The first was from the voltage and current traces of the spark itself, though since both these parameters change rapidly at breakdown there is necessarily some uncertainty in the calculation. The value determined by this method was 5×10^6 joules/m ±25%. The second calculation was made by subtracting from the stored energy of the generator 9×10^6 joules, the I^2R energy dissipated in the damping resistors of the circuit as the generator discharged, 7.2×10^6 joules. The energy per unit length in the spark calculated by this method was thus 4.5×10^6 joules/m. The value that will be used for the subsequent calculation is 5×10^6 joules/m.

Inserting this energy into the expression of Few et al. one obtains a lower limit of 1040 Hz for the dominant frequency to be expected from the spark, value that is two-thirds of the observed values.

Three points are worthy of note. First, since variations in the location, tortuosity, and energy distribution of the discharge channel, and attenuation and reflection of the sound are to a

large degree absent in the present investigation, the spark more nearly approaches the theoretical model of Few et al. Second, for the same reasons, a broad acoustic spectrum is not obtained, but rather a very narrow range of frequencies. Third, since both the dominant frequency and the energy per unit length are defined with fair accuracy, more precise checks on the theory can be made. When this is done, agreement between experiment and theory is quite good.

Why, then, were the results of Few et al. not in better agreement with theory? This was probably because they were concerned with a minimum dominant frequency and hence assumed a maximum reasonable energy input. The one that was used, 10^{10} joules, is the value frequency quoted for the energy of a complete flash rather than an individual stroke. All the strokes in a flash can be expected to contribute to the thunder spectrum, but in different ways. The first stroke usually takes a large fraction of the flash energy and therefore should provide the minimum dominant frequency. Subsequent strokes have less energy and often take place down the hot, decaying channel of a previous stroke, where the speed of sound is high. Individually, these strokes should therefore produce the higher frequency components observed. Collectively, they should produce some low frequencies by modulation at the stroke repetition rate. It is the energy that is dissipated in the first stroke of a flash, or a single stroke flash, however, that is required for comparison with the theory of Few et al. for the minimum dominant frequency.

In a paper to be submitted [*Krider et al.*, 1968], a report is given of comparative measurements on the radiant energy emitted in the wavelength range 0.4 to 1.1 μ by lightning and the long spark. These indicate that the total energy per unit length dissipated in a single lightning stroke should be less than that assumed by Few et al. by a factor of about 7, i.e., 2.3×10^{9} joules/m. The use of this energy value for lightning leads to agreement with experiment that is as good as that for the spark. The analysis of Few et al. yields 151 Hz, and the direct scaling down of the most often observed frequency from the spark (1550 Hz) gives 230 Hz, in excellent agreement with the thunder data.

It seems clear from the preceding discussion that the analysis of Few et al. gives, as it should, too low a value for the frequency, since it assumes that all the energy of a stroke is used in forming the shock wave. The following simple empirical relationship accurately fits the available data:

$$f = c \cdot P^{\frac{1}{2}}/E^{\frac{1}{2}}$$

where f is the dominant frequency (Hz), c the speed of sound (m/sec), P the atmospheric pressure (newtons/m^2), and E the energy input per unit length (joules/m).

Acknowledgments. We should like to acknowledge the cooperation and assistance of Dr. A. M. Sletten.

This work was supported in part by the Geophysics Branch of the Office of Naval Research, by Westinghouse Research Laboratories, and by the Federal Aviation Agency.

References

Few, A. A., A. J. Dessler, D. J. Latham, and M. Brook, A dominant 200 hz peak in the acoustic spectrum of thunder, *J. Geophys. Res.*, 72(24), 1967.

Krider, E. P., G. A. Dawson, and M. A. Uman, The energy dissipated in a single stroke lightning flash, *J. Geophys. Res.* (to be submitted), 1968.

(Received September 5, 1967.)

APPENDIX III

"Peak Power and Energy Dissipation in a Single-stroke Lightning Flash"

by Krider, Dawson, and Uman

JOURNAL OF GEOPHYSICAL RESEARCH Vol. 73, No. 10, May 15, 1968

Peak Power and Energy Dissipation in a Single-Stroke Lightning Flash

E. P. KRIDER[1] AND G. A. DAWSON

Institute of Atmospheric Physics, University of Arizona
Tucson, Arizona 85721

M. A. USMAN

Westinghouse Research Laboratories, Pittsburgh, Pennsylvania 15235

INTRODUCTION

A recent study comparing the acoustic output of a long air spark and lightning [*Dawson et al.*, 1968] required a reliable value for the average energy dissipated per unit length in a single lightning stroke. Previous estimates of this energy have depended on a knowledge of the average quantity of charge transferred per stroke and an educated guess at the potential difference between cloud and ground [*Malan*, 1963]. In the present study, the peak radiant power and the total radiant energy emitted within a given spectral region by a single-stroke lightning flash are compared with those given off by a long spark whose electrical power and energy inputs are known with fair accuracy.

EXPERIMENT

The measurements are similar to the measurements described by *Krider* [1966]: A calibrated silicon photodiode (E. G. & G. Model 561 detector head) was used to record the broad-band spectrally integrated light intensity radiated by the source. Briefly the characteristics of this detector are as follows: the sensitive area is 0.0728 cm^2; the spectral response covers from 4000 to 11,100 A and is essentially flat from about 5000 to 10,000 A as shown by *Krider* [1966]; the absolute sensitivity at 8000 A, as calibrated by the manufacturer, is 7.7 Mv/mw, using a 50 Ω load resistor; the output current is linear over the range of light levels studied. The output voltage pulse from the detector, when viewing the complete channel of a typical single-stroke cloud-to-ground lightning flash, is reproduced in Figure 1. (A photograph of this stroke is given in *Krider* [1966].)

With the same detector similar light measurements have been performed on a 4-meter air spark produced by the Westinghouse 6.4-Mv impulse generator at Trafford, Pennsylvania. Figure 2 shows the average photoelectric voltage pulse obtained from about thirty observations of a negative point-to-plane discharge with the generator operating voltage at 4.35 Mv. It is immediately obvious that the lightning and spark pulses differ in two important respects: rise time and over-all time scale. Apart from other factors, the rise time depends on the time necessary for the bright return wave to travel up the length of the channel. For a spark this travel time is negligible, but for lightning it causes the slow rise time seen in Figure 1 [*Krider*, 1966]. The over-all time scales are inherent characteristics of the two types of discharge.

During the spark light-intensity measurements, spark currents and voltages were recorded as functions of time by A. M. Sletten of the Westinghouse Research Laboratories. A calculation of the peak electrical power and the total energy input to the spark can be made from these records.

If some simplifying assumptions are made, comparison of the curves of Figures 1 and 2 permits calculation of the peak power and energy dissipation in the lightning stroke as follows. The signal voltages give the radiant power reaching the detector, which in turn can be related to the radiant power output of the sources from purely geometrical considerations. The radiant power versus time curves can then be integrated to obtain the total radiant energy emitted in the given bandwidth. These values for the spark are then compared with the meas-

[1] NASA Pre-Doctoral Trainee, Department of Physics, University of Arizona, Tucson.

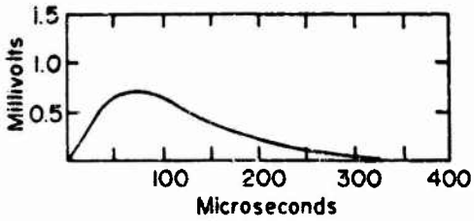

Fig. 1. The photoelectric voltage pulse corresponding to a single-stroke lightning flash at a distance of 8.2 km.

ured electrical power and energy input, and radiative efficiencies are calculated. These values are assumed to be the same for lightning (see discussion later), and hence the power and energy dissipation in the stroke can be found. The calculations will be performed first for the peak power of the lightning stroke and then for the total energy. The simplifying assumptions inherent in the calculation are discussed at the end of the paper.

Geometrical Factors

It is first necessary to determine accurately the distance dependence of the radiant flux from the sources. In the previous paper this distance dependence was assumed to be that of an infinitely long cylindrical emitter, i.e. $1/R$. However, it has since been demonstrated experimentally, using the long spark, that, with geometries very similar to those of the lightning study, the distance dependence of the radiant flux is in fact $1/R^2$ to within about 15%. This finding causes a revision in the value quoted by *Krider* [1966] for the peak radiant power output of lightning (see below). For the remainder of the discussion, a $1/R^2$ geometrical distance dependence of the radiant flux will be assumed for both lightning and the spark.

The total radiant power emitted within the detector bandwidth is given by

$$P = (V/K)(4\pi R^2/A) \qquad (1)$$

where V is the detector output voltage, K is the pulse calibration factor, R is the distance from the source to the detector, and A is the sensitive area of the detector.

For the lightning stroke, the distance R was previously estimated from the sight-sound time delay. For this note R has been found more accurately through the use of U. S. Weather Bureau cloud base height records at the time and location of the observed stroke. If we assume that the cloud base height determined the length of the stroke that was visible, we can calculate the stroke distance from the size of the photographic image and knowledge of the camera focal length. This method assumes, of course, the stroke was nearly vertical and did not slant toward or away from the camera. Since the distance is obtained in terms of the stroke length, it should be noted that the quantities sought, the power and, on integration, the energy *per unit length* of the stroke depend only linearly on stroke distance.

Results

Peak power. For the lightning stroke previously reported, the cloud base height was 1.8 km, and the distance calculated from the photographic image size was 8.2 km. At this distance, equation 1 and the signal maximum in Figure 1 yield a value for the peak power radiated from the lightning stroke of 1.1×10^{10} watts or, dividing by the stroke length, an average peak radiant power per unit length of 6.2×10^{8} w/m. These values replace and correct the peak radiant powers of *Krider* [1966] when a $1/R$ distance dependence was assumed.

The corresponding measurements for the spark were made from a distance of 23 meters, and they give, from Figure 2, a peak radiant power within the detector bandwidth of 4.0×10^{7} watts or an average of 1.0×10^{6} w/m, a value quite close to that for lightning.

The peak electrical power dissipated in the spark was obtained most accurately from direct traces of current recorded as a function of voltage. At the time of peak power, the current was

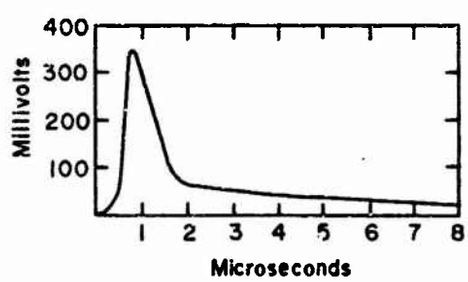

Fig. 2. The average photoelectric voltage pulse corresponding to a 4-meter air spark at a distance of 23 meters.

about 5×10^4 amp and the voltage about 10^6 volts, yielding a peak electrical power input of about 5×10^9 watts or 1.9×10^9 w/m.

Comparison of these two peak powers, radiant and electrical, yields for the spark an over-all radiative efficiency within the detector bandwidth of only 0.8%. If the same radiative efficiency is assumed for lightning at the instant of peak radiant power from the entire channel (see below), the peak electrical power dissipated in the lightning stroke, calculated from the observed radiant power, is 1.4×10^{12} watts. Dividing the above value by the stroke length gives an average peak electrical power dissipation per unit length of 7.8×10^8 w/m.

It should be emphasized that for lightning the above values for peak power, radiant and electrical, are given at the instant of peak light emission from the entire channel. Dividing a value at this instant by the stroke length probably underestimates the peak power that *actually* occurs in a given short length of channel because of the appreciable return stroke propagation time. That is, the power dissipation in a channel segment near the ground may rise quickly to peak and then decrease before the entire channel has developed. Therefore, the above results for peak radiant and electrical power per unit length represent, in the case of lightning, *minimum* values for a short channel length.

Energy. Turning now to the total radiant energy emitted by the two sources, the areas under the radiant power versus time curves can be shown to indicate a total radiant energy within the detector bandwidth of about 60 joules for the spark and 1.6×10^6 joules for the lightning stroke. Dividing the above values by the corresponding channel lengths gives average radiant energies per unit length of 15 and 870 J/m, respectively.

The electrical energy per unit length dissipated in the long spark, under the conditions of this experiment, has been calculated by two independent methods as described previously [*Dawson et al.*, 1968]. The first method consists of integrating over time the product of the current and voltage values obtained from the traces taken during the experiment; the second involves subtracting from the stored energy of the impulse generator operating on 29 stages, 8.1×10^4 joules, the energy dissipated in the series damping resistors 6.5×10^4 joules. Both methods give a spark energy input in this experiment of about 4.0×10^5 J/m ± 20%.

Again, comparing the radiant and electrical energy values, one obtains an average radiative efficiency for the spark of about 0.38%, less than the value at the instant of peak power probably because of a lower average temperature. If it is assumed that the same radiative efficiency applies to lightning, the total average energy dissipated per unit length in the stroke is calculated to be 2.3×10^6 J/m. If the *total* stroke length was 3 km, this energy per unit length is equivalent to an over-all dissipation of 6.9×10^6 joules. *Brook et al.* [1962] found that single-stroke flashes typically transfer 4.6 coulombs of charge to ground. The above energy value corresponds to a discharge to ground of 4.6 coulombs from an initial potential difference of about 3×10^6 volts, a value consistent with the 10^6–10^8 volts estimated by *Malan* [1963]. It has previously been shown [*Dawson et al.*, 1968] that the use of the energy value obtained above for a lightning stroke, 2.3×10^6 J/m, also leads to excellent agreement with the thunder data of *Few et al.* [1967].

The above estimate of energy dissipation in lightning is, as before, based on the assumption of equal radiative efficiencies of the two sources, in this case, time-averaged.

Further Calculations

Other interesting rough calculations can be made utilizing the above data. For example, the voltage applied to the spark gap at the instant of peak input power was about 10^6 volts and the current was about 5×10^4 amps. Assuming a uniformly conducting channel between the two electrodes, we find that an average electric field of about 2.5×10^6 v/cm was present during peak power dissipation. If the conductivity of the spark channel under these conditions is about 180 mho/cm [*Uman*, 1964], the above electric field and current values give an average current density of 4.5×10^6 amp/cm^2 and a channel radius of 0.6 cm at this instant.

A similar estimate can be made for lightning by assuming a current on the order of 10^4 amp [Malan, 1963] is present at the time of peak power dissipation. In this case, the calculated

peak power gives an average electric field of 7.8×10^3 v/cm, a value similar to that of the spark. Assuming a conductivity of 180 mho/cm, we obtain a lightning current density of 1.4×10^6 amp/cm^2 and a channel radius of 1.5 mm at peak power dissipation. For both the spark and lightning, the instant of peak power probably occurs before appreciable channel expansion has taken place, after which the channel diameters could be on the order of centimeters [*Uman*, 1966].

Assumptions

General comparison of the two sources. Since the detector used has a flat spectral sensitivity over most of its broad bandwidth, the signal voltages obtained should be substantially independent of the input spectral distributions and the variations of these distributions with time. Therefore, we assume the radiant power detected at a given time is proportional to the total power output of both sources within the detector bandwidth and is given by the observed voltage output of the detector divided by the pulse calibration factor.

Equal radiative efficiency at peak power. The above comparison of peak power dissipation has been based on the assumption of equal radiative efficiencies for lightning and the spark at the instant of peak light emission. This assumption is based on the following experimental evidence. Time-resolved spectroscopic studies of the spark [*Orville et al.*, 1967] and lightning [*Orville*, 1966] indicate that they are spectroscopically very similar, particularly at about the instant of peak radiant emission. Similar peak temperatures and electron densities are calculated from spectra obtained with a time-resolution of 2 μsec for the spark and 5 μsec for lightning. Also, there are strong indications that the lightning and spark channels are optically thin for most of the time of radiant emission [*Uman and Orville*, 1965; *Orville et al.*, 1967]. It is thus reasonable to assume that at peak temperature lightning and the spark have very similar radiative efficiencies. As spectroscopic sources, the major difference between them would appear to be one of size and time scale.

Equal average radiative efficiencies. The estimate of energy dissipation in lightning was based on the assumption of equal average radiative efficiencies within detector bandwidth. This assumption is based on evidence similar to that described in the preceding paragraph. Spectroscopic studies of the spark and lightning indicate that similar peak temperatures are attained and that the channels are probably optically thin for most of the time of radiant emission. In both cases the temperature appears to rise quickly to a peak value and then decrease slowly [*Orville*, 1966; *Orville et al.*, 1967]. Figures 1 and 2 indicate the major contributions to the radiated energy values come from the early time regions. Thus, since the early peak temperatures are comparable and slowly decreasing, it is quite reasonable to assume equal average radiative efficiencies for these times. It should be emphasized that this assumption is only valid for the calculation of energies associated with the early spark-like lightning channel behavior. Clearly long-duration low-power events, such as channel continuing luminosity, could not be analyzed in this way. Single-stroke lightning flashes typically lack, as does the spark, the long continuing currents sometimes found in multiple-stroke flashes [*Kitagawa et al.*, 1962].

Summary

The radiant power and energy emitted within a given spectral region from a single-stroke lightning flash have been compared with those of a long spark whose electrical power and energy inputs are known with fair accuracy. With some simplifying assumptions, the above comparison permits a calculation of the peak power and energy dissipation in the lightning channel. We obtain an average power input per unit length of 7.8×10^6 w/m, at the instant of peak radiant emission from the entire channel, and an average energy per unit length of 2.3×10^6 J/m. The peak power value represents the most reliable determination of that parameter for lightning to date, and the energy value is in good agreement with other estimates.

Acknowledgments. We are particularly grateful to Dr. A. M. Sletten of the Westinghouse Research Laboratories for operation of the spark and the records of current and voltage traces.

This research was supported in part by the Geophysics Branch of the Office of Naval Research and the Federal Aviation Agency.

References

Brook, M., N. Kitagawa, and E. J. Workman. Quantitative study of strokes and continuing

currents in lightning discharges to ground, *J. Geophys. Res.*, *67*(2), 649, 1962.

Dawson, G. A., C. N. Richards, E. P. Krider, and M. A. Uman, Acoustic output of a long spark, *J. Geophys. Res.*, *73*(2), 815, 1968.

Few, A. A., A. J. Dessler, D. J. Latham, and M. Brook, A dominant 200-hertz peak in the acoustic spectrum of thunder, *J. Geophys. Res.*, *72*(12), 6149, 1967.

Kitagawa, N., M. Brook, and E. J. Workman, Continuing currents in cloud-to-ground lightning discharges, *J. Geophys. Res.*, *67*(2), 637, 1962.

Krider, E. Philip, Some photoelectric observations of lightning, *J. Geophys. Res.*, *71*(12), 3095, 1966.

Malan, D. J., *Physics of Lightning*, English University Press, London, 1963.

Orville, R. E., A spectral study of lightning strokes, Ph.D. dissertation, University of Arizona, Tucson, 1966.

Orville, R. E., M. A. Uman, and A. M. Skeen, Temperature and electron density in long air sparks, *J. Appl. Phys.*, *38*(2), 895, 1967.

Uman, Martin A., The conductivity of lightning, *J. Atmospheric Terrest. Phys.*, *26*, 1215, 1964.

Uman, Martin A., Quantitative lightning spectroscopy, *IEEE Spectrum*, *3*, 102, 1966.

Uman, Martin A., and Richard E. Orville, The opacity of lightning, *J. Geophys. Res.*, *70*(22), 5491, 1965.

(Received October 3, 1967)

APPENDIX IV

"Four-meter Sparks in Air"

by Umam, Orville, Sletten, and Krider

Reprinted from JOURNAL OF APPLIED PHYSICS, Vol. 39, No. 11, 5162–5168, October 1968
Copyright 1968 by the American Institute of Physics
Printed in U. S. A.

A69-12406

Four-Meter Sparks in Air

M. A. UMAN, R. E. ORVILLE,* AND A. M. SLETTEN
Westinghouse Research Laboratories, Pittsburgh, Pennsylvania 15235
AND
E. P. KRIDER†
Institute of Atmospheric Physics, The University of Arizona, Tucson, Arizona 85721
(Received 4 June 1968)

Sparks of 4-m length in atmospheric air were studied, using high-speed image-converter photography, current and voltage measurements, absolute measurements of radiated light intensity, and high-speed image-converter spectroscopy. Correlated results of the various measurements are presented. The energy balance of the spark is discussed.

1. INTRODUCTION

Recently, Orville *et al.*[1] have measured the temperature, pressure, electron density, and percentage ionization in 2.5- and 5.0-m air sparks using a spectroscopic system with 2-μsec time-resolution. The sparks were generated by the Westinghouse 6.4×10^6 V Marx-circuit impulse generator at Trafford, Pa. Using the same facility, Dawson *et al.*[2] studied the acoustic output of a 4-m spark and compared that output with the acoustic output of natural lightning; and Krider *et al.*[3] measured the radiant power and the radiant energy in the 4000 to 11 000 Å wavelength range from a 4-m spark and compared those measurements with similar measurements made on natural lightning.

In the present paper we report on an experimental study of 4-m air sparks generated at Trafford. The diagnostic techniques used in the study included high-speed image-converter photography, current and voltage measurements, absolute measurements of radiated light intensity, and high-speed image-converter spectroscopy. The spark-gap geometry and electrical circuits for producing the breakdown voltage and for measuring the gap voltage and current are shown in Fig. 1. The voltage applied across the rod-plane gap would have been a standard 1.5×40 wave (1.5 μsec to peak and 40 μsec to half-value) with a crest value of approximately 3.3×10^6 V in the absence of gap breakdown and corona load. The charging voltage and thereby the stored energy were kept constant for both positive and negative rod polarity. The critical breakdown voltages for a 4-m rod-plane gap are given by Udo[4] as 1.9×10^6 V for positive rod polarity and 2.8×10^6 V for negative rod polarity. Consequently, the applied overvoltages differed considerably for the two polarities. A still photograph of a 4-m air spark is shown in Fig. 2.

2. IMAGE-CONVERTER PHOTOGRAPHY

A TRW image-converter camera was operated in the framing and streak modes at a distance of 19 m from the 4-m spark in order to photograph the luminous breakdown processes. Figures 3 and 4 show image-converter photographs of the discharge taken at 0.5 μsec intervals with 0.02 μsec exposure time.

For the case of the negative rod (Fig. 3) no luminous processes are recorded by the camera until about 3 or 4 μsec after the application of the voltage. At that time a *secondary streamer* (the terminology advocated by

* Present affiliation: State University of New York at Albany, Albany, New York 12203.
† NASA Pre-Doctoral Trainee, Department of Physics, The University of Arizona, Tucson, Arizona 85721.
[1] R. E. Orville, M. A. Uman, and A. M. Sletten, J. Appl. Phys. Res. 73, 3335 (1968).
[2] G. A. Dawson, C. N. Richards, E. P. Krider, and M. A. Uman, J. Geophys. Res. 73, 815 (1968).
[3] E. P. Krider, G. A. Dawson, and M. A. Uman, J. Geophys. Res. 73, 3335 (1968).
[4] T. Udo, IEEE Trans., PAS83, 471 (1964).

Loeb[5]) or *leader* (in analogy to the lightning leader[6]) emerges from the rod and propagates toward the plane at about 2×10^8 m/sec. Before the downward-moving leader has crossed half of the gap, one or more upward-moving leaders is initiated from the plane. The downward-moving leader and one of the upward moving leaders meet, usually just below midgap, and a bright luminosity is propagated from the junction both upward and downward toward the two electrodes at about 3×10^7 m/sec. The propagation velocity of the bright luminosity or *return stroke* (in analogy to lightning[6]) was determined by comparing [illegible] and TRW streak photographs. In Fig. 3 at 5 μsec the return stroke has crossed the gap, leaving the channel highly illuminated. The junction of the downward- and upward-moving leaders is frequently characterized by a region of multiple channels.

For the case that the rod is positive (Fig. 4), a leader appears from the rod within about 1 or 2 μsec from the application of the voltage and propagates downward initially at about 1×10^8 m/sec, increasing to about 2×10^8 m/sec near the plane. In contrast to the negative-rod breakdown, the downward-moving leader bridges essentially the whole gap, except for the last few centimeters which may be covered by an upward-moving discharge. When the positive leader reaches the plane, streak photographs show that an upward-propagating return-stroke is launched from the plane toward the rod. The return-stroke luminosity is not as distinct from the preceding leader luminosity as in the case of the negative rod, but both return-stroke velocities appear to be about the same. Note that the nine individual frames shown in Fig. 4 are not from the same discharge. Since the framing unit used in the TRW camera allowed only three frames per discharge, Fig. 4 has necessarily been constructed from three separate discharges. Further, the gain setting on each series of frames is different, the gain being increased for the earlier frames.

The image-converter photographs showed no *primary streamers* (Loeb's terminology[5]) or *impulse corona* (the notation used in most of the earlier literature[7,8]) prior to the leader's appearance as had been observed by Saxe and Meek,[7] Park and Cones,[8] Kritzinger,[9] and others for gaps about 1 m or smaller. The image tube threshold was probably not low enough to record the impulse corona. Some evidence for the existence of impulse corona is presented in Secs. 3 and 4.

[5] L. B. Loeb, Science 148, 1417 (1965).
[6] M. A. Uman, *Lightning* (McGraw-Hill Book Co., New York, 1969).
[7] R. F. Saxe and J. M. Meek, Proc. IEE (London) 102, 221 (1955).
[8] J. H. Park and H. N. Cones, J. Res. Natl. Bur. Std. 56, 201 (1956).
[9] J. J. Kritzinger, Ph.D. thesis, University of Witwatersrand, Johannesburg, 1962; Proc. Intern. Conf. Ionization Phenomena in Gases, 6th, Paris, Vol. II, (1963), pp. 295–299; Nature 197, 1165 (1966).

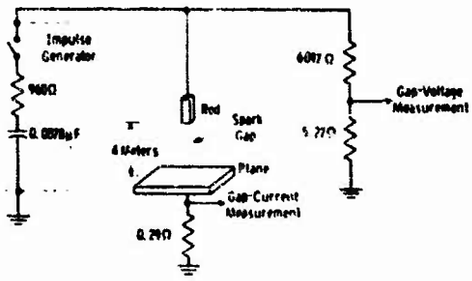

FIG. 1. Schematic diagram showing circuit for producing 4-m rod-plane sparks and circuits for measuring spark gap voltage and current.

The time scales shown in Figs. 3 and 4 are for particular discharges. For any individual discharge, the time necessary to generate a bright channel between rod and plane varied between about 4 and 6 μsec from the time of application of the voltage. The zero time value was chosen to be at the time of the initial pulse of rf radiation emitted by the spark gaps of the Marx circuit. The TRW camera was triggered on this pulse via an antenna.

3. ELECTRICAL MEASUREMENTS

Voltage and current oscillograms recorded on Tektronix No. 507 oscilloscopes, using the circuits shown in Fig. 1, are retraced in Fig. 5. The zero-time reference for the voltage and current curves of Fig. 5 may differ by as much as 0.5 μsec, so that accurate power measurements could not be obtained from these curves. However, direct traces of voltage as a function of current were recorded, from which power measurements could be more accurately derived. The current recorded in our experiments was that flowing through the shunt resistor underneath the plane. During the fast voltage changes there may be considerable difference between the measured current and the channel current flowing. Some of the small-scale structure apparent in the voltage and current curves may be due to signal reflections in the measuring system or to electromagnetic pickup. The structure shown, nevertheless, was always present. From about 7 to 30 μsec the electrical current through the gap decays approximately exponentially with the *RC* time constant of the impulse generator, about 7.5 μsec. At about 30 μsec, the gap current approaches zero, and then reverses polarity. The reverse current reaches a magnitude of about 200 A, and finally goes to zero between 60 and 80 μsec. The mechanism of current reversal is not understood.

As can be seen from Fig. 5(a), for the case of the negative rod a current of the order of 100 A appears to flow in the gap, even before the time that the image-converter camera records luminous leaders extending from the rod and the plane. The rapid current-rise to peak occurs in 1 μsec or less, and is apparently associated with the final-leaders stages and the return

FIG. 2. Still photograph of a 4-m air spark between a positive rod and a negative plane.

stroke. Prior to the rapid current increase, the voltage across the gap is roughly constant at about 3×10^6 volts for about 2 μsec. The small current pulses occurring between 1 and 2 μsec are probably similar to the pulses observed by Saxe and Meek,[7] Park and Cones,[8] and others, and associated by them with impulse corona.

For the case of the positive rod, Fig. 5(b), an appreciable current flows in the gap after about 2 μsec, consistent with the appearance of a relatively bright leader on the image-converter photographs of Fig. 4. The current rises to peak over a time of 3 or 4 μsec, during which time the gap voltage slowly collapses. The small current pulse occurring between 1 and 2 μsec is probably due to impulse corona.

The peak power input to the discharge channel from the impulse generator occurs when the voltage is collapsing and the current is rising to peak. From the measured V–I characteristics, the peak power was found to be about 6×10^9 W for the negative rod and about 5×10^9 W for the positive rod. Errors of ±20% are present in these values, due to the inaccuracy of the V–I characteristics and due to the uncertainty in the actual value of current in the gap.

The total energy input to the gap has been calculated by two independent methods. The first is by integrating the power curves over time; the second is by subtracting from the initial stored energy of the impulse generator the energy dissipated as I^2R across the 960 Ω series output resistors shown in Fig. 1. The total energy input to the gap so determined for both the positive- and the negative-rod cases was $2\pm1\times10^4$ J. It was not possible within the accuracy of the measurements to determine which discharge polarity absorbed more input energy.

If the spark is assumed to be straight and vertical, rough values for the input energy and peak power per unit length can be derived. For the positive rod these rough values are 1.3×10^9 W/m and 5×10^3 J/m; for the negative rod, 1.5×10^9 W/m and 5×10^3 J/m. In addition to the uncertainties in these values discussed above, the actual values per unit length should be lower than those given, because the spark channel is tortuous and the sparks are often not vertical.

4. LIGHT OUTPUT

Measurements were made with three calibrated photodiodes, E.G. and G. types SD-100, SGD-100, and SGD-444, of the spectrally integrated (4000–11 000 Å) light intensity emitted from the spark. Measurements were obtained of the absolute light output, both from the whole discharge channel and from a 6-cm section of the discharge channel. In Fig. 6 is shown the relative light output from a 6-cm section of the discharge from a negative rod, obtained using the SGD-444 diode. The isolated section was located 3.1 m above the plane. In Fig. 7 is shown the relative light output from a 6-cm section of the positive-rod discharge obtained using the same diode. The section observed was 2.3 m above the plane.

In Figs. 6 and 7, certain points on the curves have been labeled A, B,···H, although in some cases these

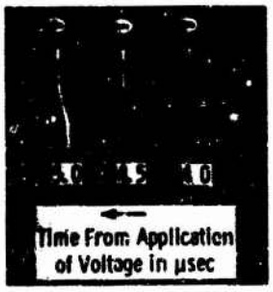

FIG. 3. Image converter photograph of the electrical breakdown between a negative rod and a positive plane separated by 4 m.

FIG. 4. Image converter photographs of the electrical breakdown between a positive rod and a negative plane separated by 4 m.

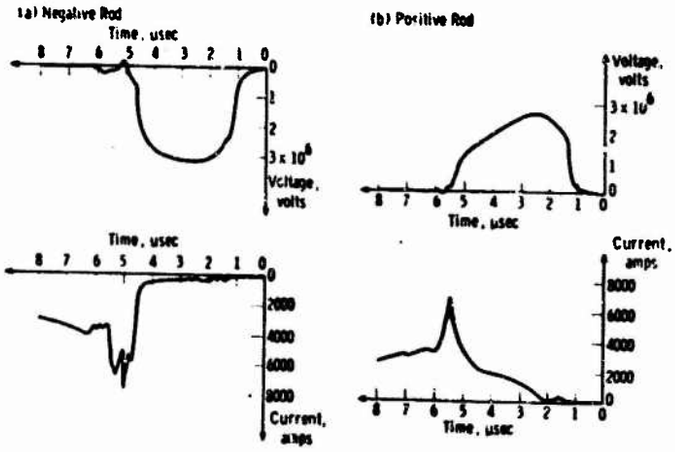

FIG. 5. Voltage across 4-m rod-plane spark gap vs time, and current through gap vs time for (a) negative rod and (b) positive rod. Zero-time reference for voltage and current curves may differ by as much as 0.5 μsec. Data given are representative. For individual sparks, time to peak current and time to voltage collapse varied and were typically between 4 and 6 μsec.

points are not well-defined. We interpret the various labeled sections of the curves as follows: Region AB represents light arriving at the detector before the leader tip crosses the gap section under observation. This light is due either to impulse corona or to scattering or reflection of the light emitted by the leader outside the gap section under observation. In region BC, a sudden increase in brightness is due to passage of the leader tip across the section of channel under observation. Region CD represents an increase in brightness of the leaders channel with time. Region DE represents a rapid increase in light due to the passage of the return stroke and formation of the high-current channel across the spark gap. After peak light intensity is reached, the light decay is relatively rapid in region EF, slow and roughly exponential in region FG, and even slower and roughly exponential in region GH.

Figures 6 and 7 are similar, with the following notable exceptions: For the positive rod (Fig. 7), a longer preleader region (AB) is apparent than for the negative rod (Fig. 6), and for the positive rod the points D and F are not well defined. That the point D is not well defined for the positive rod indicates that there is not a marked difference in intensity between the final leader and initial return-stroke phases, as noted in Sec. 2. In general, the qualitative features of the light emission are what one would expect from an examination of the image converter photographs.

The techniques for deriving values of radiant power from photoelectric measurements are discussed by

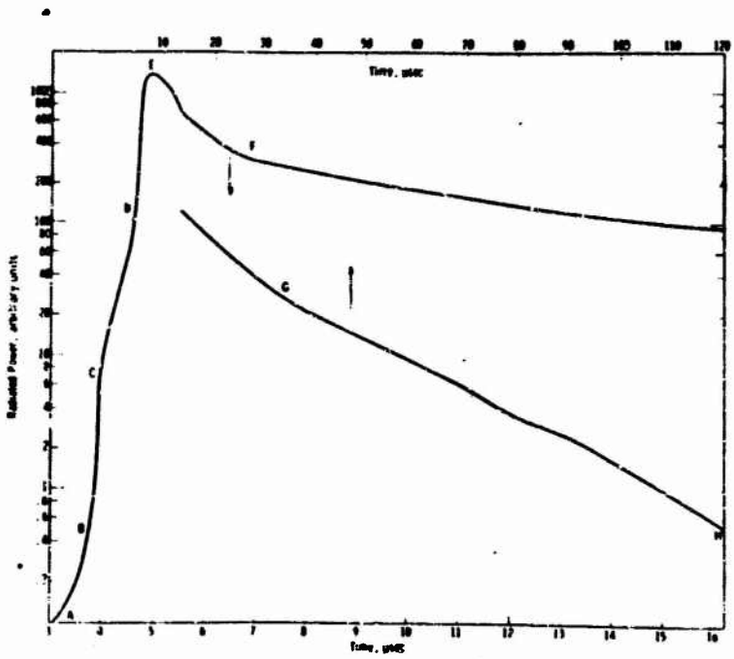

FIG. 6. Radiated power vs time from a 6-cm segment of a 4-m spark initiated from a negative rod. The observed segment was 3.1 m above the plane. Data represent average of many measurements. Peak values for individual sparks varied by ±20% from average. Time to peak for individual sparks varied and was typically between 4 and 6 μsec from application of voltage.

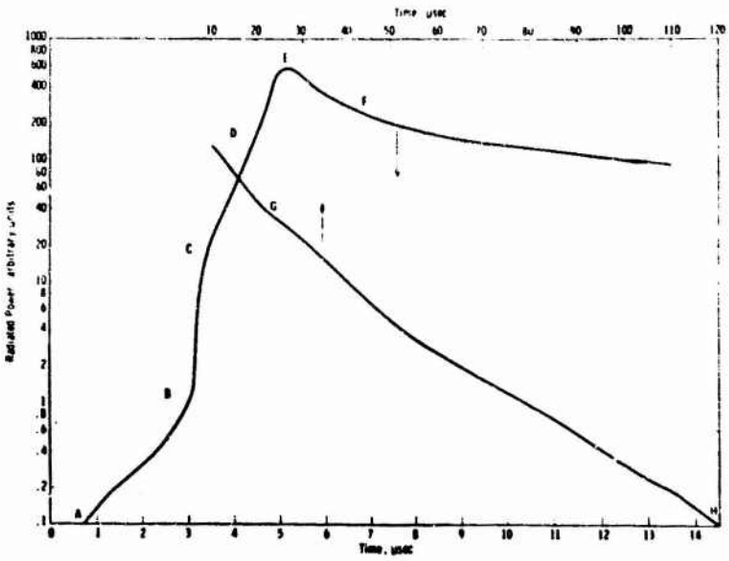

FIG. 7. Radiated power vs time from a 6 cm segment of a 4-m spark initiated from a positive rod. The observed segment was 2.3 m above the plane. Peak values for individual sparks varied by ±20% from average. Time to peak for individual sparks varied and was typically between 4 and 6 μsec from application of voltage.

Krider[10] and Krider *et al.*[3] The peak radiant power per unit length was found to be about 1×10^7 W/m for the negative rod and about 4×10^6 W/m for the positive rod. These values represent the average of many measurements of peak power. Values of radiant power obtained using each of the three calibrated diodes were in good agreement. Peak-power values for individual sparks varied by about ±20% from one discharge to another. In addition, the accuracy of the absolute measurements of power may be in error by about 25%, due to the inaccuracy of the calibration factors. The negative-rod discharge radiates about twice as much peak power as does the positive rod. As is apparent from an examination of Figs. 6 and 7, the light output from the negative rod has a faster risetime to peak and a faster decay time to half-value than does the light output from the positive rod. The total radiated light energy can be determined by integrating the power-vs-time curves. The radiant energy per unit length for the negative rod was found to be about 15 J/m, for the positive rod about 10 J/m.

As noted in Sec. 3, the discharge current goes to zero between 60 and 80 μsec. In Figs. 6 and 7, light output is presented to 120 μsec. Thus the latter times on Figs. 6 and 7 represents the decay of an air plasma in the absence of energy input to that plasma. With the SGD-444 photodiode, light was measurable to about 200 μsec, at which time the light intensity was down more than four orders of magnitude from the peak intensity.

5. SPECTRA

The TRW image-converter camera was used in the streak mode to view and record the output of a "home-made" spectrometer. A 6-cm section of discharge channel near the middle of the spark gap was isolated by a lens and slit system, and the light from that section served as input to the spectrometer. Typical streak spectra for the negative-rod discharge and for the positive-rod discharge are shown in Figs. 8 and 9, respectively. The time scales of the leader stage, stage of high luminous intensity, and the intensity decay for both positive and negative rod are in good agreement with the time scales determined photoelectrically.

Quantitative spectral measurements of long sparks were previously made on photographic film by Orville *et al.*[1] with the spectrometer coupled to a rotating film drum, the system having 2-μsec time resolution. Orville *et al.*[1] determined that the channel temperature during the first 2 μsec of bright luminosity, corresponding to 2 μsec around the peaks on Figs. 6 and 7, was about 34 000°K. (A short discussion of the meaning of the word *temperature* in a transient spark is given by Orville *et al.*) Since the light intensity changes markedly in a 2-μsec period including the peak intensity, it is clear that the temperature value determined represents at best some kind of average over the 2-μsec interval. On the other hand, temperatures determined for times several microseconds and more after peak light intensity should be relatively accurate, since for these times the luminosity does not vary rapidly. From 6 to 14 μsec after the peak luminosity, Orville *et al.* found spark temperatures which decayed from about 24 000°K to about 19 000°K. It should be pointed out that the data of Orville *et al.* are for 2.5-m and 5-m sparks. However, since the measured temperatures were, within experimental error, the same for these two lengths, it is reasonable to assume that the temperature measured is valid for the 4-m spark also.

[10] E. P. Krider, J. Geophys. Res. 71, 3095 (1966).

In order to estimate the temperature of the leader, the image-converter spectra of the leader process can be qualitatively compared with the image-converter spectra of the decaying spark channel, for which temperature is known. The leader temperature is thereby estimated to be of the order of 20 000°K. The leader is apparently a very hot arc channel whose primary radiating species is singly ionized nitrogen (NII). The transition from leader to return stroke as seen on the spectra is more pronounced in the case of the negative rod than in the case of the positive rod, although this distinction is not clearly evident in Figs. 8 and 9, because the two spectra reproduced were streaked at different rates. That the leader-to-return-stroke transition is more pronounced in the negative rod case has also been noted in Secs. 2 and 4. In both cases the spark temperature rapidly increases at the start of the return stroke phase, as is evident from the appearance at that time of spectral lines (OII, NII, and possibly NIII) of high excitation potential in the 4858 Å region.

6. THE ENERGY BALANCE

We consider now the energy balance for the spark. A significant fraction of the total energy input to the 4-m spark takes place in a time of the order of 1 μsec, while the gap voltage is collapsing and the spark current is rapidly rising to peak, probably during the final leader stages and the return-stroke stage. For the case of both positive and negative rods, the total energy input is of

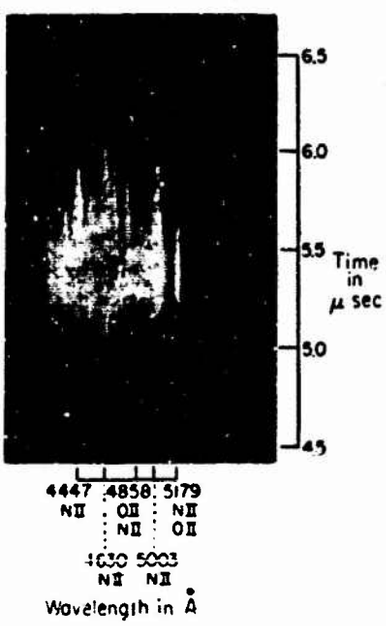

FIG. 8. A typical image converter streak spectrum of a 6-cm segment of a 4-m spark initiated from a negative rod. Segment viewed was near midgap. Times given are from application of voltage.

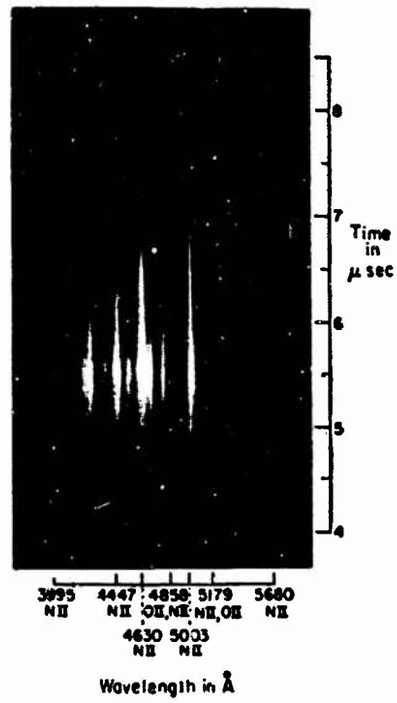

FIG. 9. A typical image-converter streak spectrum of a 6-cm segment of a 4-m spark initiated from a positive rod. Segment viewed was near midgap. Times given are from application of voltage.

the order of 5×10^3 J/m. The input energy heats the leader channel in a short time, compared to the time in which the channel can expand appreciably. Thus, the heated channel must be at a pressure exceeding ambient, and the channel will expand, creating a roughly cylindrical shock wave, which quickly relaxes to a sound wave.[2,11] The channel expands until its pressure is in equilibrium with the surrounding atmosphere. According to the data of Orville *et al.*[1], the time for the channel to reach atmospheric pressure is about 8 μsec from the first recorded light emission on film. During this 8-μsec interval, energy has been radiated from the channel, and energy has been transmitted from the channel into the shock wave. Thermal conduction and thermal convection are probably not significant as energy-loss mechanisms because of the short time involved. We conclude, then, that at about 8 μsec after the peak input power has been attained, the bulk of the input energy is divided between (1) energy of excitation, dissociation, ionization, and kinetic energy of the channel particles, (2) radiated energy, and (3) energy delivered to the shock wave. We derive now quantitative estimates of the energy stored, and of the energy radiated as light and sound.

[11] A. A. Few, A. J. Dessler, D. J. Latham, and M. Brook, J Geophys. Res. 72, 6149 (1967).

(1) According to the data of Burhorn and Wienecke,[12] the energy density of air at 30 000°K and 1 atm pressure is about 0.7 J/cm³. The total energy stored in the channel at this temperature and pressure is strongly dependent on the channel diameter. We have determined the spark-channel diameter by photographing the channel with a time integrating slitless spectrometer of high inverse spectral dispersion. Thus the width of the spectral lines, which from theory are intrinsically narrow, could be directly related to the channel diameter. A maximum diameter of 1.2 cm was observed from analysis of NII light, of 1.8 cm from analysis of NI light. That the channel is wider in the light of neutral atom than in the light of ions is due to two effects: (1) the channel widens as it cools, and (2) the NII radiation is predominantly from a hot channel core, while the NI radiation is from the cooler outer regions. The NII light from which the measurement was made was bright for about 5 μsec. If we assume a diameter of 1.8 cm, the stored energy per unit length of channel is 180 J/m, about 4% of the input energy. Since 30 000°K is an overestimation of the channel temperature 8 μsec after peak light output (Orville *et al.*[1] found 24 000°K), and 1.8 cm is probably an overestimation of the channel diameter, a value of 180 J/m for the stored energy can be considered an upper limit to the actual value.

(2) The energy radiated from the spark in the 4000 to 11 000 Å range is about 15 J/m for the negative-rod case and about 10 J/m for the positive-rod case. In both cases the radiated energy is a fraction of a per cent of the total input energy. It might be expected that the wavelength range 4000 to 11 000 Å would contain at least 10% of the total energy which escapes the channel as radiation, since little uv radiation can escape the channel because of the short optical depth for that radiation, and very little energy is radiated in the infrared at temperatures in the 20 000° to 30 000°K range. Thus the total radiated energy is probably a small fraction of the input energy. It is further interesting to note that the peak radiated power (4000 Å to 11 000 Å) is less than 1% of the peak input power.

(3) It would appear that a large fraction of the input energy goes into the shock wave. The experimental measurements of Dawson *et al.*[2] support this view. Dawson *et al.* measured the frequency of the acoustic wave emitted by the spark and, using theory relating sound wave frequency to the energy pumping the shock wave,[11] showed that a pumping energy of the order of 5×10^3 J/m yields a sound wave whose frequency is of the order of 10^3 Hz, the measured value. Thus, it would appear that the major fraction of the input energy to the spark is delivered to the shock wave.

[12] F. Burhorn and R. Wienecke, Z. Phys. Chem. 215, 269 (1960).

7. COMMENTS

The experiment described in this paper could be improved in a number of obvious ways. Most important would be a more accurate synchronizing of the zero-time reference for the TRW camera and various oscilloscope traces. With such a synchronization it would be possible to determine, for example, at what stage of the leader or return-stroke development the peak input power occurred, and how the time of the peak input power was related to the time of the peak output light. Second in importance is the design of equipment for measuring the current leaving the rod. With a knowledge of both the current out of the rod and the current under the plane, a better understanding of the current distribution could be obtained, and consequently better electrical power and energy data could be derived. Third, it should be possible to improve the absolute accuracy of the current, voltage, and light-output measurements, although it should be pointed out that the accurate measurement of high currents and voltages on a submicrosecond time scale is no simple task. Finally, the image-converter spectra should be calibrated so that quantitative data regarding such physical characteristics of the discharge channel as electron density and particle energies could be determined on a time scale of 0.1 μsec or faster.

In the experiment described in this paper, the impulse-generator-charging voltage, the energy stored in the impulse generator, and the circuit impedances have been kept constant. Undoubtedly, changes in these parameters will influence the phenomena recorded here.

ACKNOWLEDGMENTS

We wish to express our appreciation to A. J. Venturino for his assistance in performing these experiments. This research was supported in part by the Office of Naval Research and by the Federal Aviation Agency.

APPENDIX V

"A High-speed Time-resolved Spectroscopic Study of the Lightning Return Stroke, parts I, II, III"

by Orville

Reprinted from JOURNAL OF ATMOSPHERIC SCIENCES, Vol. 25, No. 5, September, 1968, pp. 827–838
American Meteorological Society
Printed in U. S. A.

A High-Speed Time-Resolved Spectroscopic Study of the Lightning Return Stroke: Part I. A Qualitative Analysis[1]

RICHARD E. ORVILLE[2,3]

Institute of Atmospheric Physics, Tuscon, Ariz.

(Manuscript received 15 December 1967)

ABSTRACT

The first time-resolved spectra of return strokes between the cloud and ground have been obtained. During the summers of 1965 and 1966 twenty-two spectra were obtained at the Institute of Atmospheric Physics, Tuscon, Ariz. The spectra were recorded with two high-speed streaking cameras converted to slitless spectrographs. The conversion was accomplished by mounting Bausch and Lomb replica transmission gratings in front of the cameras' objective lenses. The gratings are blazed for 5500Å and have 600 lines mm^{-1}. Inverse dispersions from 70–140Å mm^{-1} were used. Most of the data were obtained with a Beckman and Whitley high-speed camera. A 200-mm objective lens was used to focus the return stroke on a 0.5-mm horizontal slit. Thus, a 10-m section of the lightning channel was isolated for a discharge occurring at a distance of 4 km. Data have been obtained with a time resolution of 2–5 μsec. All spectra have been recorded on film calibrated for intensity and wavelength with a xenon source of known relative spectral emittance.

The following data have been obtained. Spectral emissions from 4000–6600Å have been recorded with 10Å wavelength resolution. All emissions have been attributed to neutral hydrogen or to neutral or singly ionized atoms of nitrogen and oxygen. No molecular or doubly ionized emissions have been identified in these spectra. The time for luminosity to rise from zero to its peak in a section of the channel is 10 μsec or less. Several faint lines due to neutral nitrogen and oxygen atoms persist for 150 μsec. The H-alpha line is present in these spectra. The recorded time sequence of spectral emissions from a section of the lightning channel is 1) line radiation from singly ionized atoms, 2) continuum, and 3) line radiation from neutral atoms. A flash has been recorded composed of at least 5 strokes. Two types of strokes are observed in this flash. The first type is characterized by intense short-lived emissions from singly ionized nitrogen atoms (NII) and a long lasting H-alpha emission. Continuum emission is relatively weak. In the second type, the singly ionized nitrogen emissions (NII) persist for a relatively long time and the H-alpha emission is very intense but short-lived. Continuum emission is relatively strong.

1. Introduction

The first time-resolved spectral studies of lightning strokes with both good spatial resolution and good temporal resolution have been obtained. A presentation and qualitative analysis of these data are reported in this paper, followed by a quantitative analysis in the next paper (Part II. A Quantitative Analysis).

The lightning discharge in its totality is called a flash which is composed of one or more strokes, consisting of a downward moving leader process of low luminous intensity followed by an upward-moving return stroke of high luminous intensity. The first leader process usually involves a multi-branched stepped leader propagating downward until contact is made with the ground by some one branch. This particular branch then becomes the channel for the return stroke and the remaining stepped leaders merely become luminous branches. The luminosity of the return stroke lasts only a few hundred *microseconds*, the interval between the strokes being variable but most frequently being about 40 msec.

Slitless spectroscopy has been used in the study of lightning for many years, but never in a quantitative way until the present decade. Pickering (1901) was one of several early workers who published spectra of the lightning flash. Of the 15 or 20 publications falling in the interval from 1900–1960, the work by Israel and Wurm (1941), Dufay (1947), and Dufay and Tcheng (1949) deserves special attention. These papers represent the most thorough studies of the lightning spectrum available up to 1962. It is significant that previous to this date all publications on the subject dealt with the spectrum of the entire flash or a number of flashes. The first spectra of the flash resolved into its component strokes were reported by Salanave (1961). His data initiated a continuing series of papers on the physical properties of lightning as determined from spectroscopic analysis. For example, Prueitt (1963) obtained the first estimates of temperature within a stroke. This was followed by calculations of peak temperature (Uman, 1964), of mass density, electron density, pressure and particle distribution for the same stroke (Uman *et al.*, 1964a, 1964b). In addition, the electron density in lightning strokes was estimated from the broadening of the H-alpha line (Uman and Orville, 1964). The assump-

[1] Research supported by the Office of Naval Research.

[2] Subsequent affiliation: Westinghouse Research Laboratories, Pittsburgh, Pa.

[3] Present affiliation: Dept. of Atmospheric Sciences, State University of New York at Albany.

tion of an optically thin emitting channel, necessary in most of the previous calculations, was checked and found to be valid for several strokes by examining the relative intensity from singly ionized nitrogen lines (Uman and Orville, 1965). An examination of the continuum radiation in the visible region indicated the continuum is probably not blackbody radiation or bremsstrahlung (Orville and Uman, 1965). All the foregoing analyses were performed on stroke-resolved spectra; that is, the lightning flash was time-resolved into its component strokes. The resulting exposure was an integration of all light received during the luminous phase from a section of the return stroke. All physical calculations therefore represented at best some kind of "average" applied to the luminous stage of the return stroke.

The desirability of time-resolving the lightning stroke, a luminous event lasting a few hundred microseconds, was recognized by several investigators. Israel and Fries (1956) constructed a scanning spectrograph with a time resolution of 20 μsec, but failed to obtain a spectrum. Vassy (1955) performed a series of laboratory experiments on the temporal characteristics of spectral emissions from sparks and intended to extend the techniques to lightning. A few years later Zhivlyuk and Mandel'shtam (1961) were more specific in their objectives and stated, "at the present time we are setting up experiments on the measurement of the lightning temperature with time sweep." Private communication with Mandel'shtam in 1966 confirms that these experiments were never performed.

The success in quantitative analysis of the integrated spectra of lightning strokes stimulated experiments designed to time-resolve the stroke itself. A time resolution of 20 msec had been obtained by Salanave *et al.* (1962) in recording the integrated spectrum of individual strokes, but an increase of three orders of magnitude was required to resolve the stroke on a microsecond scale. Krider (1965) reported the first time resolution of spectral emissions from individual return strokes using a photoelectric system with narrow passband interference filters. Although this was a significant step, it failed to isolate a narrow section of the lightning channel and yielded relative intensity measurements that were suspect. The problem of time-resolving the spectral emissions from a narrow section of the channel remained unsolved.

Experiments in our laboratory indicated a high-speed streaking camera with fast film should be capable of recording the spectral emissions from a section of the lightning channel with 5-μsec time resolution. The advantages of a photographic system include a high sensitivity and the possibility of recording simultaneously the intensities of many spectral lines. An additional advantage is that a permanent record in simple form is obtained. Among the disadvantages of film are the sensitivity variation with wavelength and the nonlinear response to light. Also, a careful calibration procedure and processing technique are required to minimize the errors in a photographic system. However, the advantages are more important than the disadvantages in a study of the lightning stroke; therefore, a high-speed streaking camera modified to a slitless spectrograph was used in the summer of 1965 to study the spectral emissions from a stroke. The initial success of this experiment was reported (Orville, 1966) and the experiment repeated in the summer of 1966. An analysis of all data from the two summers has been completed and is presented as Parts I, II and III in this issue.

2. Equipment

A high-speed streaking camera is required to time-resolve the lightning stroke spectrum. Slitless spectrographs used by Salanave *et al.* (1962) were of sufficient speed to resolve the spectrum of a *flash* into its component strokes on a time scale measured in *milliseconds*, but a high-speed camera is required to time-resolve the lightning *stroke* on a scale measured in *microseconds*, an increase of three orders of magnitude.

The slitless spectrographs used by Salanave isolate a 1-cm section of the channel in the focal plane, the image in the focal plane being focused on a film drum which spins at 1 rps. An increase of three orders of magnitude can be obtained by reducing the slit width by a factor of 10 and increasing the drum revolutions by a factor of 100. High-speed streaking cameras are uniquely designed for this task.

Figs. 1 and 2 illustrate two types of high-speed streaking cameras converted to slitless spectrographs. In Fig. 1 the light from a distant lightning stroke enters a prism-transmission grating combination and is then focused on a slit which isolates a small section of the channel. The prism-grating combination is adjusted to produce a "straight-through" path for the first-order spectrum. From the channel isolator, the lightning spectrum is focused by a lens and swept by a rotating mirror along the circumference of a stationary film drum. The result is a time-resolved spectrum, the time resolution being determined by the time required to sweep the slit image on the film. Thus, a 1-mm slit image and a writing rate of 0.2 mm $(\mu\text{sec})^{-1}$ produce a time resolution of 5 μsec.

In Fig. 2 the input optics to the high-speed streaking camera are the same as in Fig. 1. The only difference in principle is that the mirror is fixed and the film drum is rotated to streak the spectrum. Once again, a time-resolved spectrum is obtained.

The advantage of a moving mirror is that higher time resolution can be obtained compared with a system having a fixed mirror and moving film. The necessity for mirror motion restricts the size of the mirror and thus severely limits the *f* stop of the camera. The size of the mirror can be increased, however, if the mirror is fixed and the film spins in a drum. This latter technique is preferred when the light source is faint and sufficient time resolution can be obtained with the spinning drum.

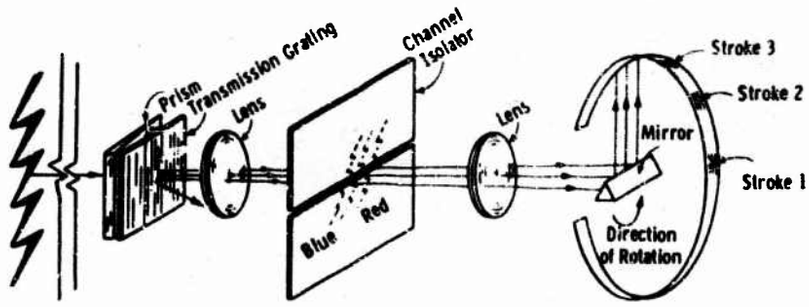

FIG. 1. Principle of a high-speed time-resolving slitless spectrograph utilizing a moving mirror and fixed film.

Two cameras were used in this experiment, representing the two types of high-speed streaking cameras available. One had a spinning mirror to obtain time resolution and the other a spinning film drum. A Model 104 high-speed streaking camera was obtained on loan from the Los Alamos Scientific Laboratory, N. Mex., and converted to a high-speed slitless spectrograph by the addition of a Bausch and Lomb replica grating. The grating is blazed for 5500Å and has 600 lines mm^{-1}. An Aero Ektar $f/2.5$ field lens with a focal length of 178 mm was mounted behind the grating to focus the spectrum on a horizontal slit with a vertical width of 0.5 mm (channel isolator). The slit can isolate a 10-m section of a cloud-to-ground stroke at a distance of 3.6 km. A three-faced mirror driven by a turbine streaks the spectrum. Compressed air drives the turbine. Although the turbine is capable of 4000 rps, it was found that 50 rps was sufficient to produce 5-μsec resolution. The spectral inverse dispersion was 143Å mm^{-1}.

In addition to the Model 104 camera, a Beckman and Whitley Model 318 high-speed streaking camera became available in the late summer of 1965. The suitability of this camera for lightning studies became very evident and the camera was used exclusively in the summer of 1966.

Fig. 3 shows the camera converted to a slitless spectrograph and mounted on a portable table with accessory equipment. Mobility is essential when the field of view is approximately 10° and the location of a lightning discharge is unpredictable. The Beckman and Whitley camera is an electrically driven moving-film streak camera capable of writing at speeds up to 0.3 mm $(\mu sec)^{-1}$. A rate of 0.12 mm $(\mu sec)^{-1}$, corresponding to a film drum rotation rate of 1.38 rps, is adequate to provide 4-μsec resolution with a 0.5-mm slit. By decreasing the slit width from 0.50 to 0.25 mm, data with 2 μsec resolution can be obtained. The film strip in the drum is 87.6 cm long. Drum and film are rotated in an evacuated housing. This produces less drum and film temperature-rise during operation and resolution loss at the image plane caused by air turbulence is minimized. The camera was converted to a slitless spectrograph by adding a Bausch and Lomb replica grating similar to the one used on the Los Alamos Model 104. A 180-mm field lens focused the lightning spectrum on a horizontal slit with a vertical width (channel isolator) of 0.53 mm. This will isolate a 10-m section of the stroke channel at 3.4 km. The inverse spectral dispersion is 80Å mm^{-1}. In the summer of 1966, a 200-mm $f/3.5$ Takumar lens was used to produce an inverse spectral dispersion of 72Å mm^{-1}. The dispersion, it should be remembered, is an average value in the visible region. The "straight-through" prism-grating combination produces a dispersion in the focal plane which is slightly nonlinear due to the dispersion of the prism superimposed on the dispersion of the transmission grating.

3. Photographic technique

Recording the spectrum of lightning on a scale measured in microseconds requires special consideration of the common sources of error in photometric work.

"Reciprocity failure" is a term referring to the fact that different film densities are obtained when the in-

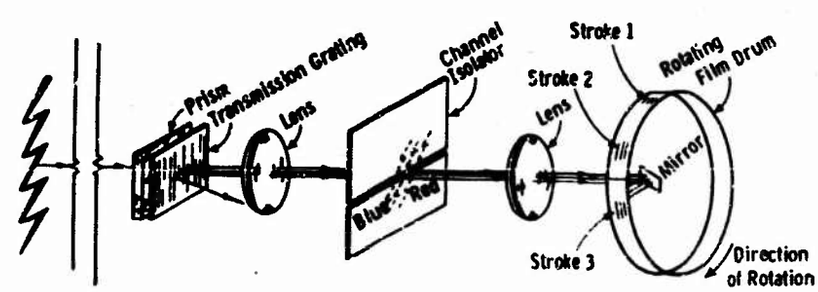

FIG. 2. Same as Fig. 1 except for a fixed mirror and rotating film.

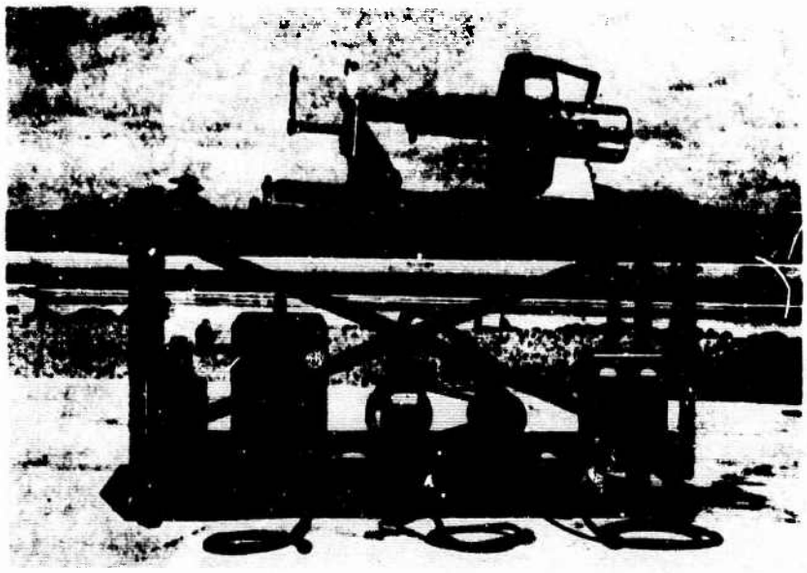

FIG. 3. The Beckman and Whitley Model 318 high-speed camera modified to a slitless spectrograph. Accessory equipment is mounted on the lower shelf of the portable table.

tensity of a light source and time are varied to produce the same exposure. The important factor controlling the failure of the reciprocity law is the time rate of formation of the latent image (Mees, 1954, p. 205). Berg (1940) performed a series of experiments on reciprocity failure at high intensities and short exposures. He noted that the latent image is formed by an electronic and ionic process. For brief exposures, the processes are separated because the electrons are more mobile than the ions. The dominance of the electronic process over the ionic process becomes complete at approximately 40 μsec, and at shorter exposure times there is no reciprocity failure. Sauvenier (1963) has studied the reciprocity failure between 10^{-6} and 10^{-4} sec. He finds no reciprocity failure between 10^{-6} and 10^{-5} sec and only a slight failure in the range 10^{-5}–10^{-4} sec. Berg's classic work and Sauvenier's results are supported by Dubovik's (1964, p. 358) recent studies.

All high-speed time-resolved lightning spectra were recorded with an exposure time ≤ 5 μsec. Reciprocity failure can therefore be neglected if a calibration source is used with an exposure time ≤ 10 μsec. A G.E. type 1531-A Strobotac unit with a xenon source was used to calibrate the film. This has an adjustable flash duration from 0.8–3.0 μsec and the latter setting was used for all calibrations.

Emulsion sensitivity is a function of the relative humidity (Mees, 1954, p. 128) and temperature (pp. 232–237). For this reason, all film was stored under identical conditions and exposed to the calibration source within a few days after each storm.

Experience obtained during the summers of 1961–1964 at the Institute of Atmospheric Physics indicated that a film emulsion with high sensitivity would be required to time-resolve the spectral emissions from a lightning stroke. Although slightly out of date, Pressman's (1962, p. 80) survey of films and developers for high-speed recording presents a thorough analysis of the possible combinations. High Speed Infrared, Agfa Isopan Record, Linagraph Orthochromatic, Tri-X, Plus-X, and Linagraph Shellburst films were initially tested for speed, gamma, fog, and wavelength sensitivity. The film speed was the determining factor. Agfa Isopan Record was selected for initial exposures despite its high background fog and lack of red extended sensitivity. This latter characteristic is necessary to record the H-alpha emission from lightning. The second choice was Linagraph Shellburst film with low background fog, high gamma, and extended red sensitivity. Agfa Isopan Record was used in the Los Alamos Model 104 camera and recorded the first time-resolved spectrum of a lightning stroke on 14 July 1965. Subsequent use of Linagraph Shellburst film resulted in complete failure due to the film's low sensitivity. All film was overdeveloped 50–100% in Kodak D-19 at 70F.

Kodak 2475 Recording film became available in the middle of the 1965 lightning season and was used exclusively after its high speed and red extended sensitivity were tested. It is a film with low resolving power, medium granularity, medium acutance, and an ASA rating of 1000.

Subsequent to the first success of 14 July, all lightning spectra were recorded on Kodak 2475 Recording film in the Beckman and Whitley Model 318 camera. It was concluded that this combination is the most sensitive photographic system for time-resolving the spectral emissions from a stroke.

Photographic film must be calibrated for its nonlinear

response to light. An acceptable process is to use a stepped slit mounted in front of the Strobotac calibration source. The stepped slit was constructed by Prueitt (1963) and consisted of steps passing known relative amounts of intensity. Since the time of exposure is constant, relative exposure changes are directly related to relative intensity changes. Therefore, density can be plotted as a function of exposure to produce a characteristic curve. Film, cut from the same roll exposed to lightning, was exposed to the standard source and developed with the film containing the lightning spectrum. In this way, density variations due to the developer temperature variations and aging were eliminated. The film was brushed continuously during development to minimize the Eberhard effect.

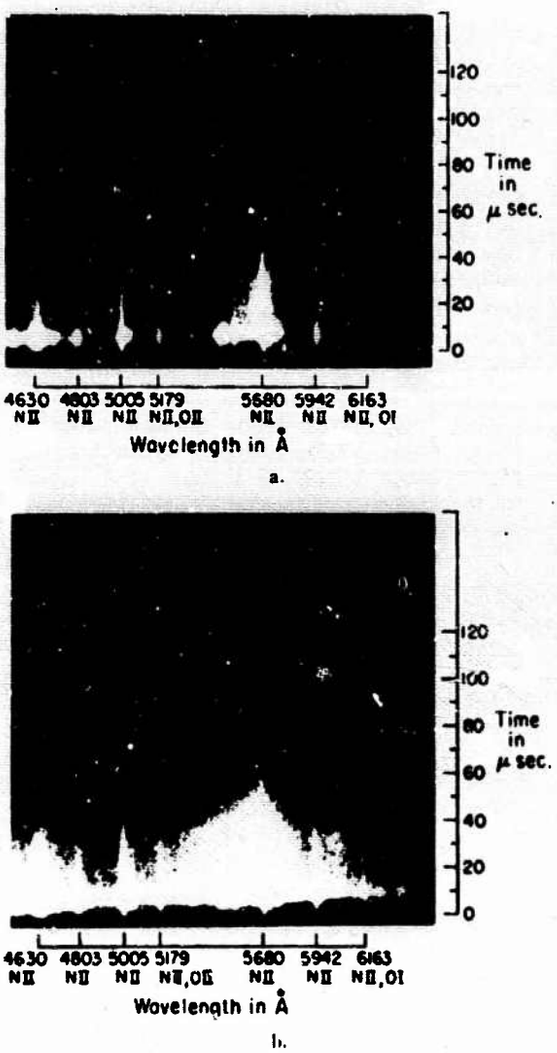

FIG. 4. High-speed, time-resolved spectrum of a lightning stroke, 14 July 1965. a. A 10-m section of a lightning return stroke has been isolated and the spectrum streaked in time. The time resolution is 5 μsec. Singly ionized atoms emit first, followed by continuum radiation. b. The same negative used in Fig. 4a has been printed with less exposure to show the persistance of several lines for approximately 120 μsec.

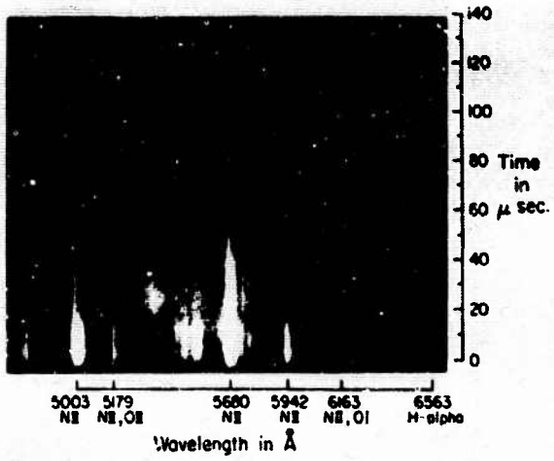

FIG. 5. Streaked spectrum of a lightning return stroke using film with red extended sensitivity. Note the appearance of the H-alpha emission at 6563Å and the dip in the continuum at 20 μsec.

4. Presentation of data

A total of 22 spectra were obtained in the summers of 1965 and 1966. The low number is indicative of the unpredictable nature of the source. To record a spectrum, the lightning stroke should occur within 10 km of the instrument and within a 10° field of view. If these conditions are met a spectrum will be recorded, assuming of course, that the camera is loaded, running at the appropriate speed, and the shutter is open. Since a time exposure is required, only lightning strokes occurring at night could be recorded. The problem of obtaining properly exposed spectra from a source as unpredictable as lightning was a major obstacle in this experiment. The small number of data is consistent with the experimental problems encountered when working in the atmospheric laboratory.

Seven time-resolved spectra are reproduced in Figs. 4–8. All spectral emissions are from approximately a 10-m section of the lightning return-stroke channel. In both Figs. 4 and 6, two prints have been made from the same negative to accurately present the dynamic range of the recorded image. The spectra cover different ranges of the optical region because the fortuitous positioning of the lightning stroke relative to the slitless spectrograph determines the wavelength range recorded. The recorded spectra will now be examined.

Figs. 4a and 4b are reproductions from the first time-resolved spectrum obtained on 14 July 1965. An extensive qualitative and quantitative analysis of this spectrum has been completed. Several weak lines at 4650, 6158 and 6456Å persist for approximately 150 μsec, but are not visible in the reproduced spectrum. All of the recorded emissions are from unresolved multiplets or

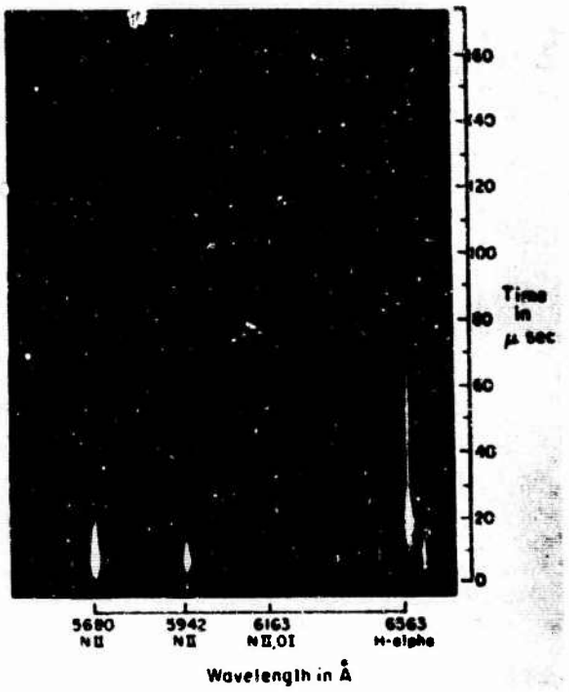

a.

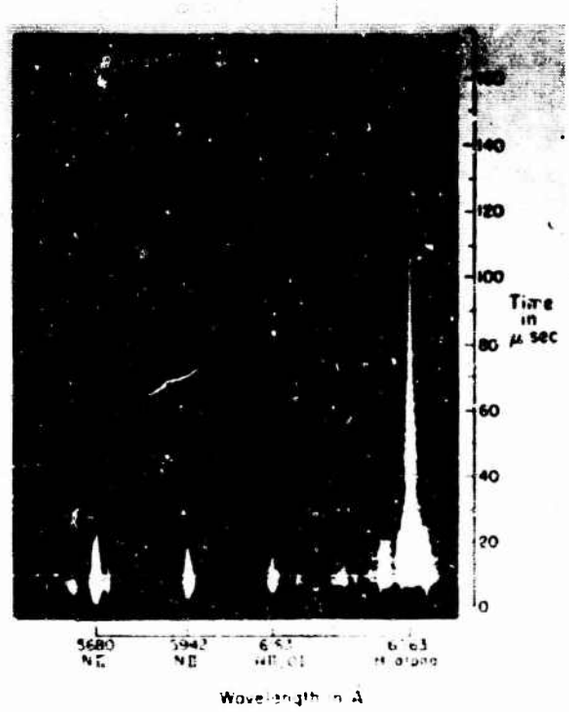

b.

[illegible] return stroke in a flash [illegible] does not record [illegible] Print from the same [illegible] continuum and persistent [illegible] line.

lines superimposed on a broad continuum. The unresolved multiplets are identified by the most intense line. For example, NII 4630 refers to the singly ionized nitrogen multiplet (NII) composed of six lines whose brightest line occurs at 4630Å. A time scale in microseconds is provided with a somewhat arbitrary zero point, arbitrary in the sense that "time zero" refers to the time when spectral emissions are first recorded. A closer stroke would shift "time zero" to an earlier point in the life of the return stroke and a more distant stroke would only have the very intense luminosity recorded, thus shifting "time zero" to a later time in the history of the stroke.

All of the intense emissions are attributed to nitrogen atoms in the singly ionized state (NII) with the exception of OII occurring at 5179Å. The identification of OII was made after attempting to calculate the temperature from the relative intensities of NII radiation at 5003 and 5179Å. Two spectra yielded temperatures in the 40,000–70,000K range. These values exceed the temperatures in the 20,000–30,000K range reported in Part II and are only presented here to confirm the OII identification. The reason for the high temperatures is that the 5179Å radiation had been attributed entirely to NII multiplets with an excitation potential of 30 eV. The contribution of OII with an excitation potential of 28.8 eV is also important and contributes to an erroneous temperature value.

It is evident in Fig. 4, and indeed in all spectra obtained, that the singly ionized species emit first, followed by continuum emission. Both types of radiation reach their peak luminosity within 10 μsec. This short time contradicts Kriders' (1965) measurement. He used a photoelectric system with narrow passband interference filters to monitor the spectral regions of interest. A curious feature of these data is the long period required for the intensity of various spectral features to rise from zero to peak luminosity. For example, NII emissions required approximatley 40 μsec to reach peak luminosity. Krider (1965) correctly suggested that the length of this period depends on the apparent time required for the leading edge of the return stroke to traverse the particular length of channel section under observation. The spectrum reproduced in Figs 4a and 4b is from a stroke 3 km or less from the observation point. The Los Alamos Model 104 camera was located 17 m above the ground and elevated 3.6°. Then at a distance of 3 km, a 10-m section of the channel is being observed approximately 200 m above the ground. If the return stroke velocity is 3.5×10^{9} cm sec^{-1} (Malan, 1963, p. 25), the leading edge of the return stroke is propagated across the section of the channel under study in about 0.3 μsec. Therefore, the contribution to the rise-time made by the propagation of the return stroke is considered negligible in these data. Current rise-times to towers, power lines and captive balloons indicate a range of 1–15 μsec with 2.5 μsec the most frequent value for the first stroke (Schonland, 1956, p. 605). Subsequent strokes have current rise-

times frequently too fast to be accurately measured. Berger and Vogelsanger (1965) indicate it is usually less than a microsecond and may be less than a few tenths of a microsecond. The spectral luminosity rise-time of 10 μsec or less is consistent with these results, but the comparison between cloud-to-ground lightning and strikes to towers, etc., may not be valid. Current rise-times are measured at the ground and spectra are obtained from a section of the return-stroke channel above the ground. It is apparent, as Krider (1966) has stated in a recent article, that he examined a large vertical section of the channel and consequently found long times for the intensity to rise from zero to peak value, the long times being due to the propagation time of the return stroke.

Fig. 5 is a spectrum from a one-stroke lightning flash recorded on 2475 Recording film. The wavelength and time scales are similar to Fig. 4 but several new features are apparent. Kodak 2475 film with its red extended sensitivity has recorded for the first time the emission at 6563Å from the H-alpha line in the Balmer series of hydrogen. The time characteristic of this emission is distinctly different from the NII and continuum emissions. The H-alpha peak emission follows by tens of microseconds the peak emissions of NII and continuum radiation. The H-alpha line was not present in Fig. 4 because the film (Agfa Isopan Record) was not sensitive to the 6563Å emission. This new feature is therefore a result of changing films and does not represent a physical difference between the strokes presented in Figs. 4 and 5.

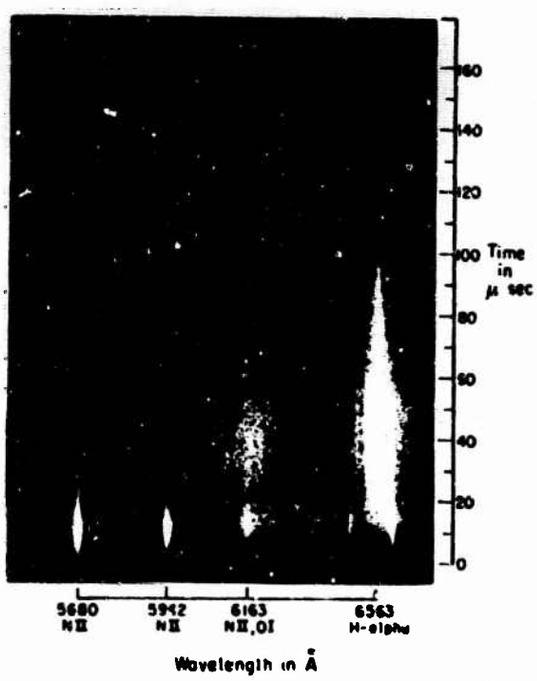

FIG. 7. Streaked spectrum from a return stroke which is subsequent to the one in Fig. 6 and believed to be from the second or third stroke. Of the five recorded return strokes, this is the most intense stroke in the flash.

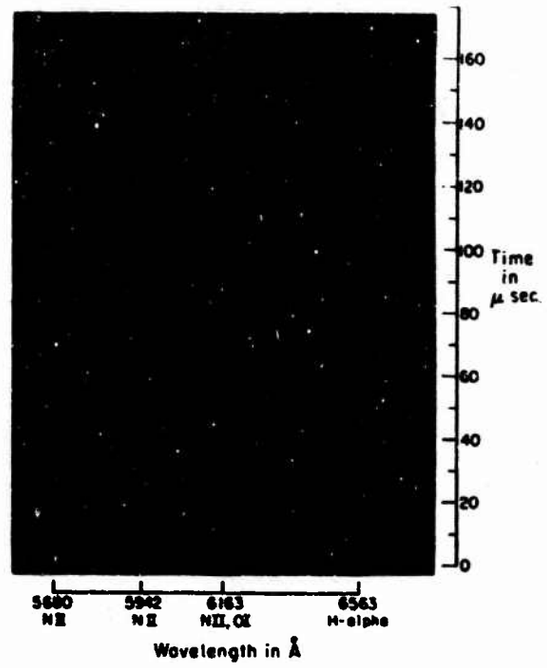

FIG. 8. Streaked spectra of the three remaining strokes in the 5-stroke flash are relatively weak. The most intense one is reproduced here. The H-alpha persistence is characteristic of all three spectra.

Two other new features do represent a physical difference between return strokes. There is a dip in the continuum intensity at approximately 20 μsec and a short streak of light appears at approximately 10 μsec between 5003 and 5179Å. A similar feature appears to the right of 5680Å. These features can be related in the following way. The dip in the continuum is reminiscent of the luminosity variations within a section of the return-stroke channel first reported by Malan *et al.* (1935) and analyzed in detail by Malan and Collens (1937). They observed that a luminosity enhancement sometimes occurred between 10 and 50 μsec. The effect of the enhancement is to produce an "intensity dip" or local minimum. Malan and Collens examined the luminosity enhancements and associated them with current variations in the channel arising from branches supplying charge to the channel. They observed luminosity enhancements when the upward moving return-stroke luminosity reached a branch point. This increase of luminosity was believed to be the result of increasing current due to the availability of another current source, the branch, and the increasing "freshness" of the charge left by the leader process.

It therefore appears that the continuum enhancement is the result of a branch point existing above the section of channel under study. Evidence of a branch appears

in the small streak of light previously mentioned between 5063 and 5179Å. This streak of light is the 5003Å emission from a branch. As mentioned previously, a similar emission appears to the right of 5680Å. Recall that it is a property of slitless spectrographs that a change in the physical position of the source changes the position of the spectrum in the focal plane. Thus, emissions from a branch displaced to the right or left from the main return-stroke channel will have the branch spectrum displaced to the right or left of the spectrum produced by the main channel.

I conclude that the return-stroke luminosity reached a branch point approximately 5 μsec after propagating along the vertical channel section under study. The luminosity then traveled down the branch and at 10 μsec passed the isolated branch section, emitting intense spectral lines in the 5000 and 5680Å regions. Less intense emissions were not recorded. The effect of tapping a new current source appears as an increasing luminosity in the main channel at approximately 30 μsec. Similar enhancements in the continuum intensity occur in three other time-resolved spectra and are probably associated with branch points above the channel section being studied.

Figs. 6, 7 and 8 present the first time-resolved spectral emissions from a multi-stroke flash. A total of five strokes were recorded of which the three most intense are reproduced. There is reason to believe that the order in which the strokes are presented is the order in which they occurred. The ambiguity of stroke order arises because the film strip is rotating at about once in 10 msec and the strokes are separated by tens of milliseconds.

Fig. 6 is believed to be the first stroke in the flash because the spectrum of a branch has been obtained. Fig. 6 is divided into parts a and b to reproduce the exposure latitude contained in the negative. Just to the left of 5680Å there is an unidentified emission which appears for 5 μsec or less. This unidentified emission is more obvious in Fig. 6b than in 6a. Similar emissions occur to the left of 5942Å. The emissions in the 5942Å region are actually composed of two lines 10Å apart. In Fig. 6b these lines are not resolved because of overexposure, but to the left of 5942Å there are two lines faintly resolved. These faint lines are the 5932 and 5942Å emissions from a branch in the return stroke. Since it is the first stroke which characteristically exhibits branching, I conclude that Fig. 6 is the first stroke in the flash.

The spectrum in Fig. 6 contains the characteristic NII lines identified in previous spectra. NII lines with the lowest excitation appear first followed by lines with a higher excitation potential. Thus, NII 5680 (20.6 eV) appears before NII 5942 (23.2 eV) and lasts longer. The time of continuum emission is best represented in Fig. 6b. The distinctive H-alpha line is absent or very faint in the first few microseconds, but quickly becomes very intense and decays slowly relative to the other emission species. H-alpha emissions are recorded beyond 160 μsec.

Fig. 7, believed to be the second stroke in the flash, exhibits several characteristics different from the first stroke. Since there is no evidence of the branching found in Fig. 6, it appears this is a subsequent stroke to the first one. Norinder and Dahle (1945) found in flashes with 1–7 strokes that the second or third strokes usually had the highest magnetic flux density and presumably the highest current. It is reasonable to assume that the highest current would be associated with the highest luminosity. Therefore, I conclude that Fig. 7 is probably the spectrum of either the second or third stroke in this flash.

In Fig. 7 all NII emissions and the continuum last longer relative to similar emissions in the first stroke reproduced in Fig. 6. Continuum emission is also more intense at longer wavelengths and cannot be explained by an increase in the film sensitivity or optical effects such as vignetting. The H-alpha emission is overexposed and decays quickly until, beyond 120 μsec, emissions are no longer recorded. A water vapor absorption band in the 5942Å region is very evident in the strong continuum radiation. Weak absorption bands in the 6260Å region are apparent and are unidentified. They were first reported by Wallace (1964).

Fig. 8 is a reproduction of the third most intense spectrum in the flash. It may have been the third stroke in the flash. The NII emissions are very brief and the H-alpha emission lasts for more than 160 μsec. The overall intensity is less than Fig. 6, but the time characteristics of the emissions are very similar. The remaining two strokes in this flash were much less intense and are not suitable for reproduction. However, the spectral emissions in the two remaining strokes are similar to Fig. 8, albeit very faint, and the H-alpha emissions are recorded for approximately 500 μsec, or 0.5 msec in each stroke.

It is indeed unfortunate that the current is unknown in the flash components reproduced in Figs. 6, 7 and 8. Two distinctive types of strokes emerge from this example. In the first type we have the intense short-lived emissions of NII followed by a long lasting H-alpha emission. Continuum emission is relatively weak. In the second type, we note a high intensity stroke at all wavelengths (5680–6600Å). The NII emission persists for a relatively long time and the H-alpha emission is intense but short-lived. Continuum emission is relatively strong.

It is interesting to consider several differences between the time-resolved slitless spectrograms of lightning reported in this paper and the slit spectrograms obtained by Wallace (1964). Wallace's spectra represent the most complete compilation of wavelength identifications in the lightning spectrum. A significant difference between the time-resolved data and Wallace's (1964) data is the relative brightness of the emissions in the 5680, 5942 and 6163Å regions. In the time resolved data (Fig. 6) we note relatively intense emissions in the 5000 and 5942Å regions and a weak short lived emission at 6163Å. An examination of the original nega-

tive indicates the apparent short-lived emission at 6163Å persists as a faint line beyond 100 μsec. The short-lived emission is due to NII and the persistent faint emission is probably OI. In Wallace's (1964) data, the 5680Å emissions are weak, the 5942Å emissions are completely absent, and the 6163Å emission is relatively bright.

There are several possible reasons for these differences. The spectrographs and films used in the two separate experiments may have different sensitivities as a function of wavelength and this may account for all the differences noted above. On the other hand, the characteristic emission times of species within the lightning stroke can be used to explain the qualitative differences between slitless spectra and slit spectra. It has already been observed that the emission in the 6163Å region on time-resolved slitless spectra is composed of a short-lived NII emission followed by a faint persistent OI emission. On a slit spectrum, however, the total amount of light would be integrated, to give the effect of an intense line. Wallace (1964) observed a strong line in this region. In the 5680 and 5942Å regions the emissions are attributed solely to NII emissions which occur for a relatively short time, on the order of 20 μsec. In Wallace's

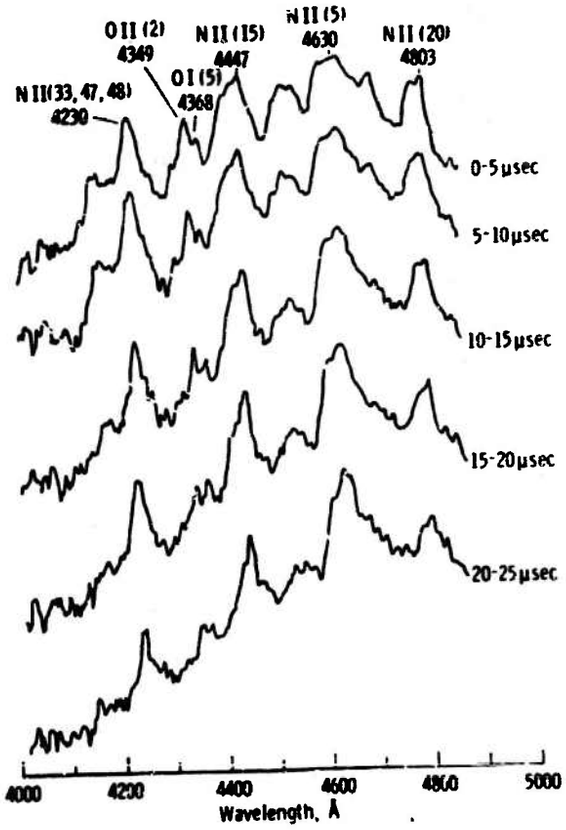

FIG. 9. Microphotometer traces in the blue region of the optical spectrum up to 25 μsec. Traces are presented every 5 μsec and are uncorrected for the nonlinear response of the film emulsion.

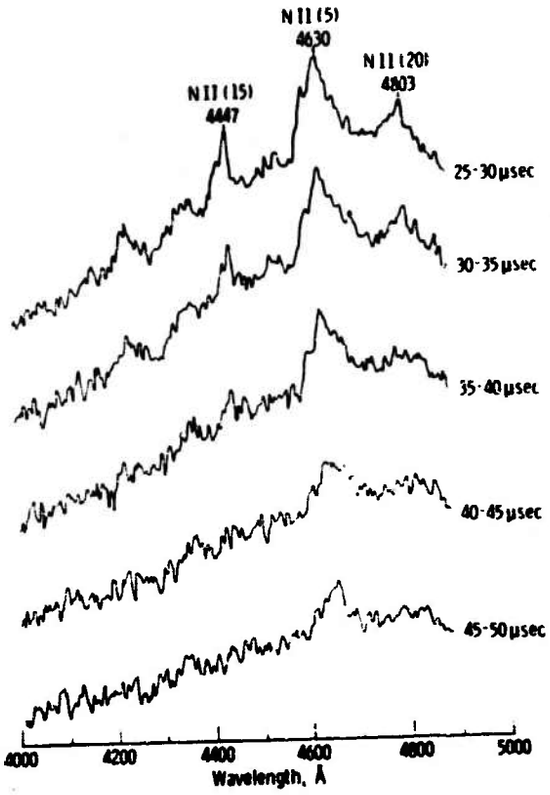

FIG. 10. Traces presented in Fig. 9 are continued to 50 μsec.

data the 5680Å emission appears as a weak line and the 5942Å emission is absent. A slit spectrograph time integrates the light from a flash and therefore favors the lines with a persistent emission. (This is particularly evident in the strong H-alpha emission recorded by Wallace.) It seems reasonable that the 5680Å emissions appear as weak lines in Wallace's data. The absence of the 5942Å emission has been suggested by Wallace (private communication) as due to a strong continuum radiation recorded in his spectra which makes it difficult to discern the 5942Å emissions and to a moderately strong water vapor absorption line at 5942Å. It appears, therefore, that a short emission time, a relatively high continuum, and a water vapor absorption band may be sufficient to explain the absence of the 5942Å emission in Wallace's data.

5. Microphotometer traces

To complete the qualitative analysis and take the first step toward quantitative analysis, it is necessary to obtain microphotometer traces. These traces represent per cent transmission through the film emulsion as a function of wavelength. They must be corrected by a tedious process to obtain relative intensity. It is sufficient to examine the uncorrected traces over most of the

spectrum to point out several important qualitative features.

In Figs. 9 and 10 the traces from a time-resolved spectrum of a lightning stroke are presented to 50 μsec in increments of 5 μsec. They were obtained by tracing across a time-resolved spectrum every 5 μsec. The spectrum from which these traces were obtained is not reproduced in this paper. The wavelength identifications have numbers associated with them which refer to multiplets of the particular species. Thus, NII (5) 4630 indicates that the unresolved NII lines at 4630Å compose the fifth multiplet of singly ionized nitrogen according to the tables of Moore (1945). Multiplet designations are a convenience and are frequently included in wavelength identifications.

As previously noted in reproductions of time-resolved spectra, NII lines are dominant. An OI line appears at 4368Å in the first 5 μsec. Compare OII 4349 and OI 4368 and note that OII 4349 is initially the most intense line, but as time increases to 20 μsec the OI 4368 line becomes stronger relative to OII 4349. This is entirely consistent with a cooling channel that was initially dominated by radiation from singly ionized species. Beyond 25 μsec the singly ionized nitrogen lines blend into the continuum until only NII 4630 is recognizable at 50 μsec. The upper excitation potential of NII 4630 is 21.1 eV and lower than the excitation potential of adjacent NII lines. Thus, we are not surprised to see its relative persistence.

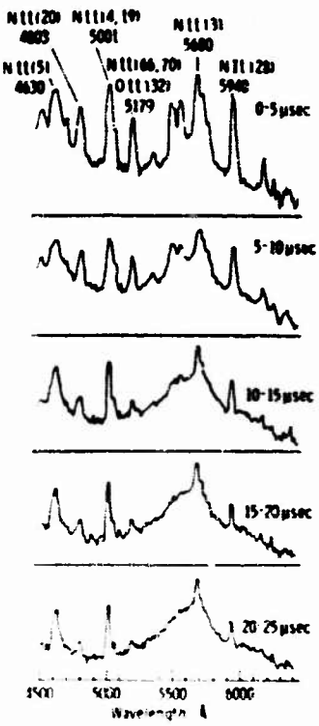

FIG. 11. Microphotometer traces from 4500–6000 Å are reproduced from tracing the spectrum in Fig. 4.

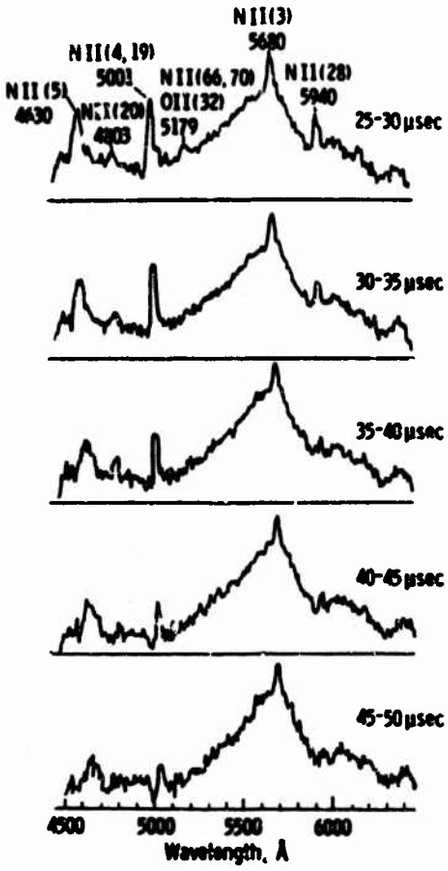

FIG. 12. Traces presented in Fig. 11 are continued to 50 μsec.

In Figs. 11 and 12, microphotometer tracings from 4500–6000Å are presented up to 50 μsec. This set of tracings was obtained by microphotometering every 5 μsec the spectrum reproduced in Fig. 4. Note how quickly the unresolved 5179Å lines decrease with time until they blend with the continuum between 20 and 25 μsec. This behavior is representative of emission lines originating from the high excitation potentials in the NII and OII atoms (~30 eV) as compared to the lower excitation potentials whose lines such as 5000Å (~23 eV) persist for 50 μsec. The shape of the 4630 multiplet changes with time as the NII radiation decreases and OI emissions in the 4650Å region increase. The profile of the "uncontaminated" 4630 multiplet can be estimated by plotting the gf values of the component lines, where g is the statistical weight of the lower level and f is the absorption oscillator strength [see, for example, Unsöld and Orville (1964b)]. A change of the profile with time indicates the qualitative effect of the OI emissions at 4650Å. In the 5680Å region the intense NII emissions are overemphasized by the sensitivity of Agfa Isopan Record film.

The last set of microphotometer tracings covers the interesting H-alpha region. In Figs. 13 and 14 the region

from 6450–6650Å is presented. These tracings were obtained from the spectrum reproduced in Fig. 6. Note in the first 5 μsec an unidentified line appears just to the left of 6563Å. This line is the NII 6611 emission from a branch. The presence of the branch spectrum was previously treated under a discussion of Fig. 6. As several spectra have previously indicated, the H-alpha emission is initially very weak relative to the NII emissions. Beyond 15 μsec the H-alpha line dominates the spectral region and the NII lines disappear. Fig. 6 indicates significant H-alpha emissions are recorded beyond 160 μsec.

6. Summary

A 10-m section of the lightning stroke has been isolated and the optical spectral emissions streaked in time. These first time-resolved spectra indicate all initial emissions are due to singly ionized species of nitrogen and oxygen. These emissions and the continuum radiation reach peak luminosity within 10 μsec. Singly ionized lines with the lowest excitation potential appear first followed by lines with a higher excitation potential. Continuum emission reaches peak luminosity after the singly ionized species and before the radiation from neutral species. Several faint lines due to neutral nitrogen and oxygen atoms persist for approximately 150 μsec.

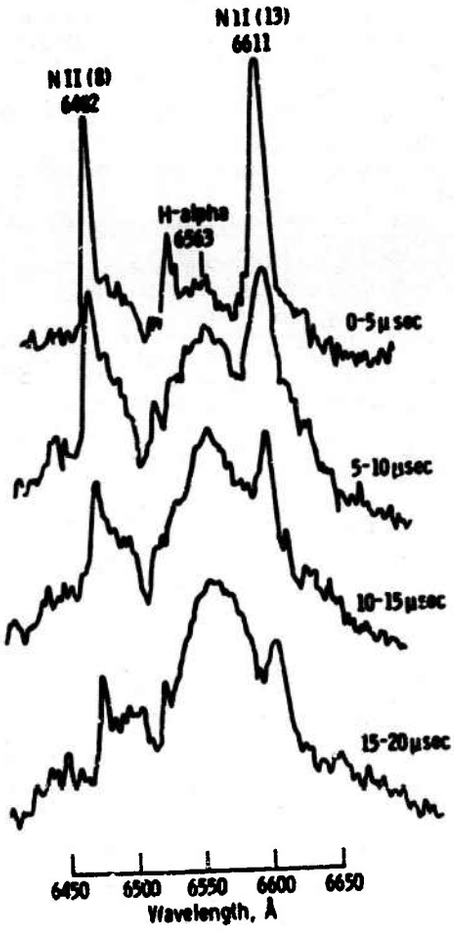

FIG. 13. Microphotometer traces in the H-alpha region are reproduced from tracing the spectrum in Fig. 6.

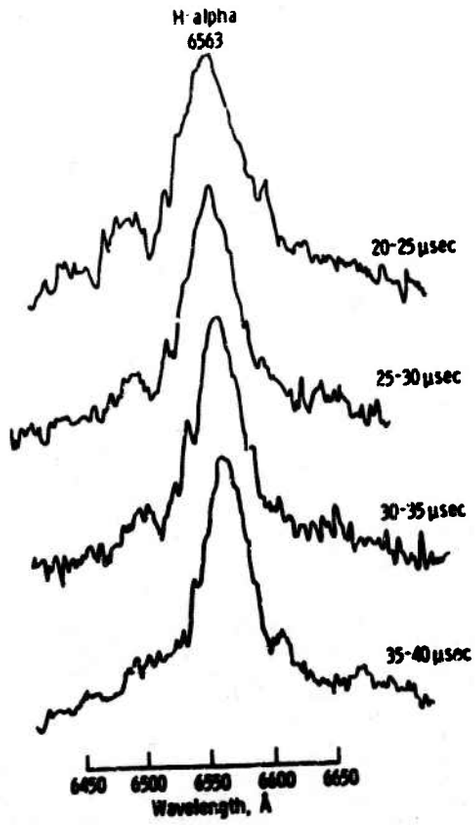

FIG. 14. Traces presented in Fig. 13 are continued to 40 μsec.

The emission features of H-alpha are distinctly different from the emissions of the singly ionized species. In the first 5 μsec the H-alpha line is very faint or completely absent in the spectrum. Its intensity rises relatively slowly and clearly peaks after 10 μsec, decaying until it is one of the few lines detected in the visible spectrum beyond 100 μsec.

Spectra from a flash composed of at least five strokes have been obtained. The spectra fall into two types. In the first type, four of the five recorded spectra exhibit relatively short-lived NII emissions and a long lasting H-alpha emission. The continuum emission is present but relatively weak. On the other hand, the remaining spectrum and second type shows NII emitting for a relatively long time compared to the same emitting species in the first four spectra. The H-alpha emission is very intense but short-lived. The continuum emission is more intense. Thus, Type I exhibits short lived NII emissions, long lasting H-alpha emission, and a

weak continuum. Type II has long lasting NII emissions, an intense short-lived H-alpha emission, and a strong continuum.

A quantitative analysis of these data is presented in the next paper.

Acknowledgments. I wish to express my appreciation to Leon E. Salanave for his encouragement and assistance in the lightning experiment and to Dr. A. Richard Kassander, Jr., for his assistance in obtaining the Beckman and Whitley streaking camera. It is a pleasure to thank Drs. Herman Hoerlin and Milton Peek of the Los Alamos Scientific Laboratory for arranging the loan of the Model 104 streaking camera. The enthusiastic support and helpful comments of Dr. Martin A. Uman of the Westinghouse Research Laboratories are gratefully acknowledged. The use of a Hilger and Watts microphotometer was generously made available by the Kitt Peak National Observatory.

REFERENCES

Berg, W. F., 1940: Reciprocity-law failure of photographic materials at short exposure times. *Proc. Roy. Soc.* (*London*), **A174**, 559–568.

Berger, K., and E. Volgelsanger, 1965: Messungen und Resultate der Blitzforschung der Jahre 1955–1963 auf dem Monte San Salvatore. *Bull. Schweiz. Elektro. Ver.*, **56**, 2–22.

Dubovik, A. S., 1964: *Photographic Recording of High-Speed Processes.* Moscow, Science Publishing House, 372 pp.

Dufay, M., 1947: Sur le spectre des éclairs dans les regions violette et ultra-violette. *Compt. Rend.*, **225**, 1079–1080.

Dufay, J., and M. Tcheng, 1949: Recherches sur les spectres des éclairs. *Ann. Geophys.*, **5**, 137–149.

Israel, H., and G. Fries, 1956: Ein Gerat zur spektroskopischen Analyse verschiedener Blitzphasen. *Optik*, **13**, 365–368.

——, and K. Wurm, 1941: Das Blitzspektrum. *Naturwissenschaften*, **29**, 778–779.

Krider, E. P., 1965: Time-resolved spectral emissions from individual return strokes in lightning discharges. *J. Geophys. Res.*, **70**, 2459–2460.

——, 1966: Some photoelectric observations of lightning. *J. Geophys. Res.*, **71**, 3095–3098.

Malan, D. J., 1963: *Physics of Lightning.* London, English Universities Press, 176 pp.

——, and H. Collens, 1937: Progressive lightning, Pt. 3, The fine structure of return lightning strokes. *Proc. Roy. Soc.* (*London*), **A162**, 175–203.

——, B. F. J. Schonland and H. Collens, 1935: Intensity variations in the channel of the return stroke. *Nature*, **136**, 831.

Mees, C. E., 1954: *The Theory of the Photographic Process.* New York, Macmillan, 1133 pp.

Moore, C. E., 1945: A multiplet table of astrophysical interest. Revised Ed., *Contrib. Princeton Univ. Obs.*, No. 20, 110 pp.

Norinder, H., and O. Dahlo, 1945: Measurements by frame aerials of current variations in lightning discharges. *Arkiv. Mat. Astron. Fysik*, **32A**, 1–70.

Orville, R. E., 1966: High-speed, time-resolved spectrum of a lightning stroke. *Science*, **151**, 451–452.

——, and M. A. Uman, 1965: The optical continuum of lightning. *J. Geophys. Res.*, **70**, 279–282.

Pickering E. C., 1901: Spectrum of lightning. *Astrophys. J.*, **14**, 367.

Pressman, Z., 1962: A comparison of high-speed photograhic films with different rigorous development conditions. *Proc. 5th Intern. Conf. High-Speed Phot.*, 80–86.

Prueitt, M. L., 1963: The excitation temperature of lightning. *J. Geophys. Res.*, **68**, 803–811.

Salanave, L. E., 1961: The optical spectrum of lightning. *Science*, **134**, 1394–1399.

——, R. E. Orville and C. N. Richards, 1962: Slitless spectra of lightning in the region from 3850 to 6900 Ångstroms. *J. Geophys. Res.*, **67**, 1877–1882.

Sauvenier, H., 1963: Étude sensitometrique d'émulsions comoerciales aux tres courts temps de pose. *Proc. 6th Intern. Cong. High-Speed Phot.*, Haarlem, Tjeenk Willink and Zoon, 388–392.

Schonland, B. F. J., 1956: The lightning discharge. *Handbuch der Physik*, Berlin, Springer, Vol. 22, 576–628.

Uman, M. A., 1964: The peak temperature of lightning. *J. Atmos. Terr. Phys.*, **26**, 123–128.

——, and R. E. Orville, 1964: Electron density measurement in lightning from Stark-broadening of H_α. *J. Geophys. Res.*, **69**, 5151–5154.

——, and ——, 1965: The opacity of lightning. *J. Geophys. Res.*, **70**, 5491–5497.

——, —— and L. E. Salanave, 1964a: The density, pressure, and particle distribution in a lightning stroke near peak temperature. *J. Atmos. Sci.*, **21**, 306–310.

——, —— and ——, 1964b: The mass density, pressure and electron density in three lightning strokes near peak temperature. *J. Geophys. Res.*, **69**, 5423–5424.

Vassy, A., 1955: Étude dans le temps spectra d'émission d'étincelles de grande longueur. *J. Phys. Radium*, **16**, 292–295.

Wallace, L., 1964: The spectrum of lightning. *Contrib. Kitt Peak National Observatory*, No. 52. (See also, *Astrophys. J.*, **139**, 994–998).

Zhivlyuk, Yu N., and S. L. Mandel'shtam, 1961: On the temperature of lightning and force of thunder. *Soviet Physics JETP*, **13**, 338–340.

Reprinted from JOURNAL OF ATMOSPHERIC SCIENCES, Vol. 25, No. 5, September, 1968, pp. 839-851
American Meteorological Society
Printed in U. S. A.

A High-Speed Time-Resolved Spectroscopic Study of the Lightning Return Stroke: Part II. A Quantitative Analysis[1]

RICHARD E. ORVILLE[2,3]

Westinghouse Research Laboratories, Pittsburgh, Pa.

(Manuscript received 15 December 1967)

ABSTRACT

A quantitative analysis has been completed of the first time-resolved spectra of return strokes. All values refer to approximately a 10-m section of the return-stroke channel. Ten return-stroke spectra, eight with 5-μsec resolution and two with 2-μsec resolution, have been analyzed to determine their temperature-time curves. The peak temperature in five of the ten spectra is in the 28,000–31,000K range despite the use of different slitless spectrographs and different multiplet intensity ratios for the measurements. The highest peak temperature was calculated to be 36,000K. Temperature errors are on the order of 10–25%. A temperature rise in two of the strokes has been calculated in the first 10 μsec from data having 5-μsec resolution. The two recorded strokes with 2-μsec resolution have monotonically decreasing temperature-time curves. It is shown that if the number density of a particular emitting species is known, the relative channel radius within which the particular radiators are contained can be calculated as a function of time. The NII radiation reaches peak intensity in 5–10 μsec, the continuum radiation attains maximum within 10–15 μsec, while the H-alpha emission is most intense in the 20–50 μsec period. The effective excitation potential of the continuum radiation lies between that of the ions and the neutrals and may therefore be due to radiative recombination or radiative attachment.

Two spectra with H-alpha emissions have been quantitatively analyzed. The first spectrum shows an increasing intensity to 50 μsec followed by a monotonic decrease. The second H-alpha spectrum attains maximum intensity in 20 μsec, decreases to a local minimum at 35 μsec, and then decreases monotonically after a small maximum at 45 μsec. The second maximum, or luminosity enhancement, is probably associated with a branch providing additional charge to the return-stroke channel. The Stark-broadened half-width of the H-alpha line has been measured as a function of time with 5-μsec resolution. From the half-width measurement an electron density on the order of 10^{18} cm^{-3} has been calculated in the first 5 μsec, decreasing to 1–1.5×10^{17} cm^{-3} in 25 μsec. Errors are on the order of 50%.

1. Introduction

Time-resolved spectrograms have been obtained from a 10-m section of the lightning return stroke and analyzed for their qualitative features in Part I. Our knowledge of the physical characteristics of the return stroke can be significantly increased if we perform a quantitative analysis of the data presented in Part I. An excellent review of these techniques has recently been published by Uman (1966).

A quantitative analysis of spectra typically yields temperature, electron density, and relative intensities of line and continuum emission as a function of time. Previously, these techniques have been applied exclusively to the time-integrated spectral emissions of a lightning stroke. Similar techniques are now applied to the first time-resolved return-stroke spectra to derive the time-dependent characteristics of the channel.

[1] Research supported by the Office of Naval Research and the Federal Aviation Agency.

[2] Former affiliation: Institute of Atmospheric Physics, Tucson, Ariz.

[3] Present affiliation: Dept. of Atmospheric Sciences, State University of New York at Albany.

2. Theory

The lightning return stroke in its most luminous phase is characterized by a high temperature (Prueitt, 1963) and a high degree of ionization (Uman *et al.*, 1964a,b). It is not surprising, therefore, as observed in Part I, that all the recorded radiation in the visible spectrum is due to atomic and ionic rather than molecular processes. In the return stroke, the interactions of the electrons with the ions and atoms control the population densities of the bound states, broaden the energy levels via the Stark effect, and cause the continuum and line radiation. Several theoretical implications of these interactions will now be examined.

a. Temperature

A calculation of the temperature in a lightning return stroke requires several important assumptions. The two most important are that the channel is in local thermodynamic equilibrium and that the channel is either optically thin or optically thick.

The assumption of local thermodynamic equilibrium (LTE) requires that the velocity distribution of the electrons be Maxwellian and that the energy levels of

the atoms and ions be populated according to Maxwell-Boltzmann statistics. This is frequently the situation in high density plasmas where collisional effects completely dominate the radiative ones. If this were not the case, then we would be forced to consider the individual reactions occurring within the return stroke and the accompanying rate coefficients and cross sections, many of which are unknown. An alternative solution would be to assume LTE and obtain answers with errors whose magnitude is unknown.

There is perhaps some question as to whether LTE does exist in the lightning return stroke as a function of time and space. Energy is continuously supplied during the return stroke phase and an intense luminosity observed. The channel can nevertheless be considered to be in a quasi-equilibrium state *relative* to the time that the physical parameters of the stroke change. In other words, the pertinent equilibration times are short compared to the time it takes for the temperature to change. Uman (private communication) has shown, using Griem's (1964) criterion, that the equilibration time for NII levels above $n=3$ and for electron and ion kinetic energies in the lightning return stroke is on the order of 0.01 μsec, an insignificant time interval relative to the time resolution of the most recent data.

A distinction is made between LTE and complete LTE. In LTE it is required that the electron velocity distribution be Maxwellian (Cooper, 1966). Upper levels in atoms and ions that are populated according to Maxwell-Boltzmann statistics can then be used to calculate the temperature. This temperature is actually the electron temperature (sometimes called the excitation temperature) of the gas because the electrons dominate the collisional excitation and de-excitation processes.

For higher values of electron density at a fixed temperature, the atomic energy levels populated according to Maxwell-Boltzmann statistics drop lower and lower until at sufficiently high densities they extend to the ground state. The gas is then in complete LTE. All atoms and ions are said to have a thermal population. The electron temperature then becomes simply the temperature of the gas. In further discussions in this paper we will not distinguish between the electron temperature and the temperature.

Under the conditions of LTE the population of a particular level N_n is given by

$$N_n=\frac{Ng_n}{B(T)}\exp(-E_n/kT), \tag{1}$$

where N_n is the number density of atoms in energy level n, N the total number density of atoms, E_n the excitation potential of the nth level, g_n the statistical weight of the nth level, k the Boltzmann constant, T the absolute temperature, and $B(T)$ the partition function, given by

$$B(T)=\sum_i g_i\exp[-E_i/kT], \tag{2}$$

where the summation is over all energy levels.

An experimental determination of the temperature within the lightning return stroke requires a knowledge of the channel opacity. If the channel is optically thin, then the mean free path for absorption of radiation is greater than the channel dimensions. Uman and Orville (1965) have examined the time-integrated lightning spectra and found the channel to be optically thin to singly ionized nitrogen atoms (NII). One time-resolved spectrum has been examined in a similar way and indicates the lightning channel is optically thin (Orville, 1966). This is, however, far from conclusive and data with better wavelength resolution are required to check the assmuption of optical thinness.

The radiated power of an emission line per unit volume of gas at uniform termperaure and density due to transitions from level n to level r measured by a detector is

$$I_{nr}=KN_nA_{nr}h\nu_{nr}, \tag{3}$$

where K is a geometrical factor representing the fraction of light entering the detector, A_{nr} the Einstein coefficient for spontaneous emission, h Planck's constant, and ν_{nr} the frequency of the emitted line. Under the assumption of LTE, N_n can be replaced using (1) to obtain

$$I_{nr}=\frac{KNg_n}{B(T)}A_{nr}h\nu_{nr}(-E_n/kT). \tag{4}$$

A similar equation could be written for another line I_{mp} representing transitions from the level m to the level p. Solving for T, after substituting for the A's ,we obtain (Griem, 1964, p. 270)

$$T=\frac{(E_m-E_n)/k}{\ln\left[\dfrac{I_{nr}\,g_p\,f_{pm}\,\lambda_{nr}^2}{I_{mp}\,g_r\,f_{rn}\,\lambda_{mp}^3}\right]}, \tag{5}$$

where f is the absorption oscillator strength for a particular transition. The intensity ratios are calculated for a line or a series of lines composing an unresolved multiplet. Ratios are calculated for various temperatures to produce a plot of intensity ratio vs temperature. A measurement of the intensity ratio is then sufficient to determine the temperature. Figs. 1 and 2 present theoretical plots of line intensity ratios for the most intense NII multiplets in the visible lightning spectrum. The numerous lines used in the ratio caluclations are listed in Orville (1966). Obviously, errors in the temperature are minimized by selecting as many lines as possible for relative intensity measurements. Criteria for selecting the most suitable lines for temperature measurements are presented in the next section.

b. Errors in the temperature measurement

The criteria for selecting lines in the emission spectrum for relative intensity measurements can be deter-

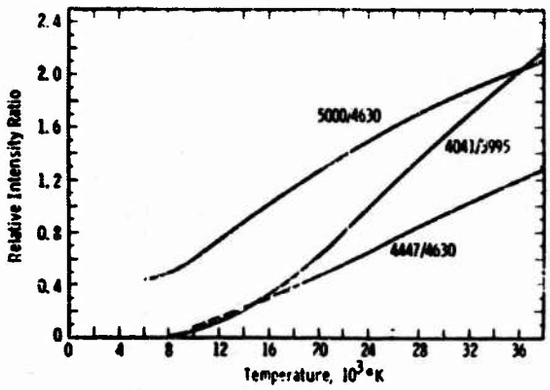

FIG. 1. Theoretical relative intensity ratios as a function of temperature (5000/4630, 4041/3995, 4447/4630).

mined by performing an error analysis on (5). Following Chuang (1965), the result is

$$\frac{\Delta T}{T}=\frac{\ln\left[\left(1+\frac{\Delta R}{R}\right)\Big/\left(1+\frac{\Delta F}{F}\right)\right]}{\frac{E_m-E_n}{kT}-\ln\left[\left(1+\frac{\Delta R}{R}\right)\Big/\left(1+\frac{\Delta F}{F}\right)\right]}, \quad (6)$$

where $1/R$ is the intensity ratio I_{nr}/I_{mp}, $1/F$ the ratio of oscillator strengths f_{pm}/f_{rn}, and ΔT the temperature error resulting from the errors in the intensity ratio ΔR and the ratio of oscillator strengths ΔF. This equation is an explicit form for the error estimate. The error in a temperature measurement is a function of the error in the intensity ratio, of the error in the ratio of oscillator strengths, and of the upper energy levels.

Several criteria for selecting emission lines are obvious. A large E_m-E_n will minimize the $\Delta T/T$. The value of ΔR is minimized by choosing strong lines of approximately equal intensity. It is apparent that ΔT will increase with increasing T, which for good accuracy should be smaller than the quantity $(E_m-E_n)/k$. Note that because of the sign and the nature of the two terms in the denominator of (6), the positive value of ΔT will be larger than the negative value at any given T.

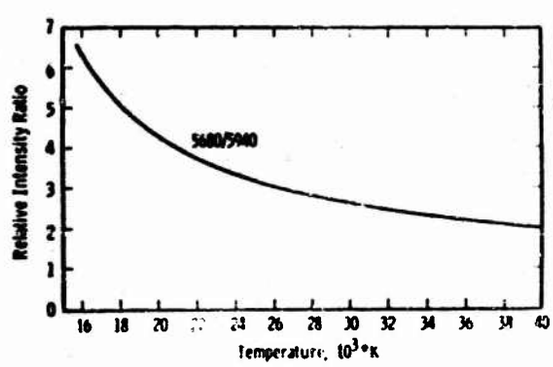

FIG. 2. Same as Fig. 1 except for (5680/5940).

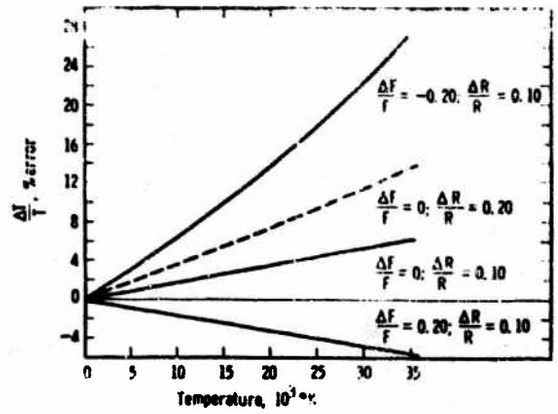

FIG. 3. Temperature errors for the 4041/3995 ratio.

Fig. 3 represents curves obtained by assuming values for the errors in R and F. The difference in the upper energy levels of NII 3995Å and NII 4041Å is 4.6 eV, i.e., $E_m-E_n=4.6$ eV. The solid lines indicate the various errors for a constant ΔR and three values of ΔF. A negative ΔF causes the largest ΔT for a given intensity ratio error. As an application of Fig. 3, consider the NII 3995Å line and the 39th multiplet of singly ionized nitrogen in the 4041Å region which were used by Prueitt (1963) to determine the temperature of a lightning stroke from time-integrated spectra. The lines NII 3995Å and NII 4041Å are one of several pairs used in this paper to calculate the temperature-vs-time curve of a lightning stroke. Assuming Prueitt's (1963) oscillator strengths were correct and his intensity errors were on the order of 20%, the errors in his temperature measurements are given by the dashed line. Thus, in the 24,200–28,400K range reported by him the temperature errors would be on the order of 10%.

c. Relative total numbers

If the temperature-vs-time curve can be determined from a time-resolved spectrum of a lightning return stroke, then it is possible to estimate the relative total number of a particular atomic species, for example NII, as a function of time.

The intensity of an emission line from a volume element v_0 at time t_0 corresponding to temperature T_0 can be written using (4) as

$$I_{nr}(T_0)=K\left(\frac{N(T_0)g_n v_0}{B(T_0)}\right)A_{nr}h\nu_{nr}\exp(-E_n/kT_0). \quad (7)$$

At some other time t and temperature T, the intensity of the *same* line is

$$I_{nr}(T)=K\left(\frac{N(T)g_n v_0}{B(T)}\right)A_{nr}h\nu_{nr}\exp(-E_n/kT). \quad (8)$$

Dividing (8) by (7) and solving for the relative total number between times t and t_0, we obtain

$$\frac{N(T)v}{N(T_0)v_0}=\left(\frac{I_{nr}(T)B(T_0)}{I_{nr}(T_0)B(T)}\right)\exp\left[-E_n\left(\frac{1}{T}-\frac{1}{T_0}\right)/k\right]. \quad (9)$$

Since the spectrograph isolates a section of the lightning return stroke, the vertical dimension of the volume is constant. Any volume change therefore results solely from a change in the channel radius. An increase in the volume by 100 would correspond to a channel radius increase of 10. It follows that if the number density $N(T)$ is known, the relative channel radius within which the particular radiators are contained can be calculated as a function of time.

d. *Electron density measurements*

The first calculation of the electron density in a lightning return stroke was accomplished by using the Saha equation and measuring the relative intensity of neutral and singly ionized lines in time-integrated slitless spectra (Uman *et al.* 1964a, b). In the lightning spectra obtained to date, however, the intensity of neutral lines has been too faint to compare their intensities to singly ionized lines. Even if this measurement could be made, however, there is still the question of whether complete LTE exists in the return-stroke channel, an assumption implicit in the use of the Saha equation. Fortunately, there is another method to measure the electron density which does not require the existence of LTE.

The Stark effect, a line-broadening phenomenon, occurs in lightning and has been observed in the H-beta (Dufay and Dufay, 1949) and H-alpha (Uman and Orville, 1964) lines of the Balmer series. This effect involves the interactions between radiating atoms or ions and charged electrons and ions and is therefore dependent on the charged particle density. In fact, the effect depends primarily on the charge number densities and is only a weak function of temperature. Line widths and profiles of hydrogen lines and many other spectral lines are given by Griem (1964, pp. 445–529). A comparison of measured H-alpha line widths with the calculated line width is sufficient to determine the electron density. The measured line width is obtained by determining the wavelength difference between the two points on the line profile where the intensity has fallen to one-half of the maximum value. This measurement is frequently called the "half width", meaning the full width of the line at half the maximum intensity. In the range of interest for the lightning stroke, the electron densities and half widths are roughly proportional to each other.

If it becomes possible to determine the electron density by the Saha equation and by the Stark effect, the degree of agreement will provide a means of checking the existence of LTE in the lightning return stroke (Uman, 1966).

TABLE 1. Photographic data appropriate to the lightning stroke analyses.

Flash	Number of recorded strokes	Date	Camera*	Film	Time-resolution (μsec)
A	2	14 July 65	LA	Agfa Isopan Record	5
B	1	14 July 65	LA	Agfa Isopan Record	5
C	2	11 Sept. 65	BW	2475**	5
D	1	11 Sept. 65	BW	2475	5
E	1	8 Aug. 66	BW	2475	5
F	5	8 Aug. 66	BW	2475	5
G	1	13 Aug. 66	BW	2475	2
H	1	18 Aug. 66	BW	2475	2

* LA = Los Alamos Model 104; BW = Beckman & Whitley Model 318.
** Eastman Kodak 2475 Recording film.

e. *Measurement of relative line intensities*

The response of a photographic emulsion at a particular wavelength depends on the intensity of the source at the particular wavelength, the sensitivity of the emulsion at the same wavelength, the time of exposure, the humidity and temperature conditions under which the emulsion is exposed, and the time, type, and temperature of the development it undergoes, not to mention other effects such as reciprocity failure intermittency, atmospheric absorption, and vignetting. In spite of these numerous sources of error, it is possible to obtain relative intensity measurements as accurate as ±10%. A few of the photographic techniques have been discussed in Part I. Additional techniques of obtaining relative line intensities and some of the inherent problems are discussed in Orville (1966).

3. Data analysis

a. *Temperature*

The temperature is calculated under the assumption that the return-stroke channel is optically thin and in LTE. It is also necessary to assume that at a given time the temperature is approximately constant across the cross section.

Temperature profiles of different lightning strokes are presented in Figs. 4–11. The error in the time scale is approximately 5 μsec. Technical data such as film type, time resolution, etc., are summarized for convenience in Table 1.

In Fig. 4, two temperature curves are plotted which were obtained from the two return strokes intense enough to be recorded by the Los Alamos Model 104 camera. The time sequence in which the strokes occurred is unknown, and so the most intense stroke is arbitrarily labeled A_1 and the second stroke A_2. The spectrum of stroke A_1 was presented in Part I, Fig. 4, and its uncor-

rected microphotometer tracings in Part I, Figs. 11 and 12.

The temperature within the strokes was determined by measuring the relative intensity of the 4630Å, 5000Å NII multiplets and then finding the corresponding temperature in Fig. 1. The horizontal bars in the temperature curve signify that the plotted value is really an "average temperature" for the 5 μsec in which the exposure occurred. The vertical error bars have been obtained by estimating the error in the measured intensity ratio of 5000/4630 and finding the corresponding temperature variation. This corresponds to using (6) and setting $\Delta F=0$. Note that the positive error bars are longer than the negative error bars due to the sign and nature of the two terms in the denominator of (6). Relative intensity errors were established as 10-20% depending upon the intensity of the line above the background continuum.

Only four points could be plotted in stroke A_2 because of the weak exposure. There is no indication of a temperature rise in the 0–10 μsec period. It is not known whether the temperature rise in A_1 in the first 10 μsec is real. The stroke may not be optically thin in the early phase and, consequently, temperatures derived from (5) would not be valid.

Fig. 5 presents a temperature curve from a flash producing one recorded spectrum. The first five temperature values are derived from the 4041/3995 ratio. The temperature dip in the 5–10 μsec range may or may not be real since the error flags allow for a smooth monotonically decreasing curve. The 4630 and 5000Å multiplets are too intense to yield relative intensities before 20 μsec but then fall within the exposure range of the film after 20 μsec. Note that the overlapping temperature measurements agree in the 20–25 μsec time to within experimental error.

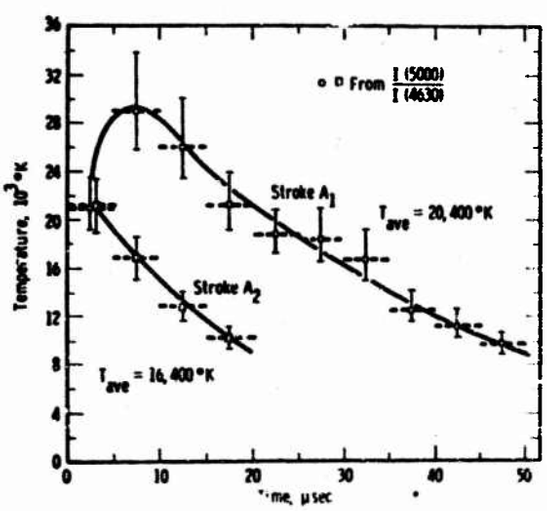

FIG. 4. Flash A: Stroke temperature as a function of time. The spectrum of stroke A_1 is reproduced in Part I, Fig. 4, and its microphotometer traces in Part I, Figs. 11 and 12.

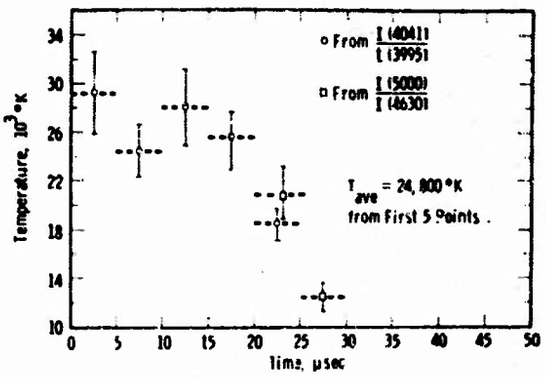

FIG. 5. Flash B: Stroke temperature as a function of time.

Flash C in Fig. 6 was observed at a distance of approximately 3–6 km and two strokes were recorded. The exposure was weak and therefore only three temperature points are plotted. Stroke C_1 corresponds to the more intense spectrum and C_2 to the weaker. The rise in temperature calculated for C_1 may once again be a spurious value; nevertheless, it occurs for the most intense stroke in agreement with the flash A analysis.

Berger (1962) and Berger and Vogelsanger (1965) have observed that the current rise-time measured at the ground is slower in the first return stroke than in subsequent strokes in a flash. If the sequence of strokes in flashes A and C is correct, the temperature rise in the first stroke is slower than in the second stroke. Whether or not the temperature has the same temporal pattern as the current at ground cannot be confirmed with these few data. Only correlated temperature and current measurements on the same time scale can answer this question.

Flash D in Fig. 7 is composed of only one recorded stroke. There is an indication of a temperature rise but a line can be drawn within the error flags indicating a monotonic decrease.

The highest recorded temperature is reported in flash E, Fig. 8. Error bars, however, indicate the true value may be anywhere between 31,000 and 40,000K.

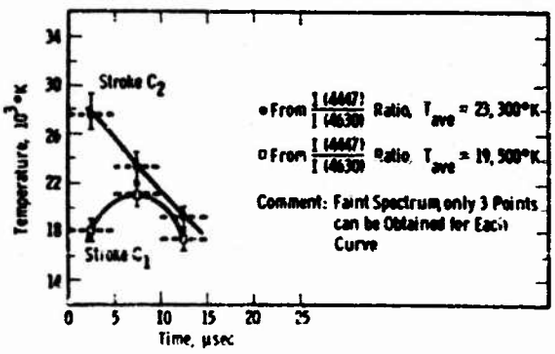

FIG. 6. Flash C: Stroke temperature as a function of time.

Fig. 9 is of special interest because flash F produced a branch spectrum in addition to the spectrum of the main channel. The spectrum is reproduced in Part I, Fig. 6. In the first 5 μsec we have the temperature of the main channel and of a branch. It is perhaps not surprising that the branch is significantly cooler. The large error bars are indicative of the increasing uncertainty in measuring high temperatures when the upper excitation levels of two lines differ by only a few electron volts. The increasing error with increasing temperature was discussed in connection with Fig. 3. That the error in calculating the temperature from the 5680/5940 ratio is a function of temperature is very evident in Fig. 2. At increasing temperatures, a small error in the relative intensity measurement produces a large uncertainty in temperature. This is evident in the first return-stroke temperatures in Fig. 9.

The last two temperature curves presented in Figs. 10 and 11 were obtained with 2-μsec resolution. A higher time resolution was used to determine if a temperature rise could be detected with several significant points in the early phase of the return stroke, i.e., during the first 10 μsec. It is clear that in the 2 one-stroke flashes, G and H, a temperature rise is not detected. The successful analysis of these two spectra with 2-μsec resolution still leaves unanswered the question of whether some lightning return strokes have temperature rise times on the order of 5–10 μsec as indicated by strokes A_1 and C_1.

No peak temperatures were measured in excess of 36,000K. The peak temperature in five of the ten spectra is in the 28,000–31,000K range despite the use of different spectrographs and multiplet intensity ratios for the measurements. Mak (1960) measured the maximum channel temperature of a short spark discharge in air and found that the peak temperature varies very little with rate of current rise in the discharge. Various current rise times produced peak temperatures in the range of 26,000–33,000K.

It is possible to obtain an "average" value for the temperature by integrating the time-resolved line intensities. This is done in the following manner. Analysis of microphotometer traces made every 5 μsec produces relative intensity values every 5 μsec. If these individual intensity values are summed, we obtain a number which represents the relative intensity of the line if the spectrum had *not* been streaked. [This is the same relative intensity used by Prueitt (1963) in his analysis of "stroke-integrated" spectra.] Relative intensities that

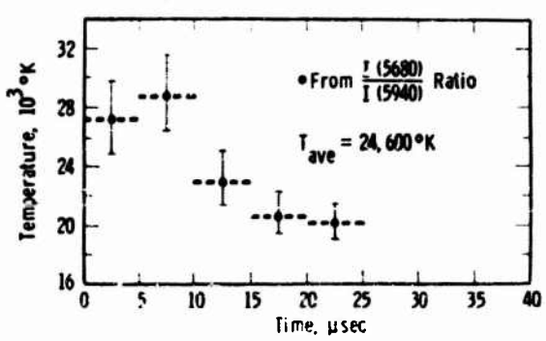

FIG. 7. Flash D: Stroke temperature as a function of time.

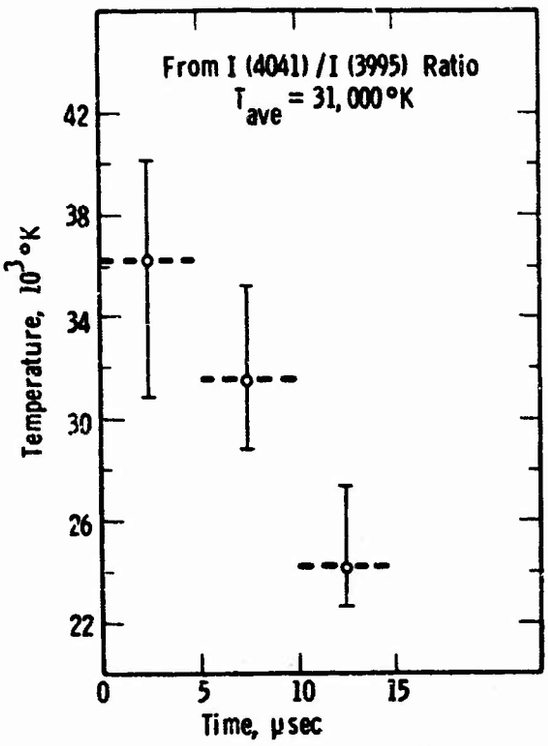

FIG. 8. Flash E: Stroke temperature as a function of time. Highest recorded temperature is in the return stroke, but note the large error flags.

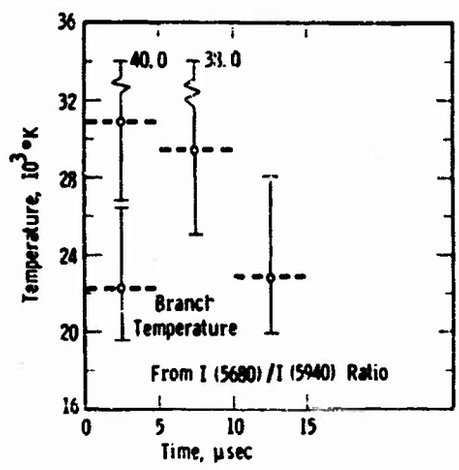

FIG. 9. Flash F: Stroke temperature as a function of time. Note that a branch temperature has been calculated and is significantly cooler than the temperature in the return-stroke channel. The spectrum of this stroke is reproduced in Part I, Fig. 6.

are summed in this manner can be compared to calculate an "average temperature." This value T_{ave} can then be compared with Prueitt's (1963) values. His temperature, determined essentially by comparing the relative intensity of two multiplets, produced a range from 22,200–33,000°K. Note carefully that this range is different from the values termed by him as the "weighted average temperature," and often quoted in the literature as a 24,200–28,400°K range for the lightning return stroke. Seven of the eight T_{ave}'s presented in this paper range from 19,000–31,000°K, in reasonably good agreement with Prueitt's 22,200–33,000°K values. The remaining T_{ave}, that of stroke A_2, is in poor agreement. It is not unreasonable that A_2 was indeed a "cooler" discharge, although another explanation is that I underestimated the experimental error in analyzing the spectrum of A_2.

Uman (1964) determined that the temperatures presented by Prueitt are within 10% of the peak value. The time-resolved temperature curves do not necessarily disagree with this conclusion. Uman examined the 4040/3995 ratio and concluded that the temperature calculated from this relative intensity ratio should be within 10% of the peak vlaue. Within experimental error, strokes B and E agree with Uman's analysis. It is unfortunate that only two spectra have been obtained from which the 4041/3995 ratio could be measured. Other spectra produce integrated temperatures which are more than 10% from the peak value. These were determined from lines having lower excitation potentials, the ions consequently emitting for longer times. Thus, the integrated temperatures will be further from the peak value. The time during which the spectral emissions are integrated in an exposure is dependent on the distance to the stroke as well as other variables.

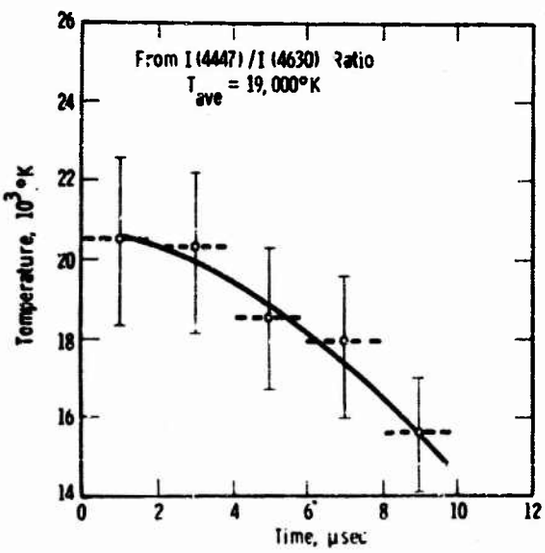

FIG. 10. Flash G: Stroke temperature as a function of time. Note 2-μsec resolution.

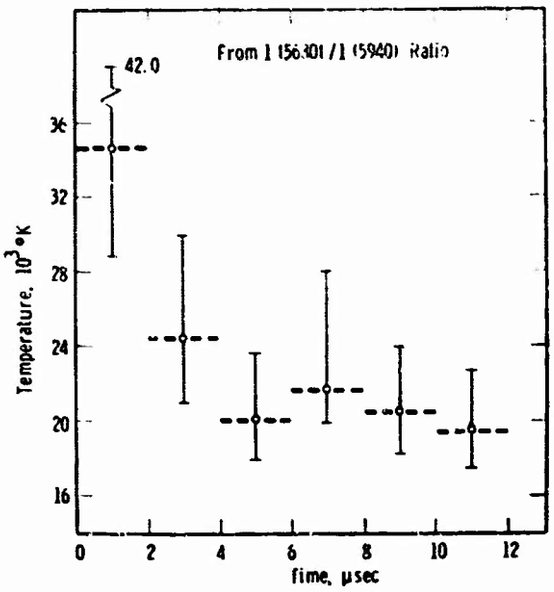

FIG. 11. Flash H: Stroke temperature as a function of time. Note 2-μsec resolution.

Thus, close strokes will have a longer integration time and produce "average" temperatures further from the peak value than those of more distant strokes.

A knowledge of the time-dependent temperature curve allows us to answer a question that was raised by Brook in 1963 at the Third International Conference on Atmospheric and Space Electricity, Montreaux, Switzerland (see Coroniti, 1965, p. 385). At this meeting, Salanave presented an unusual spectrogram in which a flash containing ten strokes had been time-resolved to produce an integrated spectrum of *each* stroke. A time resolution of milliseconds had separated the flash into its component strokes but was, of course, inadequate to time-resolve the stroke. Eight of the ten integrated spectra were suitable for analysis and temperature values were obtained from NII lines using the techniques developed by Prueitt (1963). The surprising result is that (with one exception) the temperature derived for each stroke monotonically *increased* from 21,000–27,000°K as the stroke number increased. Brook noted that this steady increase is apparently contradicted by the observation that in flashes composed of more than one stroke, the current in the first stroke is the greatest and *decreases* as the stroke number *increases*. If the current decreases with increasing stroke number, we would expect the exposure density of each spectrum to decrease with increasing stroke number. Salvanae (private communication) has re-examined his data and found that in seven of the eight analyzed spectra the density monotonically decreases and the "average temperature" monotonically increases with increasing stroke number. The physical explanation for these observations is the following.

Salanave's data is time-integrated over the duration of the lightning return stroke. The first stroke, usually the most luminous, is integrated for the longest period of time. Hence, a temperature determination from the NII lines yields a lower temperature. This temperature, we realize, is an "average temperature" determined from the integrated exposure of NII emission lines on film. Subsequent strokes to the first stroke deliver less charge, are less luminous, and the spectral emissions are recorded for a shorter period of time. The "average temperature" therefore *increases* as the integrated exposure time decreases and approaches the time of maximum temperature in the return stroke. The value of 27,000K for the last of the eight strokes agrees well with the maximum temperatures presented in this paper.

b. Relative total numbers

Knowing the temperature-vs-time curve for a particular stroke, we can calculate the relative total number from (9). Using the relative intensities from the NII 4630 multiplet in stroke A_1, the relative total number of NII ions has been calculated as a function of time. The values are presented in Fig. 12 and are expressed relative to the amount of NII present at 10 μsec.

The decreasing amount of NII in the first 10 μsec may represent the effects of increasing the temperature from 21,000K in the 0–5 μsec range to 28,000K in the 5–10 μsec range (see Fig. 4). The depletion of NII ions can be attributed to an increase of NIII ions at the expense of the NII ions. NIII ions exist in the lightning return-stroke channel but have not been detected because of their high excitation energies for optical emission.

The increase of the total number of NII ions beyond 10 μsec is undoubtedly associated with a slowly expanding channel following the rapid expansion phase. More atoms are included in the channel and we see a corresponding increase in the total number of NII ions.

c. Normalized relative intensities

Relative intensities of NII ions were measured as a function of time in order to calculate the temperature-time curves in a previous section. These relative intensities can be normalized and plotted as a function of time. Fig. 13 presents the results for Flash A composed of strokes A_1 and A_2. Note in A_1 that the intensity of lines from the higher excitation potential has a steeper slope in the first 10 μsec relative to the intensity of lines from the lower excitation potential. This is not surprising when we recall the rising temperature calculated and presented in Fig. 4. An intensity rise is not detected in the NII radiation from A_2 and a temperature rise was not calculated. Both A_1 and A_2 show the expected fast intensity decrease of NII lines originating from higher excitation potentials relative to lines originating from lower excitation potentials.

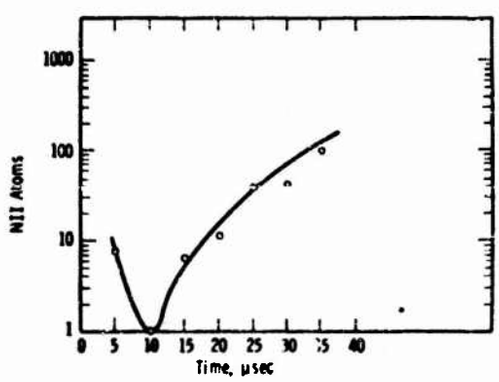

FIG. 12. Relative total number of NII ions as a function of time (stroke A_1).

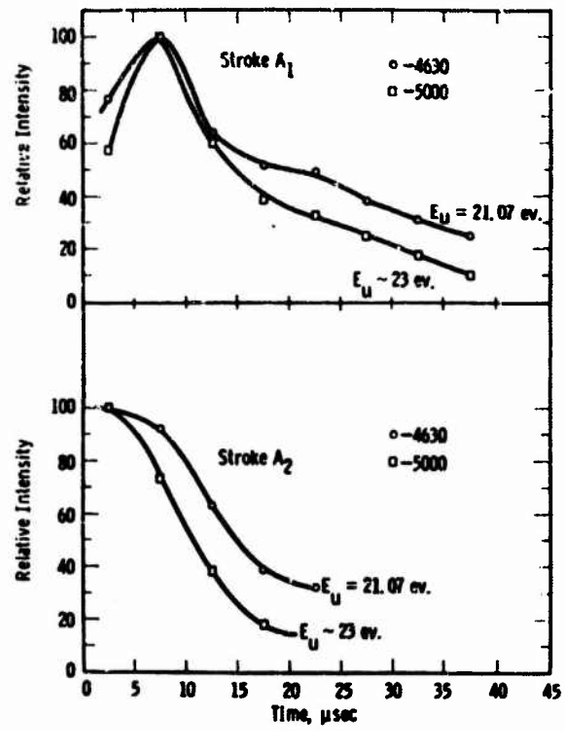

FIG. 13. Normalized relative intensity curves for two NII multiplets (4630, 5000).

That the rise and fall of the NII 4630, NII 5000 intensities follow the temperature curves is not surprising when we consider the range of temperatures involved. On the other hand, if NI emissions could be measured, we would expect their relative intensity to peak at a time following the NII peak intensity when the temperature is falling.

d. Continuum radiation

An interesting feature of all lightning spectra is the background continuum radiation that apparently emanates from the entire length of the return-stroke channel (Salanave *et al.*, 1962; Orville and Uman, 1965).

Several time-dependent curves for the continuum radiation are presented in Figs. 14, 15 and 16.

The continuum intensity for stroke A_1 is plotted at two different wavelengths in Fig. 14. Peak intensity is reached in 10 μsec and decays to its half value in approximately 100 μsec. The half-intensity point is different at separate wavelengths.

Fig. 15 indicates the peak intensity does not occur until 15 μsec. It follows the NII peak intensity by approximately 10 μsec. The sequence of maximum NII radiation followed by maximum continuum radiation was first reported by Krider (1965). A half-value cannot be measured below 65% of the peak intensity. It appears, nevertheless, that the half-value would occur at approximately 100 μsec.

Fig. 16 presents a continuum trace at 4900Å from the spectrum reproduced in Part I, Fig. 5. The first 25 μsec of the continuum curve resembles the previous two curves. Beyond 25 μsec, however, there is an enhancement of the continuum emission followed by a monotonically decreasing intensity. The effect of the enhancement is to produce a local minimum of a few per cent in the intensity. A possible explanation for this enhancement was discussed in Part I and believed to be evidence for a branch point existing above the isolated section of the return-stroke channel. The intensity half-value occurs at approximately 120 μsec. This value is later than the half-value for 4900Å in stroke A_1 and may be due to the local intensity enhancement in the channel which acts to delay the intensity decrease.

Several conclusions are apparent in these data. Clearly, the continuum radiation reaches peak intensity in 10–15 μsec, that is, 5–10 μsec after NII reaches peak intensity. We recall in Part I that the H-alpha intensity is most intense in the 20–50 μsec range. The sequence of peak intensities is then: NII radiation followed by continuum which in turn is followed by the peaking of neutral hydrogen lines. This sequence agrees with a channel characterized by a decreasing temperature and was first observed by Krider (1965) when he studied

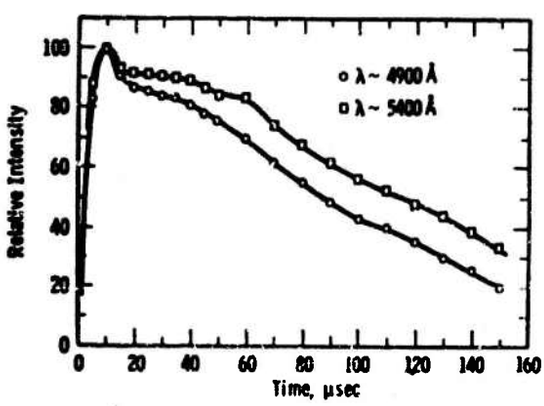

FIG. 14. Continuum intensity as a function of time for stroke A_1.

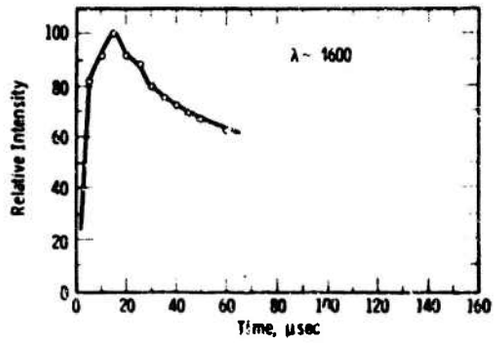

FIG. 15. Continuum intensity as a function of time. Peak emissions occur at approximately 15 μsec.

the time-dependent spectral emissions from the entire visible return-stroke channel. A final observation is that the continuum emission decays to its half value in approximately 100 μsec.

The source of the continuum radiation remains unknown. Salanave's time-integrated spectra were analyzed (Orville and Uman, 1965) and it was concluded that the source was neither blackbody radiation or electron-ion bremsstrahlung emitted at a constant temperature. Uman (1966) has pointed out that the effective excitation potential of the continuum radiation lies between that of the ions and the neutrals and may therefore be due to radiative recombination or radiative attachment.

e. H-alpha electron density measurements

The emissions from hydrogen in lightning are of particular interest. Zhivlyuk and Mandel'shtam (1961) observed the broadening of H-alpha and H-beta lines in data obtained with slit spectrographs and estimated an electron density $\geqslant 10^{17}$ cm^{-3}. These estimates were all made from spectra obtained by exposure to one or more flashes.

The first time-resolved spectrum of a lightning flash (Salanave, 1961) revealed a strong H-alpha line, which upon examination appeared to have a half-width of 15Å corresponding to an electron density of 2×10^{17} cm^{-3}

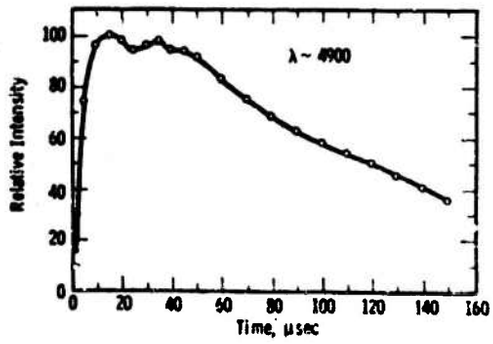

FIG. 16. Continuum intensity as a function of time. Note the local minimum near 25 μsec. This is from the spectrum reproduced in Part I, Fig. 5.

(Uman and Orville, 1964). Subsequent analysis has shown that the instrument broadening was underestimated and that the half-width was probably closer to 10 or 12Å. This is a small correction because the Stark broadening is approximately proportional to the electron density in this range of densities. Thus, a 50% error in the calculated value of 2×10^{17} cm^{-3} only reduces this to 1×10^{17} cm^{-3} or increases it to 3×10^{17} cm^{-3}.

The first time-resolved spectra of the return stroke have yielded two spectra with H-alpha emissions that can be quantitatively analyzed. These spectra are reproduced in Part I, Figs. 5 and 6. Other recordings of H-alpha emissions are either overexposed (Part I, Fig. 7) or underexposed (Part I, Fig. 8) and therefore unsuitable for quantitative analysis.

The H-alpha line in Part I, Fig. 5, has been analyzed for the relative intensity as a function of time. Fig. 17 indicates that the peak H-alpha emissions occurred approximately 50 μsec after the first light was recorded from the return-stroke channel. The emissions monotonically decrease and are not plotted beyond 140 μsec.

No electron density measurements are available from this spectrum (Part I, Fig. 5) because of a broad instrument profile superimposed on the Stark broadened H-alpha emissions. The instrument profile in this spectrum is about 25Å and completely dominates the Stark width in the H-alpha line. It is important to note that the instrument profile in these data is composed of broadening due to the instrument plus the broadening due to the orientation of the return stroke across the slit. Thus, the "instrument broadening" varies from stroke to stroke!

The spectrum reproduced in Part I, Fig. 6, is properly exposed for intensity measurements and has a narrow "instrument broadening." The wavelength resolution is on the order of 8–10Å. It is therefore possible to measure both the relative intensity and the half-width as a function of time. Fig. 17 presents these results.

The H-alpha relative intensity increases to a maximum at 15–20 μsec, decreases to a local minimum at 30–35 μsec, and then decreases monotonically after a small maximum at 40–45 μsec. If one knows to look for a local minimum at approximately 30 μsec, it is barely perceptible in the print reproduced in Part I, Fig. 6. The second maximum is probably associated with the branch detected in this spectrum. As discussed in Part I, the effect of a branch is to provide an additional source of charge to the return-stroke channel and thus cause an increase in the channel luminosity which is apparent at approximately 40 μsec. At this time, only the H-alpha emissions are recorded and the enhanced luminosity is therefore only detected in this line. A similar phenomenon was discussed in connection with the enhanced continuum of Part I, Fig. 5. It is interesting that in the two cases in which branch spectra have been recorded, indicating a junction point above the isolated channel section, an enhanced luminosity has been detected at a later time in the continuum in the first spectrum and in the H-alpha emissions in the second spectrum. It is likely that the enhanced luminosity occurs in all spectral features but is not necessarily detected.

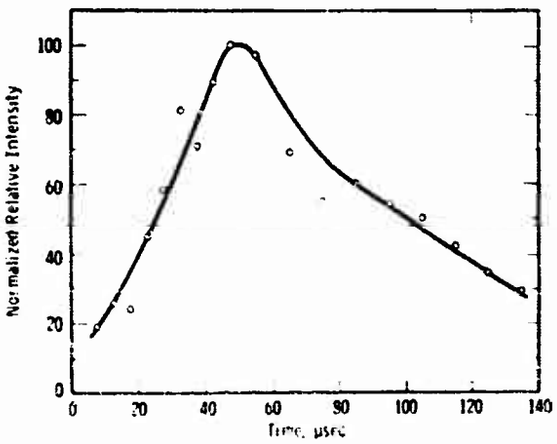

FIG. 17. H-alpha relative intensity as a function of time. The curve was obtained from the spectrum reproduced in Part I, Fig. 5.

The half-width measurements presented in Fig. 17 were obtained in the following manner. A measurement of the full line width at one-half the maximum intensity produced an uncorrected "half-width" containing the effects of the Stark broadening and the instrument broadening. The instrument broadening can be determined by first noting the narrow line on the long wavelength side of the H-alpha line which is recorded for approximately 20 μsec (Part I, Fig. 6). This is the NII 6611Å line which has a Stark width of approximately 3Å or less for temperatures <30,000K and electron densities $<10^{18}$ cm^{-3} (Griem, 1964, p. 465). The half-width of NII 6611 was variable but typically 10Å and therefore largely due to instrument broadening. By accepting the NII 6611 line as a measure of the instrument broadening, we can subtract this value from the H-alpha width to obtain the width due to the Stark effect.

Whether the line and instrument profiles are Gaussian or Lorentzian or a combination or none of these determines how the line widths are separated. The H-alpha profile can be approximated by the Lorentz dispersion curve (Griem, 1964, p. 305). The "instrument profile" is a quantity that varies from stroke to stroke as previously discussed. Assuming the instrument profile is either Gaussian or Lorentzian makes little error in the first 20 μsec when the total half-width is on the order of 30–50Å and the instrument width is 10Å. Beyond 20 μsec the difference is important. A laboratory experiment on a long spark in air similar to lightning indicates which assumption is preferred (Orville *et al.*, 1967). In this experiment it was found that by assuming a Lorentz profile for the instrument function, an electron density was obtained that was consistent with independent measurements (Orville, 1966); namely, the calculated electron density indicated atmospheric pressure was attained in the spark at the same time the luminous

spark channel was observed to stop its rapid expansion. Therefore, it appears the instrument function can be approximated by a Lorentz profile. The total width is then

$$w_t = w_l + w_i, \tag{10}$$

where w_l is the line width and w_i is the instrument width. The total line width w_t is measured from microphotometer traces of H-alpha, the instrument broadening w_i is measured from similar traces of NII 6611, and the Stark width w_l is then determined.

The top curve in Fig. 17 shows that the H-alpha Stark width is on the order of 40Å in the first 5 μsec and decreases quickly to values on the order of 10Å. Beyond 50 μsec it is impossible to accurately determine the half-width because the instrument broadening is approximately the same as the measured total line width, i.e., $w_t = w_i$. It is possible, however, to say that the H-alpha half width is less than 10Å for times exceeding 50 μsec.

Knowing the half-width, the electron density can be calculated as a function of time (Griem, 1964, p. 538). In Fig. 18 an electron density on the order of 10^{18} cm^{-3} exists in the first 5 μsec and then decreases quickly to a value between 1×10^{17} cm^{-3} and 1.5×10^{17} cm^{-3}. Errors are on the order of 50%. Beyond 50 μsec a half width of 10Å or less requires that the electron density be less than 1.5×10^{17} cm^{-3}.

A knowledge of the return-stroke temperature and electron density enables us to understand the low H-alpha intensity recorded in the first 10 μsec. It is undoubtedly associated with the high temperatures and electron densities prevailing at these times. The high temperature ionizes many of the hydrogen atoms and the Stark effect on the remaining atoms broadens the H-alpha emissions so that they tend to blend into the background continuum radiation.

The electron densities calculated here are similar to those calculated from time-resolved spectra of long air sparks (Orville *et al.*, 1967). Electron densities in the early phase of the long air spark were on the order of 10^{18} cm^{-3} decreasing to 2×10^{17} cm^{-3} in about 5 μsec. The decay in the lightning return stroke is slower because the energy input is greater and a larger channel expansion is involved.

Previous electron density estimates in lightning were made from time-integrated stroke spectra. Uman *et al.* (1964 a, b) obtained values of 3×10^{18} cm^{-3}. This calculation, however, rested upon the assumption that the spectral lines of OI, NI and NII were primarily emitted at temperatures near 24,000K, an assumption which is not supported by the first time-resolved return-stroke spectra. Uman (1966) has shown that in view of this most recent data the value of 3×10^{18} cm^{-3} should be considered as an upper limit to the electron density for temperatures on the order of 24,000K. The maximum electron density calculated in this paper is consistent with Uman's conclusion.

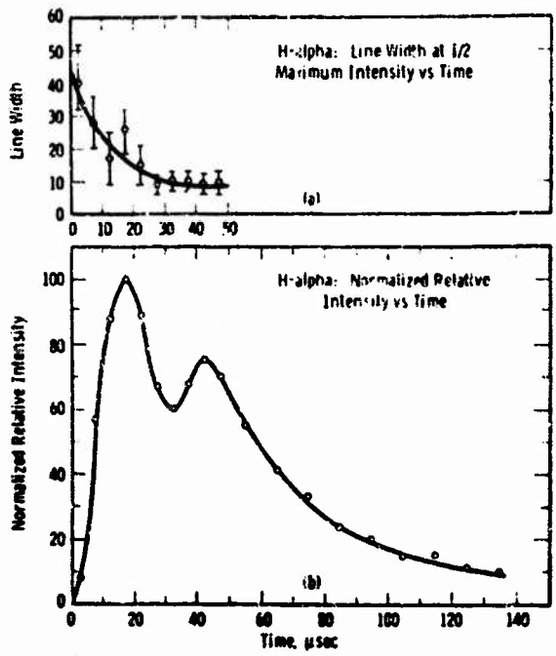

FIG. 18. H-alpha half width, a., and the corresponding relative intensity, b., as a function of time. The spectrum from which these were obtained is reproduced in Part I, Fig. 6.

The fact that the electron density decreases in 25 μsec to $1\text{–}1.5\times10^{17}$ cm^{-3} and remains constant is not surprising. Drellishak (1964) assumed LTE and calculated an electron density in nitrogen between 1×10^{17} and 2×10^{17} cm^{-3} for temperatures between 14,000 and 35,000K. Uman (1966) has pointed out that "since the Stark profiles are strong functions of electron density and only weak functions of temperature, the H-alpha profiles would not be expected to change much from the end of the shock-wave phase when the channel has attained a near-atmospheric pressure until the time at which the temperature falls below 14,000K." Thus, during the times that the electron density is constant in Fig. 18, we can assume that the channel is near atmospheric pressure and the temperature >14,000K.

If we compare Figs. 17 and 18 we note that the time when the electron density values are between 1×10^{17} and 3×10^{17} cm^{-3} corresponds to the period of maximum emissions from H-alpha. It is therefore not surprising that Uman and Orville (1964) obtained excellent agreement when integrated experimental H-alpha profiles were compared with theoretical H-alpha profiles to obtain electron density measurements on the order of 2×10^{17} cm^{-3}.

4. Conclusions and summary

Temperatures in a 10-m section of ten lightning return strokes have been calculated with 2-μsec resolution (2 strokes) and 5-μsec resolution (8 strokes). A temperature rise in two of the strokes has been detected

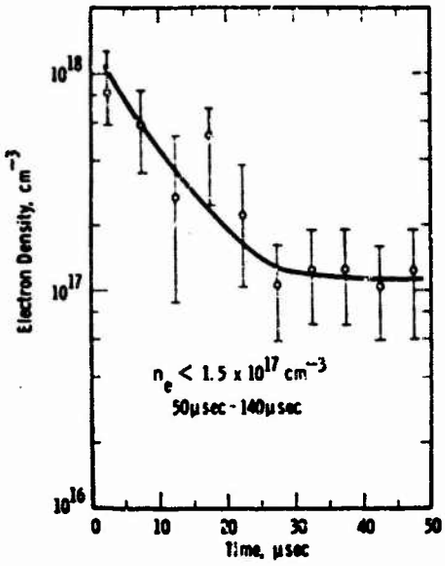

FIG. 19. Electron density as a function of time calculated from the measured half widths of H-alpha presented in Fig. 18.

in the first 10 μsec with data having 5-μsec resolution. Two strokes were recorded with 2-μsec resolution and the resulting temperature-time curve was monotonically decreasing. This leaves unanswered, however, whether *some* strokes do contain a slow temperature rise on the order of 10 μsec. It appears that typical peak temperatures in the lightning return stroke are on the order of 28,000–31,000K.

The source of the continuum radiation remains unknown, but the time characteristics of these emissions indicate it is probably associated with radiative recombination or radiative attachment

Relative intensity curves for the H-alpha emissions have been obtained in two cases with peak emissions at 20 μsec in one spectrum, and at 50 μsec in the second. The single H-alpha line suitable for electron density measurements has yielded a value of 8×10^{17} cm^{-3} in the first 5 μsec, decreasing to 1–1.5×10^{17} cm^{-3} at 25 μsec, and remaining approximately constant to 50 μsec. Beyond 50 μsec the exact electron density cannot be determined because the instrument broadening exceeds the Stark broadening.

It is unfortunate that the current characteristics in the return strokes studied here are unknown. If the enhanced luminosity recorded in a few of the time-resolved spectra is due to a branch joining the return stroke above the isolated section, then we would expect a current increase to correlate with the observed spectral enhancements. The successful simultaneous recording of spectral emissions and currents in a lightning return stroke on the same time scale opens the way to numerous calculations that will not be detailed in this conclusion. It is, however, inevitable that this lightning experiment will soon be successfully performed.

A word of caution is in order in accepting the data in Parts I and II of this paper and applying it to lightning in general. First, it should be clear that too few spectra have been obtained to know what the characteristics of the typical" stroke" are, if indeed such a typical stroke exists. Second, the so-called "typical stroke" is partly defined by the instrument studying the phenomenon and not necessarily by what is happening in nature. Any system using film as a recording device necessarily selects those strokes which produce images falling within the range of the emulsion sensitivity. The variation of distances to strokes tends to randomize the recorded data in the sense that distant intense strokes will be recorded along with close low intensity strokes. Both spectra yield meaningful physical parameters which contribute towards the average values of lightning.

Acknowledgments. I wish to express my sincere appreciation to Dr. Martin A. Uman who provided enthusiastic assistance and astute insight into problems associated with the analysis and interpretation of the lightning data. All spectra were obtained at the Institute of Atmsopheric Physics, Tucson, Ariz. The use of a Hilger and Watts microphotometer was generously made available by the Kitt Peak National Observatory.

REFERENCES

Berger, K., 1962: Front duration and current steepness of lightning strokes to earth. *Gas Discharges and the Electricity Supply Industry*, London, Butterworth, 63–72.

——, and E. Vogelsanger, 1965: Messungen und Resultate der Blitzforschung der Jahre 1955–1963 auf dem Monte San Salvatore. *Bull. Schweis. Elektro. Ver.*, 56, 2–22.

Chuang, H., 1965: Uncertainties in the measurement of helium plasma temperature by the relative intensity method. *Appl. Optics*, 4, 1589–1592.

Cooper, J., 1966: Plasma spectroscopy. *Reports on Progress in Physics*, Vol. 24, Part I, The Institute of Physics and The Physical Society, 35–130.

Coroniti, S. C., 1965: *Problems of Atmospheric and Space Electricity*. New York, Elsevier, 385–356.

Hrellishak, K. S., 1964: Equilibrium composition and thermodynamic properties of air to 24,000°K. RAND Corp. Res. Memo. RM-1543 (Defense Documentation Center, AD-84502).

Dufay, M., and J. Dufay, 1949: Spectres des éclairs photographies au prisme-objectif. *Compt. Rend.*, 229, 838.

Griem, H. R., 1964: *Plasma Spectroscopy*. New York, McGraw Hill, 580 pp.

Krider, E. P., 1965: Time-resolved spectral emissions from individual return strokes in lightning discharges. *J. Geophys. Res.*, 70, 2459–2460.

Mak, A. A., 1960: The channel temperature of a spark discharge in air. *Opt. Spectry. (USSR)*, 8, 145.

Orville, R. E., 1966: A spectral study of lightning strokes. Ph.D. thesis, University of Arizona, Tucson.

——, and M. A. Uman, 1965: The optical continuum of lightning. *J. Geophys. Res.*, 70, 279–282.

——, —— and A. M. Sletten, 1967: Temperature and electron density in long air sparks. *J. Appl. Phys.*, 38, 895–896.

Prueitt, M. L., 1963: The excitation temperature of lightning. *J. Geophys. Res.*, 68, 803–811

Salanave, L. E., 1961: The optical spectrum of lightning. *Science*, **134**, 3195-1399.

——, R. E. Orville and C. N. Richards, 1962: Slitless spectra of lightning in the region from 3850 to 6900 Ångstroms. *J. Geophys. Res.*, **67**, 1877–1882.

Uman, M. A., 1964: The peak temperature of lightning. *J. Atmos. Terr. Phys.*, **26**, 123–128.

——, 1966: Quantitative lightning spectroscopy. *Spectrum*, **3**, 102–110, 154.

——, and R. E. Ovrille, 1964: Electron density measurement in lightning from stark-broadening of H_α. *J. Geophys. Res.*, **69**, 5151–5154.

——, and ——, 1965: The opacity of lightning. *J. Geophys. Res.*, **70**, 5491–5497.

——, —— and L. E. Salanave, 1964a: The density, pressure, and particle distribution in a lightning stroke near peak temperature. *J. Atmos. Sci.*, **21**, 306–310.

——, —— and ——, 1964b: The mass density, pressure, and electron density in three lightning strokes near peak temperature. *J. Geophys. Res.*, **69**, 5423–5424.

Zhivlyuk, Yu N., and S. L. Mandel'shtam, 1961: On the temperature of lightning and force of thunder. *Sovist Physics JETP*, **13**, 338–340.

Reprinted from JOURNAL OF ATMOSPHERIC SCIENCES, Vol. 25, No. 5, September, 1968, pp. 852-856
American Meteorological Society
Printed in U. S. A.

A High-Speed Time-Resolved Spectroscopic Study of the Lightning Return Stroke: Part III. A Time-Dependent Model

RICHARD E. ORVILLE

Westinghouse Research Laboratories, Pittsburgh, Pa.

A High-Speed Time-Resolved Spectroscopic Study of the Lightning Return Stroke: Part III. A Time-Dependent Model[1]

RICHARD E. ORVILLE[2]

Westinghouse Research Laboratories, Pittsburgh, Pa.

(Manuscript received 15 December 1967)

ABSTRACT

A model of the lightning return stroke is developed using the experimental data presented in Parts I and II and Gilmore's tables for the composition of dry air in thermodynamic equilibrium. The temperature, electron density, pressure, relative mass density, per cent ionization, and specie concentration in a 10-m section of a model-return stroke are given with 5-μsec resolution from 0–30 μsec. During this period, the temperature decreases from 30,000 to 16,000K and the electron density decreases from 10^{18} to 1.5×10^{17} cm^{-3}. The channel is characterized by an average pressure of 8 atm in the first 5 μsec and attains atmospheric pressure at approximately 20 μsec. A minimum relative mass density of 3×10^{-4} is attained at the same time. Per cent ionization is on the order of 100 in the first 15 μsec and then decreases.

The largest nitrogen specie concentration in the 0–15 μsec period is NII, followed by NIII, which in turn is followed by NI. All three concentrations decrease in the 0–15 μsec time period. In the 15–30 μsec period the NI concentration increases, the NII concentration attains a quasi-equilibrium, and the NIII concentration continues to decrease rapidly. The salient characteristics of the model return stroke are discussed and related to spectral observations.

1. Introduction

In Parts I and II time-resolved spectra of lightning return strokes were presented and quantitatively analyzed. Knowledge of the temperature and the electron density for a given return stroke further enables a determination of the pressure, density, per cent ionization and specie concentrations, i.e., the concentration of NI atoms, NII ions, etc., for that stroke, all as a function of time. Since the temperature and electron density have been measured with 5-μsec resolution from a 10-m section of the return stroke, all values presented in this paper will have the same time and spatial resolution.

Previous calculations of the physical parameters of the return stroke have necessarily been derived from time-integrated slitless spectra obtained with millisecond resolution. For example, Prueitt (1963) calculated temperature in several return strokes and Uman *et al.* (1964a, b) calculated the electron density, pressure, relative mass density, per cent ionization and specie concentration in the same return strokes. Since these values, however, were obtained from data with only millisecond resolution, it was not clear whether they represented maximum values or were merely averages for the approximate 100-μsec integration time. The recent time-resolved spectra of the return stroke and consequent calculations remove some of the ambiguity in the previous parameters. The result of these calculations is a time-dependent model of the lightning return stroke in which the temperature, electron density, pressure, relative mass density, per cent ionization and specie concentration are specified with 5-μsec resolution during the initial 30 μsec of the return stroke.

2. Development of the model

From a knowledge of the temperature and electron density in a return stroke it is possible to use the tables of thermodynamic properties of air computed by Gilmore (1955, 1967[3]) to determine additional physical characteristics (all thermodynamic properties) of the stroke. Gilmore's tables present the equilibrium composition of dry air obtained from solving a number of coupled Saha equations, the equation of charge conservation, and the equation of percentage composition. Therefore, knowing the temperature and electron density of the return stroke, we can use Gilmore's tables and determine all other thermodynamic properties of the return stroke.

a. Assumptions

There are several assumptions required for the development of the time-dependent model. It is assumed 1) that the return-stroke channel is in local thermodynamic equilibrium (LTE) as a function of space and time, 2) that the return-stroke channel is optically thin to the NII lines used to calculate the temperature, 3) that the physical characteristics are constant across the stroke cross section, 4) that the thermodynamic

[1] Research supported in part by the Office of Naval Research and the Federal Aviation Agency.

[2] Present affiliation: Dept. of Atmospheric Sciences, State University of New York at Albany.

[3] Private communication.

properties of dry air and moist air are approximately the same. 5) that the broadening of the H-alpha line is due primarily to the Stark effect, and 6) that the channel is optically thin to H-alpha emissions. It is further necessary to assume 7) that the time-dependent temperature and electron density curves presented in Figs. 1 and 2 are representative values for the lightning return stroke.

The validity of assumptions 1), 2) and 3) was discussed in Part II. Assumption 4) is reasonable in that the maximum amount of water vapor in the air prior to the lightning stroke is no more than a few per cent. It is unlikely that the presence of a small percentage of hydrogen will strongly affect the properties derived from Gilmore's tables. Assumptions 5) and 6) have previously been discussed in Part II and by Uman and Orville (1964, 1965).

It is quite possible that 7) is not true. The peak temperature of 30,000K in Fig. 1 is approximately the value calculated from five of the eight spectra with 5-μsec resolution. Since a much higher temperature could exist in the channel for a microsecond or less and not be detected, the concept of peak temperature refers to the highest "average temperature" measured within the channel with a time resolution of 5 μsec. The remaining five temperature points in Fig. 1 fall within the experimental error of the temperatures calculated for stroke A presented in Fig. 4, Part II. Only one curve for the electron density as a function of time has been obtained. Fig. 2 is a reproduction of the electron density plotted in Fig. 19, Part II, for stroke F. The first three temperature points in Fig. 1 agree, within experimental error, with the temperature values calculated for stroke F in Fig. 9, Part II. For the purpose of the model development, it will be assumed that the entire temperature-time curve (Fig. 1) and the electron density-time curve (Fig. 2) apply to the same stroke, in this case, the model stroke.

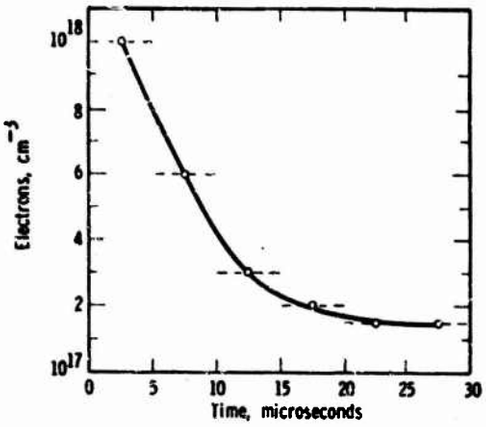

FIG. 2. Electron density vs time based on Fig. 19 in Part II.

b. *Return-stroke model*

Figs 1–6 present the time-dependent physical characteristics in a 10-m section of the model lightning return stroke. The time scale is the same in all figures; namely, 0–30 μsec with 5-μsec resolution. Figs. 1 and 2 are based on experimental data and have just been discussed. Figs. 3–6 are derived from the tables of Gilmore (*loc. cit.*).

The pressure-time curve in Fig. 3 indicates an average pressure of 8 atm in the first 5 μsec, decreasing to atmospheric pressure in 20 μsec. A high pressure within the channel produces rapid channel expansion. The rapid expansion soon reduces the channel pressure to approximately the ambient value. Unfortunately, the peak pressure is a poorly determined quantity reflecting the large errors in the electron density measurement. For example, a factor of 2 error in the electron density produces a similar error in the pressure. If, on the other hand, a pressure of 8 atm is correct, based on a correctly determined electron density, it is still possible that much higher pressures exist in the first microsecond or so and are not detected. For example, it does not seem

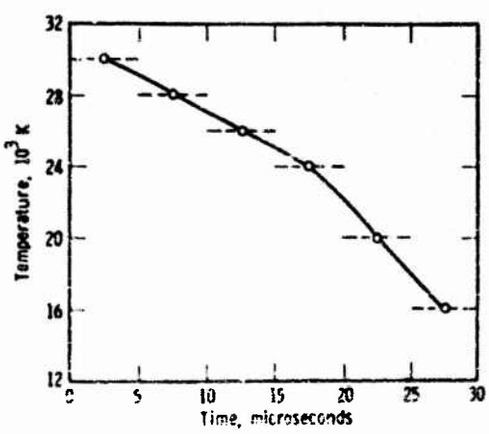

FIG. 1. Temperature vs time based on the experimental temperature data presented in Part II.

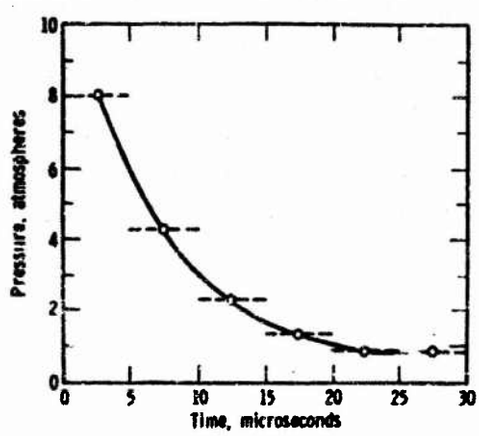

FIG. 3. Pressure vs time. The pressure in the first microsecond may exceed 8 atm by an order of magnitude.

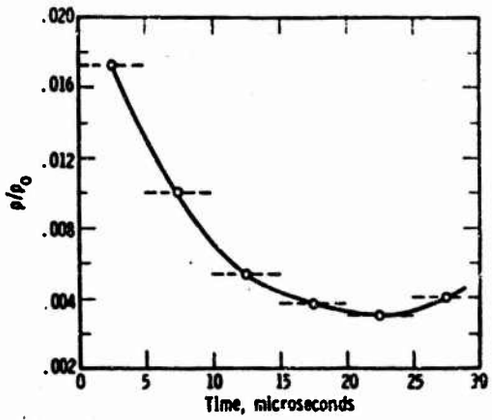

FIG. 4. Relative mass density vs time where ρ_0 is the mass density of air at STP and ρ is the mass density in the return-stroke channel.

unreasonable for a temperature on the order of 36,000K and an electron density of approximately 7×10^{18} cm^{-3} to exist in the first microsecond of a return stroke. (Even higher temperatures and electron densities may exist.) At these values the pressure would be roughly 60 atm. For a value of 7×10^{18} cm^{-3}, extrapolation of Griem's (1964) tables indicates the H-alpha Stark width would be on the order of several hundred angtroms. Clearly, this line would blend into the continuum and be undetected. Electron densities calculated from the H-alpha half-width in the first 5 μsec are weighted toward densities existing in the latter part of the 5-μsec exposure time. Consequently, the pressure is weighted, in a similar way, toward lower pressures. Therefore, the "peak pressure" of 8 atm in the return stroke model can only be accepted as an indication of the high pressures within the channel in the first 5 μsec.

Fig. 4 presents the relative mass density, ρ/ρ_0, as a function of time, where ρ_0 is the mass density of air at STP (1.29×10^{-3} gm cm^{-3}) and ρ is the mass density in the return-stroke channel. The rapidly expanding model-channel, characterized by high temperatures and high electron density and pressure, has a mass density that decreases in the 0–25 μsec period. The minimum relative mass density is 3×10^{-3} attained in approximately 20–25 μsec. At 25 μsec, atmospheric pressure has been attained in the return-stroke channel and further cooling of the channel produces an increase in the relative mass density.

Fig. 5 presents the per cent ionization as a function of time in the model return stroke. A value of 100% ionization means that in a given volume the number of electrons equals the number of molecules, atoms and ions. Molecular species, however, are effectively nonexistent for the temperatures and electron densities existing in the 0–30 μsec period of the return stroke. The physical implication of a channel characterized by 100% ionization is that the dominant species is singly ionized.

We see in the early stages of the model return-stroke development that the per cent ionization is 110, increasing to 120 at 15 μsec and then monotonically decreasing. During the 0–15 μsec period the channel is characterized by a falling temperature and pressure. A decreasing temperature would reduce the per cent ionization and a decreasing pressure would increase the per cent ioniza-

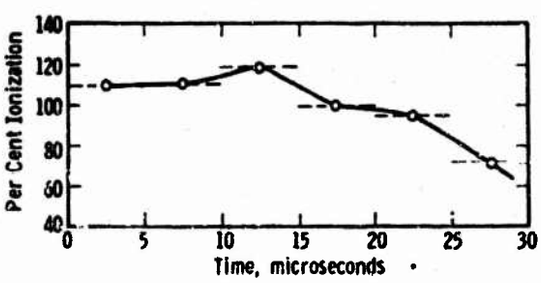

FIG. 5. Per cent ionization vs time where 100% means the number of electrons equals the number of atoms and ions in a given volume.

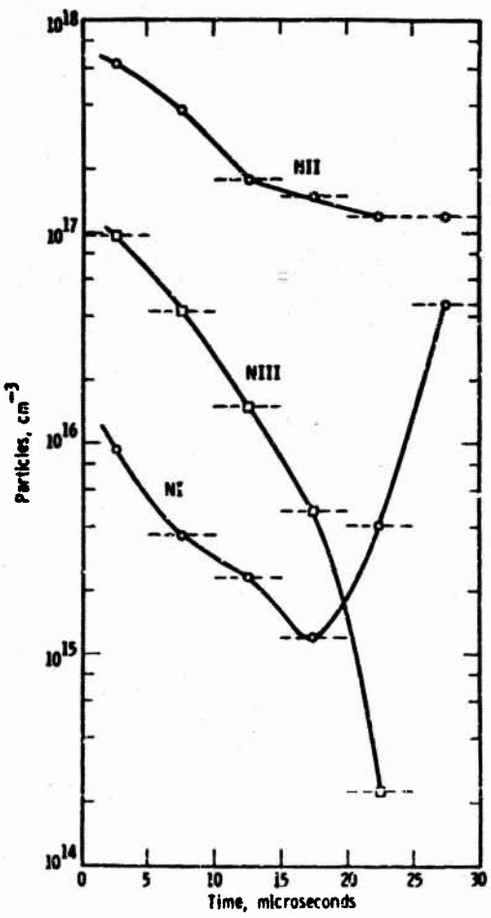

FIG. 6. Nitrogen species vs time. The relative values are significant, but the absolute values may be in error by an order of magnitude.

tion. It is apparent that the pressure effect dominates the temperature effect in the 0–15 μsec period. Consequently, we see a slight increase in the per cent ionization. Beyond 15 μsec the channel is near atmospheric pressure and the decreasing temperature begins to significantly reduce the per cent ionization. For the temperature and electron densities of interest, the per cent ionization is not a sensitive function of the electron density. An error by a factor of 2 in the electron density at 30,000K changes the per cent ionization by less than 10%.

A representative variation of specie concentrations is presented in Fig. 6. Although Gilmore's tables for the equilibrium composition of air contain the concentrations of 38 species, it is sufficient to plot the variation for three species of the principal constituent of air. Neutral nitrogen atoms (NI), singly ionized nitrogen atoms (NII), and doubly ionized nitrogen atoms (NIII) have concentrations which vary relative to each other in precisely the same way as similar species of oxygen. The concentrations are a sensitive function of the electron density. For example, a factor of 2 error in the electron density affects the specie concentrations as much as an order of magnitude, depending upon the species.

Consider the 0–20 μsec period in Fig. 6. All three specie concentrations are decreasing. In the particular temperature and electron density ranges existing in this time period (see Figs. 1 and 2), and at constant relative mass density, Gilmore's tables indicate a decreasing temperature will increase the NI and NII concentrations and decrease the NIII concentration. On the other hand, a decreasing pressure will reduce all concentrations. Therefore, in the case of the NIII concentration, the falling temperature and pressure have additive effects and the result is a rapidly decreasing concentration. In the case of the NI and NII concentrations the falling temperature and pressure produce opposite effects. Since Fig. 6 indicates the NI and NII concentrations decrease with time in the 0–20 μsec period, the falling pressure dominates the concentrations. Recall from Fig. 3 that during this time period the channel rapidly expands to reduce the channel pressure from 8 atm to the ambient value. This rapid expansion is sufficient to insure the reduction of the NI and NII concentrations, in addition to accelerating the reduction of the NIII concentration.

Consider the time beyond 20 μsec as shown in Fig. 6. The channel pressure is in approximate equilibrium with the ambient air and the dominant physical characteristic within the channel is now the decreasing temperature. Once again consider the effect of a falling temperature upon the specie concentrations for the temperature and electron densities of interest (see Figs. 1 and 2). At constant pressure the falling temperature increases the NI concentration (Drellishak, 1964). However, now the temperature and electron density have attained values such that any further decrease of the temperature decreases the NII concentration. As we would expect, the NIII concentration continues to rapidly decrease. Note in Fig. 6 that the NI concentration increases and the NIII concentration decreases in accord with the expected effects of a falling temperature, at the prevailing electron densities. The NII concentration, however, instead of the anticipated monotonic decrease, has apparently attained a plateau in the 20–30 μsec period. This may be the net effect of the increasing relative mass density (Fig. 4) and the decreasing per cent ionization (Fig. 5).

The results of Fig. 6 agree in a qualitative way with the time-resolved spectral features presented in Part I. For example, the NII emissions in the visible region dominate the optical spectrum in the early phase of the return stroke and the NI emissions (and H-alpha) appear at later times, consistent with the relative concentrations in Fig. 6. NIII emissions have not been identified in the lightning spectrum, although Fig. 6 indicates a concentration approximately one-sixth that of the NII concentration. It appears that the channel temperature is insufficient to excite the NIII ions to the states from which optical emissions (in the ranges measured by previous spectroscopy) occur (30–40 eV). The NII and OII ions radiate in the visible region from energy levels 20–30 eV above their ground states. If doubly ionized species are eventually detected in the lightning return stroke, it is clear the emissions will occur in the very early phase of the stroke.

3. Summary and conclusion

A model of the lightning return stroke has been obtained based upon time-resolved spectrograms and Gilmore's tables of the thermodynamic properties of heated air. The physical properties of the model stroke have been presented for a 10-m section of the return stroke for the first 30 μsec with 5-μsec resolution. A rough picture of the stroke development is the following.

The rapid input of energy into the return-stroke channel, following the leader process, produces a gas characterized in the first 5 μsec by a temperature of 30,000K and an electron density on the order of 10^{18} cm^{-3}. At these high temperatures and electron densities the pressure is about 8 atm and the per cent ionization is approximately 110. The dominate species in the channel is NII. Pressures within the channel greatly exceed the ambient pressure and the channel expands. The decreasing pressure accompanying the rapid expansion in the 0–20 μsec period seems to dominate the changes in the relative mass density, per cent ionization, and the specie concentrations. In other words, the relative mass density falls to a minimum of 3×10^{-2}, the per cent ionization increases to a maximum of 120, and the NI, NII and NIII concentrations decrease. At 20 μsec, with the channel in approximate pressure equilibrium with the surrounding air, the decreasing channel tem-

perature dominates the previously mentioned physical characteristics. Between 20 and 30 μsec the cooling channel at atmospheric pressure is characterized by an increasing relative mass density and a decreasing per cent ionization. During this same period the NI concentration is increasing at the expense of the NII and NIII ions.

It is important to remember that the rough model presented here is based on only a few time-resolved spectra quantitatively analyzed in Part II. The difficulties involved, however, in obtaining high-speed time-resolved data of the return stroke seem to justify the formation of a model based on these few spectrograms. It is clear that there are several ways to improve this model. Spectra with a time-resolution of 1 μsec will improve the estimate of the "peak temperature." Electron densities exceeding 10^{18} cm^{-3} in the initial few microseconds can be calculated by obtaining time-resolved spectrograms in the infrared where the Stark effect in neutral oxygen lines can be measured to determine the electron density (Griem, 1964; Orville *et al.* 1967). An interesting addition to the model would be simultaneous current oscillograms on the same time scale as the spectral measurements. Simultaneous current data, similar to that obtained by Berger (1962), and Berger and Vogelsanger (1965), would add a significant variable to the time-dependent model of the lightning return stroke.

Acknowledgments. I am grateful to Dr. Martin A. Uman for his helpful comments in the preparation of this paper.

REFERENCES

Berger, K., 1962: Front duration and current steepness of lightning strokes to earth. *Gas Discharge and the Electricity Supply Industry*, London, Butterworth, 63–73.

——, and E. Vogelsanger, 1965: Messungen und Resultate der Blitzforschung der Jahre 1955–1963 auf dem Monte San Salvatore. *Bull. Schweiz. Elektro. Ver.*, 56, 2–22.

Drellishak, K. S., 1964: Partition functions and thermodynamic properties of high temperature gases. AEDC-TDR-64-22 (Defense Documentation Center, AD-428210).

Gilmore, F. R., 1955: Equilibrium composition and thermodynamic properties of air to 24,000K. RAND Corp., Res. Memo. RM-1543 (Defense Documentation Center, AD-84502).

Griem, H. R., 1964: *Plasma Spectroscopy*. New York, McGraw-Hill, 573 pp.

Orville, R. E., M. A. Uman and A. M. Sletten, 1967: Temperature and electron density in long air sparks. *J. Appl. Phys.*, 38, 895–896.

Prueitt, M. L., 1963: The excitation temperature of lightning. *J. Geophys. Res.*, 68, 803–811.

Uman, M. A., and R. E. Orville, 1964: Electron density measurement in lightning from Stark-broadening of H_α. *J. Geophys. Res.*, 69, 5151–5154.

——, and ——, 1965: The opacity of lightning. *J. Geophys. Res.*, 70, 5491–5497.

——, —— and L. E. Salanave, 1964a: The density, pressure, and particle distribution in a lightning stroke near peak temperature. *J. Atmos. Sci.*, 21, 306–310.

——, —— and ——, 1964b: The mass density, pressure, and electron density in three lightning strokes near peak temperature. *J. Geophys. Res.*, 69, 5423–5424.

APPENDIX VI

"Determination of Lightning Temperature"

by Uman

JOURNAL OF GEOPHYSICAL RESEARCH VOL. 74, NO. 4, FEBRUARY 15, 1969

Determination of Lightning Temperature

MARTIN A. UMAN

Westinghouse Research Laboratories, Pittsburgh, Pennsylvania 15235

The assumptions on return-stroke channel opacity, temperature profile, and energy-state distribution that have been used in lightning temperature calculations are examined. It is shown that the assumptions used are probably valid, except perhaps during the initial few microseconds of the discharge, and that a reasonable approximation to local thermodynamic equilibrium exists within the return-stroke channel.

INTRODUCTION

Return-stroke channel temperatures have been reported by *Prueitt* [1963], *Uman* [1964], and *Orville* [1968]. These temperature determinations have been made by relating the intensity ratios of N II spectral lines to theory. No detailed analysis of the theoretical techniques used to calculate temperature has been published. In order for the temperature calculations to be meaningful, the following criteria for channel properties must be satisfied: (1) the channel must be optically thin to the spectral lines of interest, (2) the region of the channel cross section from which the radiation of interest is observed must to some reasonable approximation be at uniform temperature, and (3*a*) the discrete atomic energy levels from which the transitions leading to the measured N II line emission occur must be populated according to Boltzmann statistics. If these three criteria are satisfied, the temperature determined is, at the least, the electron temperature, since for the range of interest of electron density (equal to and greater than 10^{17} cm^{-3}) the electrons will have a Maxwell-Boltzmann energy distribution and it is electron excitation and de-excitation collisions with the atoms that maintain the Boltzmann distribution among the bound atomic energy levels [*Griem*, 1964]. If criterion 3*a* is replaced by the more restrictive requirement: (3*b*) that the lightning channel be in local thermodynamic equilibrium (LTE), the temperature determined by analysis of the N II line radiation is a true temperature in the thermodynamic sense. The lightning channel is said to be in LTE as a function of position and time if each small volume of that channel at local temperature $T(\mathbf{r}, t)$ satisfies the conditions for thermodynamic equilibrium of a classical gas. A classical gas is said to be in thermodynamic equilibrium at temperature T if *all* energy states, continuous and discrete, are populated according to Boltzmann statistics. In particular, the kinetic energy distribution of each group of particles is described by a Maxwell-Boltzmann distribution function, the population of the discrete atomic energy levels is described by a Boltzmann distribution, and the relation between the populations of discrete atomic energy levels and continuum levels is described by a Saha equation.

The validity of the application of the concept of temperature to the lightning channel has been questioned by *Hill and Robb* [1968], who suggest that the electron–heavy-particle kinetic-energy equilibration time is of the order of tens of microseconds. In a reply to the comments of *Hill and Robb* [1968], *Dawson et al.* [1968] present theory to show that the equilibration time is, in fact, of the order of tenths of a microsecond. In this paper we examine the procedures previously used to determine lightning channel temperature and show that they are for the most part valid and that, in fact, to a reasonable approximation LTE exists in the lightning channel.

DISCHARGE PROPERTIES

Orville [1968] found that the peak temperatures in ten return-stroke channels occurred within the first 10 μsec of the discharges and were of the order of 30,000°K. These peak temperatures were derived from an analysis of the time-resolved N II radiation recorded by a

Copyright © 1969 by the American Geophysical Union.

spectrometer with a time resolution of a few microseconds; thus, if the temperature was not essentially constant during that period of time, they represent some sort of average temperature. *Orville's* [1968] temperature data are in good agreement with the temperatures previously derived from analysis of time-integrated spectra [*Prueitt*, 1963; *Uman*, 1964]. In gengeneral, *Orville* [1968] found that N II line intensities were strong enough to be observable from distant lightning only when channel temperatures were above about 10,000° to 15,000°K. The return-stroke temperatures for all strokes studied were below 30,000°K after 10 μsec and were near or below 20,000°K after 20 μsec. Only 3 of 10 measured peak temperature points were in excess of 30,000°K, although the error bars about the points show that 6 of the 10 strokes might have had peak temperatures in excess of 30,000°K.

Electron densities in lightning return-strokes have been measured by *Uman and Orville* [1964] and by *Orville* [1968] by the technique of comparing the Stark width of the $H\alpha$ line with theory. The Stark width of $H\alpha$ is independent of the population of the bound atomic energy levels and is only a weak function of the electron temperature. According to *Orville* [1968], the electron density averaged over the first 5 μsec of the return stroke has a value of about 10^{18} cm^{-3}. This electron density and the measured channel temperature averaged over a similar initial time interval yield a channel whose pressure is about 8 atm, an average value that is probably weighted toward lower pressures [*Orville*, 1968]. In any event, the initial channel pressure exceeds ambient, and the lightning channel must, therefore, expand, apparently reaching pressure equilibrium with the surrounding atmosphere in a time of the order of 10 μsec [*Orville*, 1968]. When pressure equilibrium is reached, the measured electron density is about 10^{17} cm^{-3}, and thereafter it stays constant for at least as long as the N II lines are recorded. According to the calculations of *Drellishak* [1964], a nitrogen plasma in LTE at 1 atm pressure will have an electron density of about 10^{17} cm^{-3} for all temperatures between 13,000° and 35,000°K. Since nitrogen and air plasmas can be expected to be very similar, the theoretical results provide good confirmation of the measured values.

The time resolution of the spectrometer used by *Orville* [1968] was 2 μsec for some strokes and 5 μsec for others. In the spectroscopic measurement of channel properties, it is necessarily assumed that the time resolution of the spectrometer exceeds the characteristic time in which the discharge changes its properties. This situation probably occurs after the initial few microseconds of the discharge but may not occur during the initial few microseconds. There is apparently no literature on the actual light output of a short section of the return-stroke channel on a submicrosecond time scale. In the sections to follow we assume that errors in computed channel properties due to possible inadequate time resolution of the spectrometer or due to the techniques used for handling the photographic film on which the lightning spectrum is recorded are not important, and we concentrate rather on errors due to the possible inadequacy of the assumptions made about channel properties.

Analysis

We consider now the criteria for channel properties (presented in the first section) that must be satisfied if the measured lightning temperatures are to be meaningful.

1. Measurements of the lightning channel opacity to visible N II line radiation have been made by *Uman and Orville* [1965] and *Orville* [1966]. *Uman and Orville* [1965] analyzed time-integrated spectra and found the lightning channel to be transparent to the visible N II line radiation during the greater part of the time that the radiation was emitted. *Orville* [1966] analyzed one time-resolved stroke spectrum for opacity and found some deviations from optical thinness in the early part of the discharge. He states, however, that his results are far from conclusive and that more data with greater spectral dispersion are needed to check the opacity as a function of time. According to the theory presented by *Uman and Orville* [1965], the volume of the lightning channel radiating the visible N II lines must have a diameter of the order of a millimeter or less if the temperature is 30,000°K and of the order of a centimeter or less if the temperature is 20,000°K in order for that volume to be optically thin to the visible N II lines. The results of theory and of experiments with long laboratory sparks indi-

cate that initially the return-stroke diameter is considerably less than 1 cm [*Uman*, 1969]. Theory and direct measurements made on the lightning discharge indicate that the return-stroke channel expands to a diameter of the order of a centimeter [*Uman*, 1969]. It would appear therefore that the lightning channel is transparent to the visible N II line radiation except possibly during the initial phases of the return stroke.

2. It has not been practical to measure radiation from the lightning channel as a function of radial position within the channel. Hence all lightning spectra thus far obtained yield at best the total radiation at a given wavelength emanating from a short length of channel regardless of where within the channel that radiation originated. Strictly speaking, lightning temperature measurements are not meaningful unless the radial temperature profile of that part of the channel from which the N II radiation occurs is relatively flat. The temperature profile of the channel is determined primarily by the initial conditions and by the means available for transporting heat out of the channel. The initial condition of the channel is that of a high-temperature, high-pressure plasma rapidly expanding behind the cylindrical shock wave that it initiates [*Uman*, 1966; *Orville*, 1968]. The initial temperature profile of the channel is not known, but it is probably not unreasonable to consider that the profile is flat. If, subsequently, the dominant energy loss mechanism is radiative energy loss from an optically *thin* channel, the temperature profile will remain flat [see, for example, *Lowke and Capriotti*, 1968]. If the dominant energy loss mechanism is optically thin radiation and even if the initial temperature profile is not flat, the profile will rapidly tend to become flat because regions of higher temperature will have greater radiative cooling rates than regions of lower temperature. Even if the channel is optically thick at various wavelengths (e.g., parts of the ultraviolet and some line centers), the dominant energy loss mechanism may still be optically thin radiation with the result that the channel profile will be flat. This is the case, for example, for a steady-state air arc at a pressure of 30 atm and a temperature of 25,000°K [*Lowke and Capriotti*, 1968]. If the lightning channel has been in pressure equilibrium with the ambient atmosphere for a time of the order of 1 msec (see below) and its temperature is below about 20,000°K, the dominant energy loss mechanisms will probably be thermal conduction and convection. Thermal conduction necessitates a decreasing temperature with radius and hence a rounded temperature profile. Steady-state nitrogen arcs (a good approximation to steady-state air arcs) at atmospheric pressure and temperatures below about 15,000°K have rounded profiles [*Maecker*, 1964]. On the other hand, according to the calculations of J. J. Lowke (private communication, 1968) using the method of *Uman and Voshall* [1968], if an air arc of 1 cm in radius has a flat temperature profile initially and even if energy loss by radiation is completely ignored (only thermal conduction is considered), the profile will remain relatively flat for a time of the order of 0.1 msec. It does so because 0.1 msec is insufficient time for the channel particles to diffuse across the channel and alter the initial profile. In a time of the order of 1 msec the profile will be rounded. No return-stroke temperatures have been measured for times in the discharge later than 50 μsec, and hence it would appear that for the lightning temperature measurements that have been made the assumption of a flat temperature profile is a reasonable one.

If a temperature determination is made for a channel whose temperature profile in the region from which the visible N II line radiation originates is not flat but rather is rounded, some weighted average temperature will be measured. The average temperature will be weighted toward the temperature of that part of the channel in which the visible N II line radiation is the strongest. Of the visible N II multiplets of interest, the one with the lowest upper excitation potential, N II(3), will increase in intensity at fixed pressure near atmospheric for increasing temperature up to about 30,000°K because of the increased population of the upper excitation potential from which that line is radiated. The intensity will decrease for increasing temperature above about 30,000°K because the N II density is depleted by formation of N III. For pressures in excess of atmospheric the temperature at which the N II density is depleted is in excess of 30,000°K. Since all visible N II lines with multiplet numbers higher than 3 have upper excitation potentials higher than that of

N II(3), these lines will reach peak intensity at atmospheric pressure at a temperature higher than about 30,000°K. Thus, for atmospheric pressure and above and temperatures below about 30,000°K, the maximum intensities of all the visible N II lines will be radiated from the center of the channel where the temperature is maximum. For these conditions the temperature measured will be weighted toward the central temperature. For atmospheric pressure and temperatures above about 30,000°K, different N II lines will reach peak intensity at different temperatures. For the case of a rounded profile, different N II lines will be effectively radiated from different radial positions in the channel, and thus any temperature determination made from the ratio of N II lines under these conditions is subject to considerable error. Fortunately, all temperature measurements thus far made for times after about 10 μsec (when the channel can be expected to be near atmospheric pressure) were below 30,000°K. If the early temperature profile of the channel is rounded, early temperature measurement in excess of 30,000°K may be subject to some errors for channel pressures not much in excess of atmospheric. On the other hand, at early times one would expect a relatively flat temperature profile and pressures considerably in excess of atmospheric.

3a. We wish to show that the atomic energy levels involved in the transitions leading to the visible N II line radiation are populated according to Boltzmann statistics. According to *Griem* [1964], this will be true if for these levels the collisional-rate processes (electron-ion collisional excitation and de-excitation) dominate the radiative process (radiative decay and recombination). In general, for a fixed electron density and electron temperature, there will be an energy level of the N II atom above which a Boltzmann distribution of the bound energy levels exists and below which one does not. This is the case, at least in the hydrogenic approximation, because collisional rate processes increase as the spacing between energy levels decreases (that is with increasing energy level), while the radiative decay rates decrease with increasing energy level [*Griem*, 1964].

All N II spectral lines used in lightning temperature measurements result from transitions with lower energy levels at or above the lowest $n = 3$ level, the $3s^3P^o$ at about 18.4 ev, of N II. This level will be in Boltzmann equilibrium with all higher levels if the total transition probability for radiative decay from it is much smaller than, for instance, the total rate of collisional excitation from it to all higher levels. If $A_{q'q}$ is the Einstein transition probability for a transition from state q to state q', and $C_{q'q}$ is the collision transitional rate per atom from state q to state q' (discrete and continuum levels), we require that

$$\sum_{q'>q} C_{q'q} \gg \sum_{q'<q} A_{q'q} \qquad (1)$$

where q is the $3s^3P^o$ state.

According to *Seaton* [1962] and *Griem* [1964], a reasonable approximation for the collision transitional rate between discrete energy levels of ions is

$$C_{q'q} \approx 9 \times 10^{-8} f_{q'q} N_e \left(\frac{E_H}{\Delta E}\right)\left(\frac{E_H}{kT_e}\right)^{1/2} \cdot e^{-\Delta E/kT_e} \ \text{sec}^{-1} \qquad (2)$$

where $f_{q'q}$ is the absorption oscillator strength, ΔE is the energy difference between levels q and q', E_H is the ionization potential of hydrogen, T_e is the electron temperature, k is Boltzmann's constant, and N_e is the electron density in cm^{-3}. To determine the conditions under which (1) is satisfied without having to perform a great amount of detailed calculation, we can underestimate $\Sigma_{q'>q}C_{q'q}$ and overestimate $\Sigma_{q'>q}A_{q'q}$. The conditions thus calculated will be more stringent than necessary. We underestimate $\Sigma_{q'>q}C_{q'q}$ by considering only three multiplets in the summation: the N II(3) multiplet consisting of 6 lines resulting from transitions from the $3p^3D$ level at about 20.6 ev, the N II(4) multiplet consisting of 3 lines resulting from transitions from the $3p^3S$ level at about 20.9 ev, and the N II(5) multiplet consisting of 6 lines resulting from transitions from the $3p^3P$ level at about 21.1 ev. Using the oscillator strengths and the energy level data compiled by *Wiese et al.* [1966], we can sum (2) over the lines comprising these three multiplets and determine the collision transitional rate as a function of temperature. After performing these operations, we find that

$$\sum_{e'>e} C_{e'e} \cong 4 \times 10^{-7} N_e \ \text{sec}^{-1} \quad \text{for} \quad T_e = 10{,}000°\text{K}$$
$$\cong 8 \times 10^{-7} N_e \ \text{sec}^{-1} \quad \text{for} \quad T_e = 15{,}000°\text{K}$$
$$\cong 11 \times 10^{-7} N_e \ \text{sec}^{-1} \quad \text{for} \quad T_e = 20{,}000°\text{K} \qquad (3)$$
$$\cong 16 \times 10^{-7} N_e \ \text{sec}^{-1} \quad \text{for} \quad T_e = 40{,}000°\text{K}$$

The collision transitional rate increases monotonically for increasing temperature and fixed electron density for temperatures between 10,000° and 40,000°K.

The radiative transition probability $A_{e'e}$ can be related to the *emission* oscillator strength $f'_{e'e}$ by

$$A_{e'e} = 4.3 \times 10^7 (\Delta E)^2 f'_{e'e} \qquad (4)$$

with ΔE in electron volts. Equation 4 can be derived from the expression given by *Allen* [1963, p. 55] using λ (in angstroms) equal to $12{,}400/\Delta E$. The energy levels found below the $3s^3P^0$ at 18.4 ev to which transitions might occur are listed by *Moore* [1949] and given in Table 1. Dipole transitions from the $3s^3P^0$ to all lower levels are forbidden by the dipole transition selection rules: $\Delta L = \pm 1$ and $\Delta S = 0$. Nevertheless, dipole forbidden transitions can be expected to occur. For example, *Kelly* [1964] has reported a transition probability of 1.3×10^6 sec^{-1} for the intercombinational ($\Delta S \neq 0$) transition to the ground state.

As stated previously, in order to make the conditions for the existence of a Boltzmann distribution above the $n = 3$ level as restrictive as possible, it is appropriate to overestimate the total radiative transition rate from the $3s^3P^0$ level. Thus we will assume that transitions can occur from the $3s^3P^0$ level to *all* lower levels subject to the restriction on the multiplet members, $\Delta J = 0, \pm 1$ with $0 \rightarrow 0$ not allowed. (This assumption is equivalent to making the calculations essentially *model* calculations and is, in fact, necessary if the calculations for the $3s^3P^0$ level are to be valid for levels above the $3s^3P^0$, which may have allowed transitions to some of the $n = 2$ levels.) We will also assume that for all transitions occurring $f'_{e'e} = 1$, the maximum value of f' for one electron transitions. Further, we ignore the effects of the possible imprisonment of ultraviolet radiation which will tend to reduce the net downward transition rate.

TABLE 1. Energy Levels of the N II Atom Found below the $3s^3P^0$ Level at 18.4 ev According to *Moore* [1949]

Level	Approximate Energy, ev
$2p^3\ ^1D^0$	17.8
$2p^3\ ^3P$	13.5
$2p^3\ ^5D^0$	11.4
$2P^3\ ^5S^0$	5.8
$2p^2\ ^1S$	4.05
$2p^1\ ^1D$	1.9
$2p^2\ ^3P$	Ground state

If we perform the summation indicated above, we find for the total radiative transition rate from the $3s^3P^0$ level

$$\sum_{e'<e} A_{e'e} \cong 1 \times 10^{11} \ \text{sec}^{-1} \qquad (5)$$

The total radiative transition probability is dominated by the probability of transitions to the ground state.

The combination of (1), (3), and (5) yields as the condition for the existence of a Boltzmann distribution at and above the lowest $n = 3$ level

$$N_e \gg 3 \times 10^{17} \ \text{cm}^{-3} \quad \text{for} \quad T_e = 10{,}000°\text{K}$$
$$N_e \gg 1 \times 10^{17} \ \text{cm}^{-3} \quad \text{for} \quad T_e = 15{,}000°\text{K}$$
$$N_e \gg 9 \times 10^{16} \ \text{cm}^{-3} \quad \text{for} \quad T_e = 20{,}000°\text{K}$$
$$N_e \gg 6 \times 10^{16} \ \text{cm}^{-3} \quad \text{for} \quad T_e = 40{,}000°\text{K} \qquad (6)$$

We have, however, underestimated the collision transitional rate per ion and overestimated the radiative transition probability. It is reasonable, therefore, to adopt in place of (6) the requirement

$$N_e \geq 10^{17} \ \text{cm}^{-3} \qquad (7)$$

As noted in the previous section, electron densities of about 10^{17} cm^{-3} are to be expected in the lightning channel after pressure equilibrium has been reached and for the time during which

the N II lines are recorded. Early in the discharge, the electron density is in excess of 10^{17} cm^{-3}. It would appear, therefore, that a Boltzmann distribution will be established between the lowest $n = 3$ energy level of the N II atom and all higher energy levels.

From (3) it is apparent that for $N_e = 10^{17}$ cm^{-3} the collision transitional rate from the $3s^3P^0$ level is in excess of 10^{16} sec^{-1}. Thus more than a hundred collision-induced transitions occur in 0.01 μsec. If the lightning discharge changes its properties on a time scale measured in 0.01 μsec or longer, it is to be expected that a Boltzmann distribution will exist above the lowest $n = 3$ level as a function of time.

For completeness, it is important to mention that the Boltzmann distribution can only be maintained if the spatial variation of the electron temperature is small in comparison with the distance an N II atom can diffuse in the order of an equilibration time for the lowest $n = 3$ level. This condition is considerably less restrictive than the condition (discussed previously) that the temperature profile must be relatively flat in the region from which the N II atoms are radiating.

Although the spectral lines of O I, N I, and O II have not as yet been used in lightning temperature measurements, they may well be used in the future. Channel temperatures in long sparks have been measured using the O I(1), O I(4), O I(35) multiplets in the near infrared [*Orville et al.*, 1967]. It is appropriate then to consider whether a Boltzmann distribution exists among the bound energy levels of O I, N I, and O II. The lowest energy level involved in visible or near-infrared radiation from O I is about 9.1 ev above the ground state and from N I is about 10.3 ev above the ground state. The ionization potential of O I is about 13.6 ev and of N I is about 14.5 ev. If the calculations previously performed for N II are repeated for O I and N I, the calculated radiative transition rates are found to be smaller for the neutral atoms than for N II, since the energy gap between excited levels and ground state is smaller for the neutrals (see equation 4). The collisional rates are roughly the same for the neutrals as for N II [*Griem*, 1964]. Thus we would expect that at and above 9.1 ev in O I and 10.3 ev in N I a Boltzmann distribution would be maintained. The lowest energy level involved in visible radiation from O II is about 22.9 ev above the ground state. The calculations for O II are very similar to the calculations for N II, and we would expect the O II states at and above 22.9 ev to be Boltzmann distributed if the N II states above 18.4 ev are.

3*b*. We wish to show now that the lightning temperatures measured are more than simply electron temperatures and that, in fact, to a reasonable approximation LTE exists in the return-stroke channel. We consider first the Boltzmann distribution of bound atomic energy levels; second, the kinetic-energy equilibration time between electrons, ions, and neutrals; and third, the effect of a strong electric field on the temperature of electrons and heavy particles.

Deviations from a Boltzmann distribution among the bound energy states of an atom occur because below some atomic level the radiative transition rates become equal to or exceed the collision transitional rates. The effect of these deviations is to overpopulate the lower energy levels relative to the Boltzmann distribution that exists among the upper levels. The overpopulation may be reduced somewhat by the effects of imprisoned ultraviolet radiation, which will tend to reduce the net downward radiative transition rate. For N II, then, some reasonable approximation to a Boltzmann distribution may exist even below the lowest $n = 3$ level. For O I, N I, and O II, some reasonable approximation to a Boltzmann distribution may exist even below the lowest levels involved in visible or near-infrared radiation.

If one is to speak of a return-stroke channel temperature, the electrons, the ions, and the neutrals in the channel should have the same average kinetic energy. The bulk of the input energy to the channel is initially delivered to the electrons because of their high mobility in the applied electric field. The energy gained by the electrons is then transferred by collisions to the ions and the neutrals. The equilibration time for electron-ion temperatures is given by [*Griem*, 1964]

$$\tau_{KE} \approx \frac{M}{m} \frac{1}{\langle \nu_{ei} \rangle} \tag{8}$$

where m is the electron mass, M is the ion mass, and $\langle \nu_{ei} \rangle$ is the average electron-ion collision frequency. In the formulation of (8) only elastic

collisions are considered, and thus τ_{KE} from (8) represents the maximum value of the electron-ion equilibration time. Electron-ion interactions are the dominant interactions in the lightning channel in the temperature and electron density ranges of interest. *Griem* [1964] shows that since

$$\langle \nu_{ei} \rangle = \frac{4(2\pi)^{1/2}}{3} N_e \left(\frac{2}{4\pi\epsilon_0 kT_e}\right)\left(\frac{kT_e}{m}\right)^{1/2} \ln \Lambda \tag{9}$$

with

$$\Lambda = 1.24 \times 10^{17}(T_e/n_e^{1/2}),$$

(8) can be written

$$\tau_{KE} \approx \frac{M}{m}\left[3 \times 10^{-7}\left(\frac{E_H}{kT_e}\right)^{3/2} N_e\right]^{-1} \text{ sec} \tag{10}$$

where the electron density is expressed in cm^{-3}. In (9) single ionization has been assumed.

From (10), the equilibration time calculated is

$$\begin{aligned} \tau_{KE} &\approx 7 \times 10^{8}/N_e \text{ sec} \quad \text{for } T_e = 10{,}000°\text{K} \\ \tau_{KE} &\approx 1 \times 10^{9}/N_e \text{ sec} \quad \text{for } T_e = 15{,}000°\text{K} \\ \tau_{KE} &\approx 2 \times 10^{9}/N_e \text{ sec} \quad \text{for } T_e = 20{,}000°\text{K} \\ \tau_{KE} &\approx 5 \times 10^{9}/N_e \text{ sec} \quad \text{for } T_e = 40{,}000°\text{K} \end{aligned} \tag{11}$$

Thus for $N_e = 10^{22}$ cm^{-3}, the electron-ion equilibration time is less than 0.1 μsec. If the discharge parameters change on a time scale measured in 0.1 μsec or longer, the kinetic energy of the ions will be equal to that of the electrons. Further, energy transfer between the ions and the neutrals will be relatively rapid, owing to their similar masses, and thus electrons, ions, and neturals should all have the same kinetic temperature on a 0.1-μsec time scale. A similar but less detailed discussion of the kinetic-energy equilibration time in the return-stroke channel has been given by *Dawson et al.* [1968]. The results obtained were essentially the same as the results given here.

In the preceding discussion of the kinetic-energy equilibration time, it was assumed that the applied electric field is not large enough to separate the electron and heavy-particle temperatures on a steady-state basis. We can use theory to obtain a rough estimate of the electric field that will in the steady state separate the electron and ion kinetic temperatures by a given per cent. Following *Finkelnburg and Maecker* [1956], we balance the energy gained by the electrons from the electric field in a mean free time with the net energy delivered from the electrons to the gas per collision:

$$\tfrac{3}{2}k(T_e - T_g)f = \tfrac{1}{2}\frac{e^2E^2}{m}\left(\frac{1}{\langle \nu_{ei} \rangle}\right)^2 \tag{12}$$

where T_g is the gas temperature, f is the electron average fractional energy loss per collision, and E is the electric field.

If (12) is divided by T_e and rearranged, we obtain

$$\chi = \frac{T_e - T_g}{T_e} = \frac{1}{3kT_e}\frac{1}{f}\frac{e^2E^2}{m}\left(\frac{1}{\langle \nu_{ei} \rangle}\right)^2 \tag{13}$$

From (13) and (9), E can be determined as a function of T_e for fixed values of the fractional electron-gas temperature difference χ. Results obtained using (13) should be considered accurate only to a factor of 2 or 3.

Equation 13 has been evaluated for nitrogen (a good approximation to air) with $\chi = 0.1$ and 0.01. The collision frequency was calculated using the data on electron density given by *Drellishak* [1964]. For simplicity, it is assumed that for temperatures above 10,000°K, electron collisions with ions (the dominant collisions) are primarily elastic, so that $f = 2m/M$. Since the value of f used is the minimum value to the actual f, the electric field intensity calculated for a given value of χ is the minimum value to the actual field. At atmospheric pressure the electron and heavy-particle temperatures are separated by 10% at an electric field intensity of the order of 20 v/cm and by 1% at an electric field intensity of the order of 6 v/cm for temperatures between about 13,000° and 30,000°K. At a pressure of 10 atm the comparable electric fields are about an order of magnitude higher. Electric fields in high-current arcs in air at atmospheric pressure are of the order of 10 v/cm [*King*, 1962], so that the

effect of the electric field in separating particle temperatures in the return stroke channel should not be significant during the time the channel is near atmospheric pressure. In the first few microseconds of the return-stroke history, the channel pressure is high and so probably is the channel electric field. Very little information is available on the magnitude of either parameter at early times. It is possible that the electron temperature might exceed the heavy-particle temperature during the initial microseconds of the discharge owing to the presence of a relatively strong electric field in the channel.

Conclusions

The assumptions on return-stroke channel properties that have been used to determine return-stroke temperatures from a comparison of the ratios of visible N II spectral lines with theory would appear to be valid, except possibly during the first few microseconds of the discharge. If during the initial microseconds of the discharge the channel temperature is near 30,000°K and the radius of the volume radiating N II is larger than about 1 mm, the N II lines will be self-absorbed, leading to an erroneous temperature measurement. It is likely that the temperature profile of the return-stroke channel is relatively flat during the first 0.1 msec of the discharge. If, however, temperature profiles are rounded after the initial microseconds of the discharge, measured temperatures will be weighted toward the central temperature. If temperature profiles are rounded during the initial microseconds of the discharge and if the central temperature is above 30,000°K, the channel is optically thin, and the pressure is not considerably in excess of atmospheric, erroneous temperature measurements will occur because different N II lines will radiate their peak intensities from different radial positions in the channel. However, it is in the initial microseconds of the discharge that high channel pressures are to be expected.

The concept of a temperature would appear to be a valid concept when applied to the return-stroke channel. In fact, to a reasonable approximation, the channel can be considered to be in LTE: The lowest energy levels of the N II, O II, N I, and O I atoms that are involved in visible or near-infrared radiation and possibly even lower levels are populated according to Boltzmann statistics on a 0.01-μsec time scale. The kinetic temperatures of the electrons, ions, and neutrals are equilibrated on a 0.1-μsec time scale except possibly during the initial discharge phase. If a strong electric field is present in the channel during the initial discharge phase and if the channel pressure is not considerably in excess of atmospheric, the electron and heavy particle temperatures may be separated by the electric field. The separation of electron and heavy-particle temperatures, if it does occur, would be expected to last for a few microseconds or less.

Acknowledgments. I wish to thank Drs. A. V. Phelps, J. J. Lowke, R. E. Orville, and L. S. Frost for their helpful comments regarding this paper.

The research reported in this paper was supported in part by the Atmospheric Science Division of the Office of Naval Research and by the Federal Aviation Agency.

References

Allen, C. W., *Astrophysical Quantities*, 2nd ed., Athlone Press, London, 1963.

Dawson, G. A., M. A. Uman, and R. E. Orville, Discussion of the paper by E. L. Hill and J. D. Robb, 'Pressure pulse from a lightning stroke,' *J. Geophys. Res.*, *73*, 6935, 1968.

Drellishak, K. S., Partition functions and thermodynamic properties of high temperature gases, *Defense Documentation Center AD 428 210*, January 1964.

Finkelnburg, W., and H. Maecker, Electric arcs and thermal plasmas, *Handbuch der Physik*, *22*, 254-444, 1956.

Griem, H. R., chapter 6, in *Plasma Spectroscopy*, McGraw-Hill, New York, 1964.

Hill, E. L., and J. D. Robb, Pressure pulse from a lightning stroke, *J. Geophys. Res.*, *73*, 1883, 1968.

Kelly, P. S., Transition probabilities in nitrogen and oxygen from Hartree-Fock-Slater wave functions, *J. Quant. Spectry. Radiative Transfer*, *4*, 117, 1964.

King, L. A., The voltage gradient of the free burning arc in air or nitrogen, *Proceedings of the 6th International Conference on Ionization Phenomena in Gases, Munich, 1961*, pp. 871-877, North-Holland, Amsterdam, 1962.

Lowke, J. J., and E. R. Capriotti, Calculation of temperature profiles of high pressure electric arcs using the diffusion approximation for radiation transfer, *J. Quant. Spectry. Radiative Transfer*, *8*, 1968.

Maecker, H., Arc measurements and results, in *Discharge and Plasma Physics*, edited by S. C. Haydon, pp. 266-288, Department of University Extension, University of New England, Armidale, N.S.W., Australia, 1964.

Moore, C. E., *Atomic Energy Levels as Derived from Analyses of Optical Spectra*, vol. 1, *NBS Circ. 567*, June 15, 1949.

Orville, R. E., A spectral study of lightning strokes, Ph.D. thesis, University of Arizona, Tucson, 1966. (Available from University Microfilms, Inc., Ann Arbor, Michigan, no. 67-147.)

Orville, R. E., A high-speed time-resolved spectroscopic study of the lightning return stroke, 1, A qualitative analysis; 2, A quantitative analysis; 3, A time-dependent model, *J. Atmospheric Sci.*, *25*, 827, 1968.

Orville, R. E., M. A. Uman, and A. M. Sletten, Temperature and electron density in long air sparks, *J. Appl. Phys.*, *38*, 895, 1967.

Prueitt, M. L., The excitation temperature of lightning, *J. Geophys. Res.*, *68*, 803, 1963.

Seaton, M. J., chapter 11, in *Atomic and Molecular Processes*, edited by D. R. Bates, Academic Press, New York, 1962.

Uman, M. A., The peak temperature of lightning, *J. Atmospheric Terrest. Phys.*, *26*, 123, 1964.

Uman, M. A., Quantitative lightning spectroscopy, *IEEE Spectrum*, *3*, 102 and 154, 1966.

Uman, M. A., chapter 7, in *Lightning*, McGraw-Hill, New York, 1969.

Uman, M. A., and R. E. Orville, Electron density measurement in lightning from Stark-broadening of Hα, *J. Geophys. Res.*, *69*, 5151, 1964.

Uman, M. A., and R. E. Orville, The opacity of lightning, *J. Geophys. Res*, *70*, 5491, 1965.

Uman, M. A., and R. E. Voshall, Time interval between lightning strokes and the initiation of dart leaders, *J. Geophys. Res.*, *73*, 497, 1968.

Wiese, W. L., M. W. Smith, and B. M. Glennon, *Atomic Transition Probabilities*, vol. 1, *Hydrogen thru Neon*, National Standard Reference Data Series 4, National Bureau of Standards May 20, 1966. (Available from Superintendent of Documents, U. S. Government Printing Office, Washington, D. C.)

(Received September 9, 1968;
revised November 6, 1968.)

APPENDIX VII

"Time Interval between Lightning Strokes and the Initiation of Dart Leaders"

by Uman and Voshall

JOURNAL OF GEOPHYSICAL RESEARCH VOL. 73, NO. 2 JANUARY 15, 1968

Time Interval between Lightning Strokes and the Initiation of Dart Leaders

MARTIN A. UMAN AND ROY E. VOSHALL

Westinghouse Research Laboratories, Pittsburgh, Pennsylvania 15235

The temperature decay of a lightning channel during the interstroke period is determined theoretically. It is shown that, in the absence of input energy to the channel, the channel temperature will decay sufficiently slowly so that conditions conducive to the initiation and propagation of a dart leader will exist in the channel after a typical interstroke period of 40 msec. Thus, it would appear unnecessary to invoke the special mechanisms suggested by Brook et al. and by Loeb to explain the 'long' interstroke period. The calculations indicate that the lightning channel radius during the latter stages of a lightning stroke is of the order of centimeters. A mechanism is suggested to explain the phenomenon of bead lightning and to account for the observed long-lasting luminosity occurring at certain points on the normal discharge channel.

INTRODUCTION

A complete lightning flash to ground is composed of one or more partial discharges known as strokes. Each stroke begins with a faintly luminous predischarge, which travels from cloud to ground, a distance of the order of kilometers. The predischarge preceding the first stroke in a flash is called the 'stepped leader,' because its luminosity moves earthward in steps of typically 50 meters with about a 50-μsec time delay between steps [*Schonland*, 1956]. The stepped leader forges its way earthward through essentially un-ionized air. Subsequent strokes in a multiple-stroke flash are preceded by 'dart leaders.' The dart leader appears to the camera as a luminous dart about 50 meters in length, which travels smoothly toward ground along the path of the previous stroke. Dart leader velocities have been reported by *Schonland* [1956] to be between 1.0×10^6 and 2.1×10^7 m/sec, with a most frequent value of 2.0×10^6 m/sec. *Schonland et al.* [1935] found that, in general, the longer is the time from the cessation of measurable luminosity of the previous stroke, the lower is the dart leader velocity. Brook and Kitagawa (published in *Winn* [1965]) have presented data illustrating this effect. *Schonland et al.* [1935] suggested that the effect is due to the decrease in channel conductivity with time, lower conductivity yielding a slower dart leader. Other factors that may affect the dart leader velocity are the change in the channel radius with time and the increase in the channel particle density with time. A typical value for the time between cessation of the previous stroke and the initiation of a dart leader is about 40 msec, most time intervals being between 10 and 100 msec [*Schonland*, 1956]. A minimum time interval of 3 msec has been reported by M. Brook (private communication, 1967). According to *Kitagawa et al.* [1962], if the time interval between strokes is longer than about 100 msec, there is probably continuing current flowing in the channel during the time interval.

During the time interval between two stroke-current peaks, the total lightning channel may increase in luminosity without the prior appearance of a dart leader. This increase is known as an *M* component. It would appear that *M* components generally occur during the few milliseconds of low current occurring at the termination of some lightning strokes [*Malan and Schonland*, 1947] or during the flow of continuing current [*Kitagawa et al.*, 1962] following some strokes. It is, therefore, reasonable to assume that, when *M* components do occur, the lightning channel is sufficiently conducting that dart leaders cannot occur.

The lightning stroke current, as measured at the ground, rises to a peak value of the order of 10 kA in microseconds for first strokes and in tenths of microseconds for subsequent strokes [*Lewis and Foust*, 1945; *Hagenguth and Anderson*, 1952; *Berger and Vogelsanger*, 1965]. The current decreases to half of peak value in

about 20 to 60 μsec [*Hagenguth and Anderson*, 1952; *McCann*, 1944]. Thereafter, currents of the order of 100 to 1000 amp may flow with characteristic decay times of milliseconds [*Hagenguth and Anderson*, 1952; *Berger and Vogelsanger*, 1965].

Several spectroscopic determinations of lightning temperature versus time have been made by *Orville* [1966] (and private communications, 1967). Using 5-μsec time resolution, Orville found peak lightning temperatures near 30,000°K. Orville's data indicate that stroke temperature decreases to about 10,000°–15,000°K in 20 to 50 μsec. No temperature determinations below these values were possible, owing to the low light levels characteristic of the visible spectrum at these temperatures. *Maecker* [1953] has reported that a short laboratory arc in nitrogen carrying 200 amp of current has a central temperature of about 11,000°K. *Edels and Holme* [1966] report that short arcs in air with currents between 10 and 25 amp have central temperatures between 6000° and 7000°K. On the basis of the foregoing discussion, we might reasonably expect the lightning temperature in the latter stages of the discharge to be of the order of 10,000°K.

Lightning channel radii between 1.5 and 6 cm have been reported by *Evans and Walker* [1963] from measurements made on 2-μsec photographic exposures of the lightning channel. *Schonland* [1937] has photographically measured lightning channel radii between 7.5 to 11.5 cm. Unless great care is taken, the photographic measurement of channel radius can be expected to yield an overestimation of the channel radius. *Uman* [1964], from a measurement of the damage caused by lightning when that lightning was allowed to pass through insulating screens, found that the lightning channel was at most 1 or 2 cm in radius. *Flowers* [1943] has investigated the variation in radius of lightning-like sparks in air. He found that sparks 9 cm in length reaching peak currents of the order of 20,000 amp in a few microseconds were initially contained within very narrow channels. By the time peak current was attained, those channels had expanded to radii of 0.5 to 1.0 cm. After peak current, the channel radii continued to increase, reaching a value of a few centimeters in tens of microseconds. On the basis of the foregoing discussion, we might reasonably expect the lightning channel radius in the latter stages of a lightning stroke to have a value between 1 and 8 cm.

The pressure existing in the lightning channel as a function of time can be estimated as follows: Prior to the return stroke, the channel pressure and particle density are that characteristic of the leader. The pressure is probably near atmospheric, and the particle density, owing to the elevated leader temperature, is probably somewhat less than that characteristic of atmospheric air. The return stroke heats the leader channel to a temperature of the order of 30,000°K. Since the heating of a short section of channel occurs quickly, the particle density will not have time to change appreciably during the heating process. The resultant high temperature and relatively high air density yield a channel pressure that is probably an order of magnitude, or more, greater than atmospheric pressure. The channel will therefore expand until it is in pressure equilibrium with its surroundings. If we assume that the temperature remains constant, the channel volume must increase 10 to 100 times in order to lower the channel pressure to atmospheric. Thus, we would expect that the channel pressure would be near atmospheric after the channel radius had expanded 3 to 10 times its initial value. The initial radius is probably less than 1 cm, since (as we shall see) the final radius is of the order of 1 cm. The channel will probably expand at supersonic velocity. A velocity of Mach 3 corresponds to a radial expansion of 1 cm in about 10 μsec. We would therefore expect that, in a time measured in tens of microseconds, the channel pressure would approach atmospheric and, furthermore, would remain near atmospheric for the duration of the slow monotonic stroke temperature decay.

In this paper, we will present calculations of the temperature decay in the lightning stroke channel during the interstroke period. We will assume reasonable values for stroke temperature and radius at effective current cessation and begin the calculations from those initial conditions. By 'at effective current cessation' we mean at the time at which the channel current falls to a sufficiently low value so that the energy input to the channel is small compared with the energy dissipated by the channel.

It has been suggested by *Brook et al.* [1962]

that a small, steady current flowing in the lightning channel during the interstroke period might be necessary to maintain a level of ionization sufficient to allow a dart leader to traverse the path of the previous stroke. *Brook et al.* [1962] calculate that this current might be about 10 amp and still escape detection by photographic and electric-field-change measurements. It has been suggested by *Loeb* [1966] that ionizing waves may traverse the lightning channel during the interstroke period, keeping the degree of ionization above some minimum level necessary to support the dart leader. We shall show that neither of these suggested mechanisms is necessary, that the temperature decay in the lightning channel is sufficiently slow so that appreciable temperature and electrical conductivity exist in the lightning channel tens of milliseconds after the effective current cessation.

Theory

To describe the behavior of the decaying lightning channel after effective current cessation, we write the following four equations for the air composing the channel and regions around the channel: an energy balance equation

$$-\nabla\cdot\kappa\nabla T + \rho c_p \frac{DT}{Dt} + \rho \frac{D}{Dt}\left(\frac{v^2}{2}\right) - \frac{\partial P}{\partial t} = 0 \tag{1}$$

a momentum balance equation

$$\rho \frac{D\mathbf{v}}{Dt} = -\nabla P \tag{2}$$

a mass conservation equation

$$\frac{\partial \rho}{\partial t} + \nabla\cdot\rho\mathbf{v} = 0 \tag{3}$$

and an equation of state

$$P = P(\rho, T) \tag{4}$$

(see, for example, *Liepmann and Roshko* [1957]). In (1)–(4), P is the gas pressure, T is the absolute temperature, ρ is the mass density, $\mathbf{v}$ is the gas velocity, c_p is the specific heat at constant pressure, and κ is the thermal conductivity. The operator D/Dt is defined as

$$\frac{D}{Dt} = \frac{\partial}{\partial t} + \mathbf{v}\cdot\nabla \tag{5}$$

The validity of the set of equations used in describing the decaying lightning channel is dependent on the following assumptions: (1) local thermodynamic equilibrium is present in the system as a function of position and time, and (2) heat loss from the channel by radiation and by gravity-driven convection is negligible. These assumptions will be considered later.

To obtain a more tractable set of equations, we make the following additional assumption: (3) the pressure within and around the channel is always nearly atmospheric; that is, spatial and temporal pressure variations are small. The validity of this assumption will be considered later. With this assumption, we can set equal to zero the third and fourth terms on the left-hand side of (1). That the third term is proportional to ∇P can be seen by comparing it with (2) for the case that the air flow is only in the radial direction (see assumption 4 below).

We will solve, then, with the aid of a digital computer the following set of equations:

$$-\nabla\cdot\kappa\nabla T + \rho c_p\left(\frac{\partial T}{\partial t} + \mathbf{v}\cdot\nabla T\right) = 0 \tag{6}$$

$$\frac{\partial \rho}{\partial t} + \nabla\cdot\rho\mathbf{v} = 0 \tag{7}$$

$$P = P(\rho, T) = \text{constant} \tag{8}$$

Values for the mass density $\rho(T)$ and the specific heat $c_p(T)$ of air, both evaluated at 1 atmosphere pressure, were taken from the data of *Burhorn and Wienecke* [1960] and *Hansen* [1959]. Values for the thermal conductivity $\kappa(T)$ of air at 1 atmosphere pressure were taken from the data of *Yos* [1963]. The equations given above are sufficient to allow the determination of ρ, $\mathbf{v}$, and T as a function of position and time.

To obtain a solution of (6)–(8), it is necessary to choose a temperature profile for the channel and for the region surrounding the channel at the time of effective current cessation and also to assume a boundary value for the temperature at some distance from the channel. Further, we assume, for simplicity, our fourth and final assumption: (4) the channel is straight, cylindrically symmetrical, and infinitely long. Thus, we disallow turbulence or other air flow that is in a direction other than radial. We have arbitrarily chosen the initial temperature profiles to be roughly parabolic. On the time scales

used to measure the temperature decay, the temperature versus time curves are only slightly affected by the choice of initial profile. That is, any initial channel profile will relatively quickly revert to a profile characteristic of the channel. Some channel profiles as a function of time are given in Figures 1 and 2. In Figures 3 and 4 the central temperature of the decaying discharge channel is plotted as a function of time. In Figures 3 and 4, the channel radius is designated by that value of initial radial coordinate at which the temperature profile becomes essentially flat. Thus, the value assigned to the radius is somewhat larger than would be the luminous radius for the same temperature profile. Data have been presented for channel radii of 1.0, 2.0, 4.0, and 8.0 cm, and initial central temperatures of 8,000° and 14,000°K. In each case the temperature was arbitrarily assumed to be 500°K at a radius equal to twice the initial channel radius. For the times considered, the profile decay is only slightly affected by the presence of the arbitrary temperature boundary. If the boundary were moved to larger radius, the decay in the central temperature would take place at a slightly slower rate.

Since the ability of a decaying channel to support a dart leader depends, at least in part, on the electrical conductivity of the channel, it is appropriate to consider now the electrical conductivity of air at 1-atmosphere pressure as a function of temperature. This data, calculated by *Yos* [1963], assuming local thermodynamic equilibrium and assuming that the air does not contain water vapor, is given in Table 1. Further, as can be determined from the calculations of *Gilmore* [1955], an order of magnitude value for the equilibrium electron density in

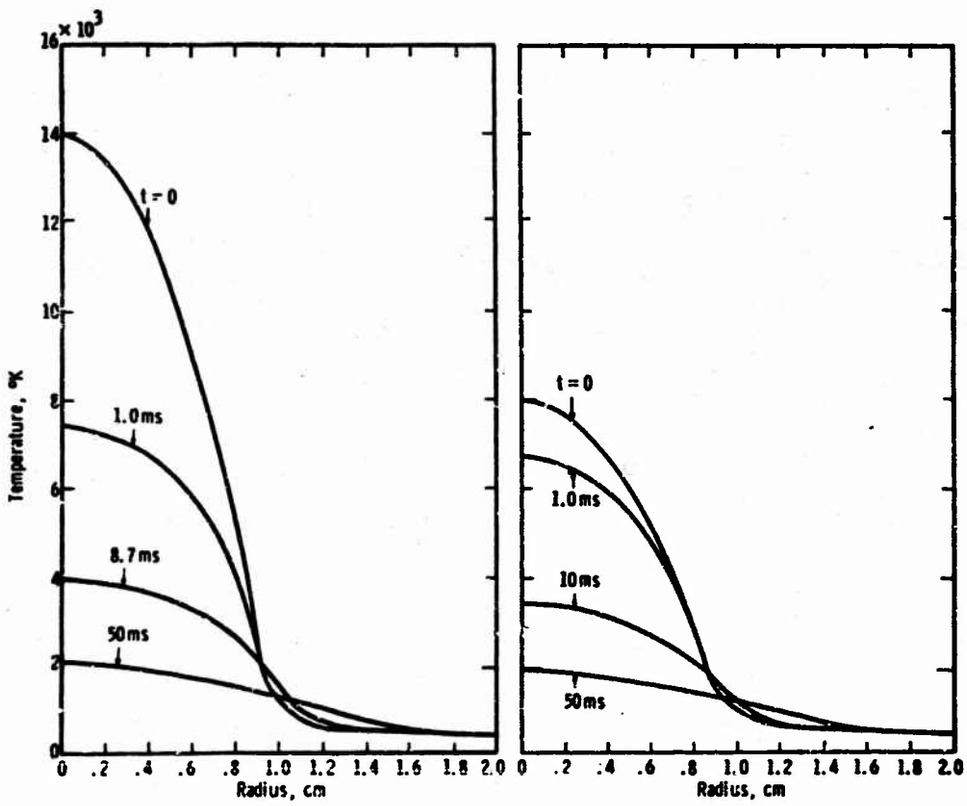

Fig. 1. Channel temperature profiles at various times for an initial radius of 1.0 cm and for initial central temperatures of 14,000° and 8000°K. The initial temperature profile is chosen to be roughly parabolic.

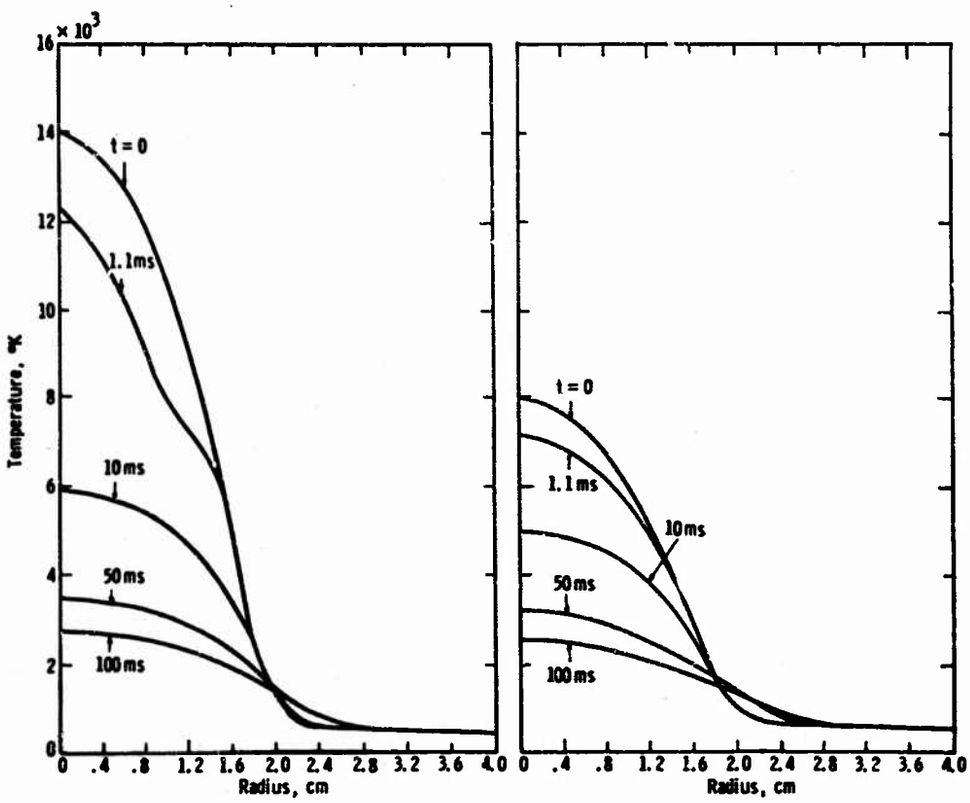

Fig. 2. Channel temperature profiles at various times for an initial radius of 2.0 cm and for initial central temperatures of 14,000° and 8000°K. The initial temperature profile is chosen to be roughly parabolic.

cm^{-3} of dry air can be obtained by multiplying the conductivity in mhos/cm by 10^{16}. At 4000°K, the electrical conductivity is about 10^{-8} mhos/cm and the electron density is about 10^{12} cm^{-3}. The channel at 4000°K is, thus, a poor conductor. At 2000°K, the electrical conductivity is about 10^{-8} mhos/cm and the electron density is about 10^{7} cm^{-3}. The channel at 2000°K is essentially nonconducting. It would appear likely that the level of conductivity necessary to support a dart leader would occur for a value of temperature between 2000° and 4000°K. Although the above data are valid only for air that does not contain water vapor, the presence of water would not be expected to change the conductivity values by an order of magnitude or to change the relation between conductivity and electron density by an order of magnitude.

Discussion of Results

It can be seen from the figures that the time for a discharge channel to decay from a given initial temperature to a given final temperature is roughly proportional to the square of the channel radius. If we consider the temperature decay from an initial 8000° to 14,000°K temperature range to a final 3000°K, we find that the time involved for a 1.0-cm channel is 15 to 20 msec and for a 2.0-cm channel 60 to 80 msec. Channels with radii over 4.0 cm take over 150 msec to relax from an initial 8000° to 14,000°K temperature range to a final 3000°K. If we assume that near 3000°K the lightning channel is ripe for a dart leader and recall that the interstroke time intervals are between 3 and 100 msec, the lightning channel radius at effective current cessation must, according to the theoret-

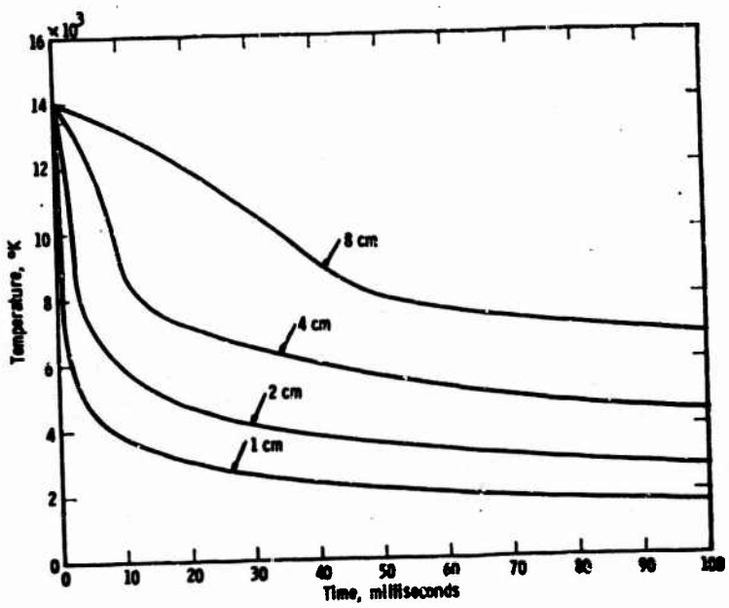

Fig. 3. Decay of the central temperature for channel radii of 1, 2, 4, and 8 cm. The initial central temperature is 14,000°K.

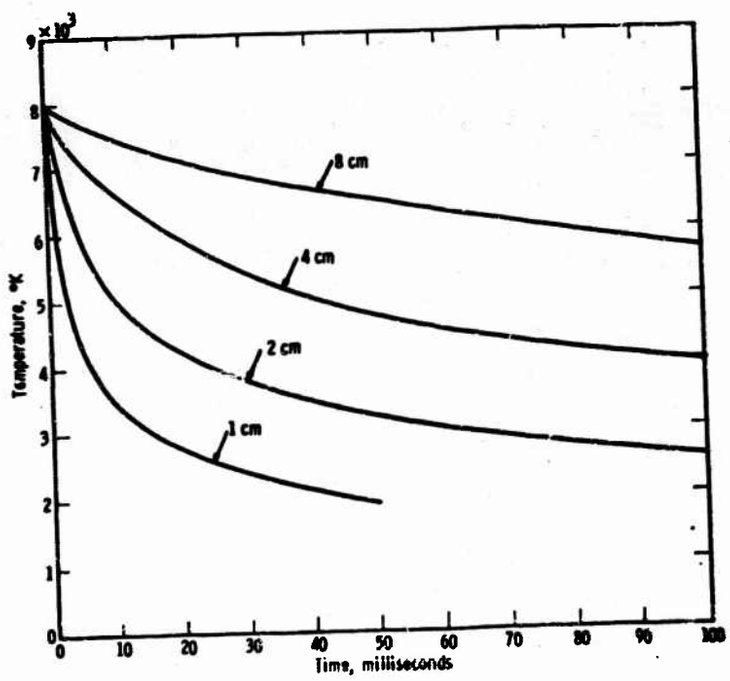

Fig. 4. Decay of the central temperature for channel radii of 1, 2, 4, and 8 cm. The initial central temperature is 8000°K.

TABLE 1. Equilibrium Electrical Conductivity of Dry Air at 1 Atmosphere, as Calculated by *Yos* [1963]

Temperature, °K	Electrical Conductivity, mhos/cm
2000	9.98×10^{-9}
3000	2.14×10^{-4}
4000	2.43×10^{-2}
5000	2.94×10^{-1}
6000	1.13
7000	3.90
8000	10.4
9000	19.0
10,000	27.3

ical data given above, be between about 0.5 and 2.5 cm. This calculated radius for lightning is in relatively good agreement with other determinations of that radius. Since in our formulation of the equations describing the decaying channel we neglected all channel heat loss other than loss by thermal conduction, the calculated radius given above should be considered a minimum value to that actually existing at current cessation. For example, in order for a channel with both conductive and convective heat loss to decay to 3000°K in about 50 msec, the channel might have to have an initial radius of, say, 4.0 cm instead of the 2.0 cm necessary if only conductive heat loss were considered. It would appear that, for reasonable lightning channel radii, one would expect to obtain the measured interstroke time intervals if channel temperature decays to near 3000°K between strokes. It is probably not coincidental that, in the 2000° to 4000°K temperature range, air changes from a conductor to an insulator.

The total particle density present in the lightning channel near 3000°K at 1-atmosphere pressure is about an order of magnitude less than that existing outside the channel. This value of channel particle density provides a part of the environment conducive to dart leader initiation and propagation. This is the case because ionization rates and charged particle velocities in the presence of a strong electric field are dependent on the quantity E/N, electric field intensity divided by particle density. For given electric field provided by the dart leader, the high value of E/N in the channel relative to regions outside the channel serves to make the channel a preferred path for the dart leader. The discharge channel radius does not change significantly with time, and thus its change is apparently not important in the dart-leader initiation process.

If no continuing current flows in the lightning channel between strokes, the channel is observed photographically to decay in luminosity until it is dark. Often, however, certain points of the discharge channel (often associated with bends in the channel) are observed to remain luminous for an appreciable fraction of the interstroke time interval. (See, for example, the Boys camera photographs in *Schonland* [1956].) It is appropriate to examine the expected change in channel luminosity with time to see if that change is consistent with experiment. *Morris et al.* [1966] report that the continuum radiation from air at atmospheric pressure at wavelengths above 2000 A falls off about two orders of magnitude as the temperature decreases from 16,000° to 9000°K. Presumably, the continuum is a reasonable measure of the total radiation. According to the data presented by *Allen* [1965], the total optical radiation emitted by air at atmospheric pressure decreases about two orders of magnitude as the temperature is lowered from 14,000° to 9000°K and about three orders of magnitude as the temperature is lowered from 9000° to 4000°K. Since the peak lightning temperature is near 30,000°K [*Orville*, 1966, and private communication, 1967], the change in total luminosity from the peak lightning temperature to the 2000° to 4000°K range at least is five orders of magnitude. The change in luminosity in the *visible* wavelengths may be even greater, since a large part of the visible radiation is due to singly ionized nitrogen, which does not exist at low temperatures. If a streak camera with photographic films is used to record the stroke luminosity as a function of time and if the camera diaphragm is set so that the peak luminosity does not strongly overexpose the film, one would not expect, even under the best of conditions, to record luminosity more than two or three orders of magnitude below the peak luminosity. Therefore, with such an arrangement one might reasonably expect to fail to record photographically the lightning channel after it has fallen much below a temperature of about 10,000°K. As mentioned above, certain

positions on the channel, often apparently bends in the channel, are observed to retain their luminosity for relatively long times. It is suggested that these positions of long-lasting luminosity are sections of the lightning channel of enlarged radius. As noted earlier, a tripling of the channel radius will increase by about an order of magnitude the effective time constant for temperature decay. Further, a higher initial temperature for a fixed radius would also serve to increase the decay time, particularly for a section of channel of large initial radius (compare data on Figures 3 and 4).

As an extension of the preceding discussion, we are able to offer a possible physical mechanism for the phenomenon of bead lightning. If the lightning channel radius were somehow periodically modulated as a function of height, then, as the channel luminosity decayed, the channel would take on the appearance of a string of beads. That is, the regions of enlarged radii would be visible for a longer time than the regions of smaller radius would. One mechanism for such a modulation of radius is the pinch effect in the presence of standing wave phenomena, as has been suggested by *Uman* [1962]. The proposed regular modulation of channel radius may, on the other hand, be an accident of nature, occurring, for example, when the channel consists of a large number of kinks or bends.

Discussion of Approximations

We have made a number of approximations in the foregoing analysis. The validity of the results obtained may depend on the validity of the approximation. It is appropriate therefore to consider the approximations. We have assumed (1) that local thermodynamic equilibrium is present in the system as a function of position and time, (2) that heat loss from the channel by radiation and by gravity-driven convection is negligible, (3) that the pressure within and around the channel is always nearly atmospheric, and (4) that the channel is straight, cylindrically symmetrical, and infinitely long and thus that all air flow is radial, that is, that the effects of turbulence and other nonradial air flow can be neglected.

1. For thermodynamic equilibrium to exist in the channel as a function of time, all relevant particle-interaction times must be short compared with the characteristic time in which the channel changes its properties and the collisional rate processes must dominate the radiative rate processes, radiative decay and recombination [*Griem*, 1964]. In the temperature range of interest, the electron-neutral and neutral-neutral energy equilibration times are always less than 1 msec, so that kinetic energy is equilibrated on a time scale short compared with a millisecond. Data on electron-ion recombination times for air in the low-temperature ranges are apparently rare. If we assume that the results of *Bates and Dalgarno* [1962] for hydrogen are roughly valid, we find an equilibrium electron-ion recombination time of the order of 1 μsec for temperatures near 8000°K. At 5000°K, the recombination time is less than 1 msec; at 3000°K it is about 1 sec. The hydrogen recombination times at temperatures near 3000°K are probably long compared with the actual air recombination times, as can be inferred from the data of *Stein et al.* [1964]. *Stein et al.* [1964] found electron-NO^+ recombination times of less than 1 msec for air at 2900°K and 0.1 atmosphere. Radiative energy loss from the channel will be relatively small, as is evident from the data of *Allen* [1965], so that it is reasonable to assume that the rate processes are collision dominated. Thus, for temporal variation on a millisecond scale, the assumption of thermodynamic equilibrium would seem to be reasonable. For thermodynamic equilibrium to exist in the channel as a function of position, the spatial variation of the temperature should be small over the distance that particles can diffuse in times of the order of the equilibration times discussed above [*Griem*, 1964]. For times of the order of 1 msec in the temperature range of interest, the particle diffusion length is of the order of 0.1 cm. Thus, for spatial variations on a 0.1-cm scale, the assumption of thermodynamic equilibrium would seem to be reasonable.

Even if local thermodynamic equilibrium is not present within the channel, deviations from equilibrium will probably not cause an order of magnitude change in the computed temperature-decay data. This is the case because the thermal conductivity, specific heat, and mass density are relatively insensitive functions of temperature and might be expected to differ from their equilibrium values by only a factor

of 2 or 3. On the other hand, the electrical conductivity given in Table 1 for low temperatures is a very sensitive function of temperature. In view of this fact, some of our comments about the temperatures at which certain conductivity levels are reached may be in error in the absence of thermodynamic equilibrium.

2. That radiative energy loss is negligible compared with heat loss by thermal conduction can be easily shown by comparing the thermal-conduction loss with the calculations of the radiative emission of air by *Allen* [1965]. Gravity-driven convection may be an important heat-loss mechanism. A reasonable upper limit to the convective air velocity is a velocity of the order of the speed of sound, about 1 cm in 30 μsec. The convective velocity is probably one or two orders of magnitude below the speed of sound. Let us assume that the convective velocity is 1 cm/msec. Then appreciable convective motion can occur in the tens of milliseconds between lightning strokes. Although convective heat loss occurs from the lightning channel, the primary effect of convection may be to carry away the heat delivered from the channel core to the channel perimeter by thermal conduction.

3. We have assumed that the pressure within and around the channel does not deviate appreciably from atmospheric as the channel cools. As the channel temperature decreases, the mass density in the channel must increase if the pressure is to remain constant. The inward flow of air needed to maintain the channel at near atmospheric pressure is driven by a time-varying pressure gradient. An upper limit on the size of the pressure terms, the third and fourth terms on the left-hand side of (1), can be obtained by assuming that for any computed spatial and temporal change in channel temperature the mass density remains fixed. The pressure terms are then compared in magnitude to the other terms in (1). The results of such an analysis indicate that the pressure terms are negligible if the discharge properties change on a time scale measured in milliseconds. Thus, except possibly for the initial rapid temperature decay, the constant pressure approximation would appear to be valid for the lightning discharge.

Another way of looking at the approximation of constant pressure is the following: If the pressure is to remain constant as the channel cools, air must flow radially into the channel. Equations 6–8 allow no pressure variations but force the velocity to assume a value necessary to keep the pressure constant. The average radial velocity in the 10,000° to 14,000°K temperature range computed for the 1.0-cm channel is about 0.1 cm/msec and for the 8.0-cm radius is about 0.04 cm/msec. If these velocities are realizable without significant pressure variation, the constant pressure assumption is reasonable. For channels with radii 1 cm and over, the flow velocity is relatively small and thus might be expected to exist in the absence of strong pressure variation.

4. The assumption of cylindrical symmetry should have little effect on the temperature decay in the absence of turbulence or other nonradial air flow. The effects of turbulence and other nonradial air flow in transferring heat from the channel are similar to the effects of gravity-driven convection. In addition, however, turbulence or strong wind could physically break or fragment the channel. Since the interstroke time interval has been measured many times under various different conditions of wind velocity and since the various measurements are in relatively good agreement, it would seem reasonable to assume that the effects of turbulence and other nonradial air flow on the discharge parameters could be neglected.

Acknowledgment. The research reported in this paper had its origins in similar research on laboratory arcs initiated at the Westinghouse Research Laboratories by Mr. H. C. Ludwig. We are indebted to Dr. W. Frie of Siemens Aktiengesellschaft for suggesting (in a letter to H. C. Ludwig) a technique for manipulating equations 6–8, so that they could be easily programmed for a digital computer. Further, we wish to acknowledge stimulating and helpful conversations with Drs. J. J. Lowke, A. V. Phelps, and B. W. Swanson of the Westinghouse Research laboratories.

This research was supported in part by the Geophysics Branch of the Office of Naval Research and by the Federal Aviation Agency.

References

Allen, R. A., Air radiation graphs: Spectrally integrated fluxes including line contributions and self absorption, *Res. Note 561, Avco Everett Res. Lab.*, Everett, Mass., July 1965.

Bates, D. R., and A. Dalgarno, Electronic recombination, in *Atomic and Molecular Processes*, edited by D. R. Bates, pp. 245–271, Academic Press, New York, 1962.

Berger, K., and E. Vogelsanger, Messungen und Resultate der Blitzforschung der Jahre 1955-1963 auf dem Monte San Salvatore, *Bull. Schweiz. Electrotech. Vereins, 56*, 2, 1965.

Brook, M., N. Kitagawa, and E. J. Workman, Quanitative study of strokes and continuing currents in lightning discharges to ground, *J. Geophys. Res., 67*, 649, 1962.

Burhorn, F., and R. Wienecke, Plasmazusammensetzung, Plasmadichte, Enthalpie, und spezifische Wärme von Stickstoff, Stickstoffmonoxyd und Luft bei 1, 3, 10, und 30 atm in Temperaturbereich Zwischen 1000 and 30,000°K, *Z. Phys. Chem., 218*, 270, 1960.

Edels, H., and J. C. Holme, Measurements of the decay of arc column temperature following interruption, *Brit. J. Appl. Phys., 17*, 1595, 1966.

Evans, W. H., and R. L. Walker, High-speed photographs of lightning at close range *J. Geophys. Res., 68*, 4455, 1963.

Flowers, J. W., The channel of the spark discharge, *Phys. Rev., 64*, 225, 1943.

Gilmore, F. R., Equilibrium composition and thermodynamic properties of air to 24,000°K, *Rand Corp. RM-1543*, Santa Monica, California, August 24, 1955. (Available from Defense Documentation Center as AD 84052.)

Griem, H., *Plasma Spectroscopy*, pp. 129-168, McGraw-Hill, New York, 1964.

Hagenguth, J. H., and J. G. Anderson, Lightning to the Empire State Building, 3, *Am. Inst. Elec. Eng., 71*(3), 641, 1952.

Hansen, C. F., Approximations for the thermodynamic and transport properties of high-temperature air, *NASA Tech. Rept. R-50*, 1959.

Kitagawa, N., M. Brook, and E. J. Workman, Continuing currents in cloud-to-ground lightning discharges, *J. Geophys. Res., 67*, 637, 1962.

Lewis, W. W., and C. M. Foust, Lightning investigation on transmission lines-VII *Trans. Am. Inst. Elec. Eng., 64*, 107, 1945.

Liepmann, H. W., and A. Roshko, *Elements of Gasdynamics*, pp. 178-191, John Wiley & Sons, New York, 1957.

Loeb, L. B., The mechanisms of stepped and dart leaders in cloud-to-ground lightning strokes, *J. Geophys. Res., 71*, 4711, 1966.

Maecker, H., Elektronendichte und Temperatur in der Säule des Hochstromkohlebogens, *Z. Phys., 136*, 119, 1953.

Malan, D. J., and Schonland, B. F. J., Progressive lightning, 7, Directly correlated photographic and electrical studies of lightning from near thunderstorms, *Proc. Roy. Soc., A, 191*, 513, 1947.

McCann, G. D., The measurement of lightning currents in direct strokes, *Trans. Am. Inst. Elec. Eng., 63*, 1157, 1944.

Morris, J. C., G. R. Bach, R. V. Krey, R. W. Liebermann, and J. M. Yos, Continuum radiated power for high-temperature air and its components, *AIAA J. 4*, 1223, 1966.

Orville, R. E., A spectral study of lightning strokes, Ph.D. Dissertation, Department of Meteorology, University of Arizona, Tucson, 1966.

Schonland, B. F. J., The diameter of the lightning channel, *Phil. Mag., 23*, 503, 1937.

Schonland, B. F. J., The lightning discharge, *Handbuch der Physik, 22*, 576, 1953.

Schonland, B. F. J., D. J. Malan, and H. Collens, Progressive lightning, 2, *Proc. Roy. Soc., A, 152*, 595, 1935.

Stein, R. P., M. Scheibe, M. W. Syverson, T. M. Shaw, and R. C. Gunton, Recombination coefficient of electrons with NO^+ ions in shock-heated Air, *Phys. Fluids, 2*, 1641, 1964.

Uman, M. A., Bead lightning and the pinch effect, *J. Atmospheric Terrest. Phys., 24*, 43, 1962.

Uman, M. A., The diameter of lightning, *J. Geophys. Res., 69*, 583, 1964.

Winn, W. P., A laboratory analog to the dart leader and return stroke of lightning, *J. Geophys. Res., 70*, 3265, 1965.

Yos, J. M., Transport properties of nitrogen, hydrogen, oxygen, and air to 30,000°K, *Avco Corp. Tech. Memo RAD-TM-63-7*, Wilmington, Delaware, March 22, 1963. (Available from Defense Documentation Center as AD 435053.)

(Received July 20, 1967;
revised August 25, 1967.)